The Thesis committee for Udit Shankar Dasgupta
Certifies that this is the approved version of the following thesis:

Design of Laterally Loaded Monopile Foundations in Sand for Offshore Wind Turbines

APPROVED BY

SUPERVISING COMMITTEE:

Robert B. Gilbert, Supervisor

Shin-Tower Wang

Design of Laterally Loaded Monopile Foundations in Sand for Offshore Wind Turbines

by

Udit Shankar Dasgupta, B.E.

THESIS

Presented to the Faculty of the Graduate School of

The University of Texas at Austin

in Partial Fulfillment

of the Requirements

for the Degree of

Master of Science in Engineering

THE UNIVERSITY OF TEXAS AT AUSTIN

May 2017

Dedicated to my Grandmother Nila Roy and my Parents without whom I wouldn't be the man that I am today.

Acknowledgments

Graduate school has been an important journey in my life and I have met many people on the way who deserve credit for enriching it. Dr. Robert Gilbert would be the number one person on that list. Starting from day one in his risk class, I have admired him. Though short, my interactions with him have made me grow exponentially, as an engineer and as a person. In short - He's the best.

I would like to thank my reader, Dr. Shin-Tower Wang for closely following my work and giving valuable insight into the research. I would also like to thank Professors Rathje, Cox, El-Mohtar, Stokoe and Zornberg for being my teachers. I don't think I could have had better. I am especially grateful to Dr. Charles Woodruff for exposing me to the world of geology as he did. Geology will be my lifelong passion, and he has a lot to do with it.

One of the best things about UT has been the peers I have been able to interact with. The Pickle Research Group - Hande, Asitha, Ying, Yunhan and Jim - I could always count on you guys - for technical advice or otherwise. My fellow geotechs - Alejandro, Yuta, Aaron, Anna, Ritika, Hamza, Kaleigh, Patricia, Calvin - people I am sure to cross paths with once again in industry. That is something I look forward to. Special thanks goes out to the superstar Julia Roberts and omnipotent Subu for their great advice on life always.

My friends from Pilani were a major source of support throughout this endeavor - Piyush, Digveer, Prateek, Sanjana, Gauravi, Ruchir, and Shantanab - I'm glad we kept in touch and I intend to keep it that way.

There's another bunch of people without whom my Austin life would have been a major drag. Kshitiz and Priyadarshan - for being my fellow sufferers of grad school and wonderful roommates; Devendra - for all the amazing discussion we've had and for showing me what true humility is; Ronak - for always motivating me and being part of the "NoPinzNoGinz" regime; and Tanvi - for the inspiration and positivity that you brought to me.

This section would be incomplete if I didn't mention my two best buddies from middle school - "Niju" and "Aki". The perilous but beautiful trip to the Himalayas filled with adventure, introspection and discussion was the best of my life yet. They got me through some tough times, and I will always be grateful. I look forward to many more adventures with these fine gentlemen in this lifetime.

Lastly, but most importantly I would like to thank my family. They are the ones who have watched over me throughout this journey. My parents "Piu-Ma" and "Baba" for always supporting me and pushing me to strive for more. My brother "Dada" and my sister-in-law "Boudi" for always checking up on me. Finally, my dear nephew Arjo a.k.a. "Chubbles" for lighting up my days with his cute, chubby, and kind heart.

Design of Laterally Loaded Monopile Foundations in Sand for Offshore Wind Turbines

Udit Shankar Dasgupta, M.S.E.
The University of Texas at Austin, 2017

Supervisor: Robert B. Gilbert

Globally renewable energy is gaining popularity with the largest scope in offshore wind energy. Although USA is one of the leaders in the onshore wind industry, it is yet to tap into the abundance of coastline it has available for this offshore wind development. High costs of installation have been a deterrent, with the foundation being a major part of that cost. Among the various options for offshore foundations, the most popular and at the forefront of feasibility in construction are the monopiles. The aim of this research is to see how well the p-y method specified in the American Petroleum Institute (API) design standard predicts the response of these laterally loaded piles in sands. This thesis also investigates possible approaches to modify the codes to better predict the response and improve the efficiency of the design of the monopiles. The p-y approach was developed for analyzing laterally loaded long slender piles which are widely used for offshore oil and gas platforms. These piles tend to bend and fail through formation of flexural plastic hinges.

The large diameter relatively short monopiles for wind turbine applications are relatively stiffer and behave differently. They tend to rotate and/or translate instead of bending, evidenced by sizeable movements of the tip of the pile. Additionally, there is a serviceability criteria of the wind turbines to operate at low displacements i.e. low strain levels. This research focuses on the small strain response of the piles. The main behavior investigated with the long-slender pile load tests historically has been the response at large strain levels i.e. failure. The empirically calibrated API method may not be valid for such short-rigid piles and need to be verified before they can be used with confidence.

A database of laterally loaded piles in sands is compiled and presented. Specifically the impact of the initial stiffness modulus (k) on the response was investigated using the finite difference code LPILE. The Embedded Length to Diameter Ratio (L/D) is an important factor of design that influences the response. Based on the few field tests chosen for analysis from the database, it is observed that the API code overestimates the initial stiffness of the pile for piles with lower L/D ratios for monotonic loading. For cyclic loading, the LPILE analysis does not lead to much change in initial stiffness from the monotonic simulation, but the actual measurements suggest an increase in stiffness. There is an added effect of base shear which might be an important force that is taken into consideration for short rigid piles, that the current code does not specify. Higher stresses locked into the soil due to pile driving might lead to higher base shear. Finally, since the problem is one of small strain,

feasibility of future in-situ seismic testing is looked at by collection of sands from Mustang Island, TX, where the original field load tests were conducted that led to the specifications in the API code.

Table of Contents

List of Tables

List of Figures

Chapter 1

Introduction

Renewable sources of energy have taken up a sizeable share of the global electricity market as shown in Figure 1.1.

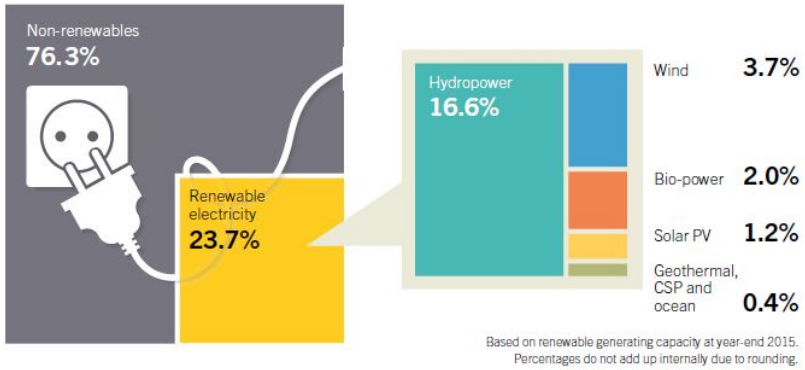

Figure 1.1: Estimated Renewable Energy Distribution of Global Electricity Production, End-2015 (Sawin, 2015)

According to Sawin (2015), employment in the renewable energy sector (not including large-scale hydropower) increased in 2015 to an estimated 8.1 million jobs (both direct and indirect). Additionally, as per IEA (2016)(Figure 1.2), global emissions of carbon dioxide were at 32.1 billion tonnes in 2015, having stabilized since 2013. Preliminary data from IEA (2016) suggest that electricity generated by renewables accounted for around 90% of new electricity

generation in 2015.

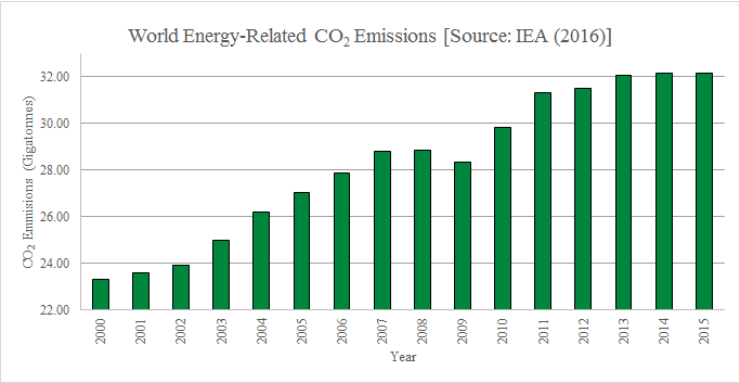

Figure 1.2: World Energy-Related CO_2 Emissions upto 2015 (IEA, 2016)

1.1 Global Wind Energy Market

Although a small segment in the renewable energy sector, wind energy has seen consistent growth over the last decade, growing from approximately 433 Gigawatts to 487 Gigawatts in 2016 alone (as illustrated in Figure 1.3 (GWEC, 2017)).

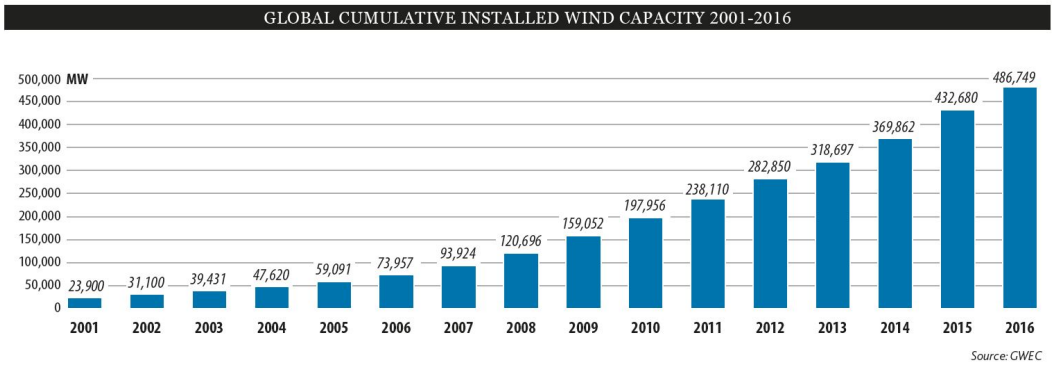

Figure 1.3: Global Cumulative Installed Wind Capacity from 2001-2016 (GWEC, 2017)

The major players in the overall wind market (offshore and onshore collectively) have been the People's Republic of China, USA and Europe. This is shown in Figure 1.4 with PR China at 34.7 %, USA at 16.9 % and Europe at a share of 22.4 % of the global market.

The potential of offshore wind is enormous. According to some estimates, it could meet the energy demand of Europe seven times over and that of USA four times over (Senanayake, 2016). There are several benefits to operating offshore wind farms. There is convenient access to less turbulent, high-speed winds, leading to efficient electricity generation. The idea of visual pollution is also pertinent. Many times, on-shore wind farms impact the aesthetics of the environment and encroach on usable land. This visual impact is a factor that leads to opposition from local communities.

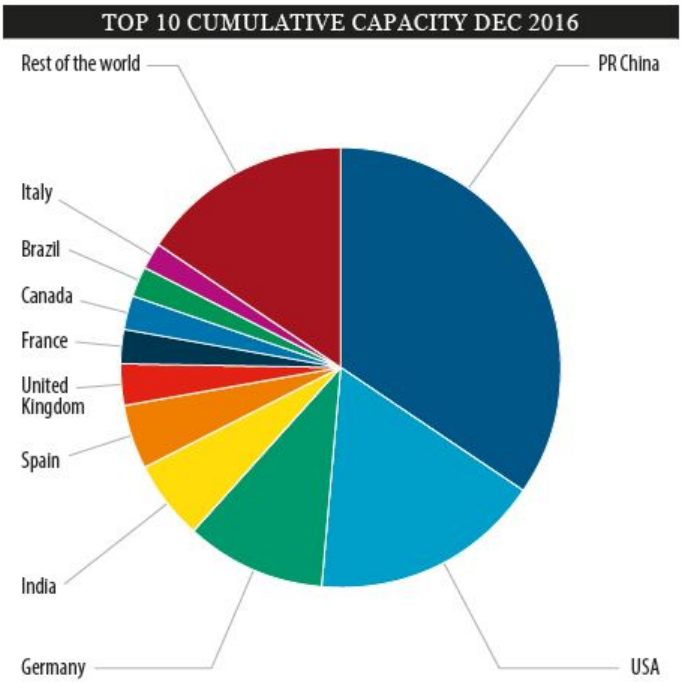

Country	MW	% Share
PR China*	168,690	34.7
USA	82,184	16.9
Germany	50,018	10.3
India	28,700	5.9
Spain	23,074	4.7
United Kingdom	14,543	3.0
France	12,066	2.5
Canada	11,900	2.4
Brazil**	10,740	2.2
Italy	9,257	1.9
Rest of the world	75,577	15.5
Total TOP 10	**411,172**	**84**
World Total	**486,749**	**100**

Source: GWEC

Figure 1.4: Global Top Ten Cumulative Wind Capcity Installed upto Dec 2016 (GWEC, 2017)

There has been a rise in the offshore wind sector as evidenced in Figure 1.5. On closer inspection, the data shows that Europe and China have been

the major parties responsible for that growth. In the following section, this thesis will report the scope and status of the offshore wind industry in USA.

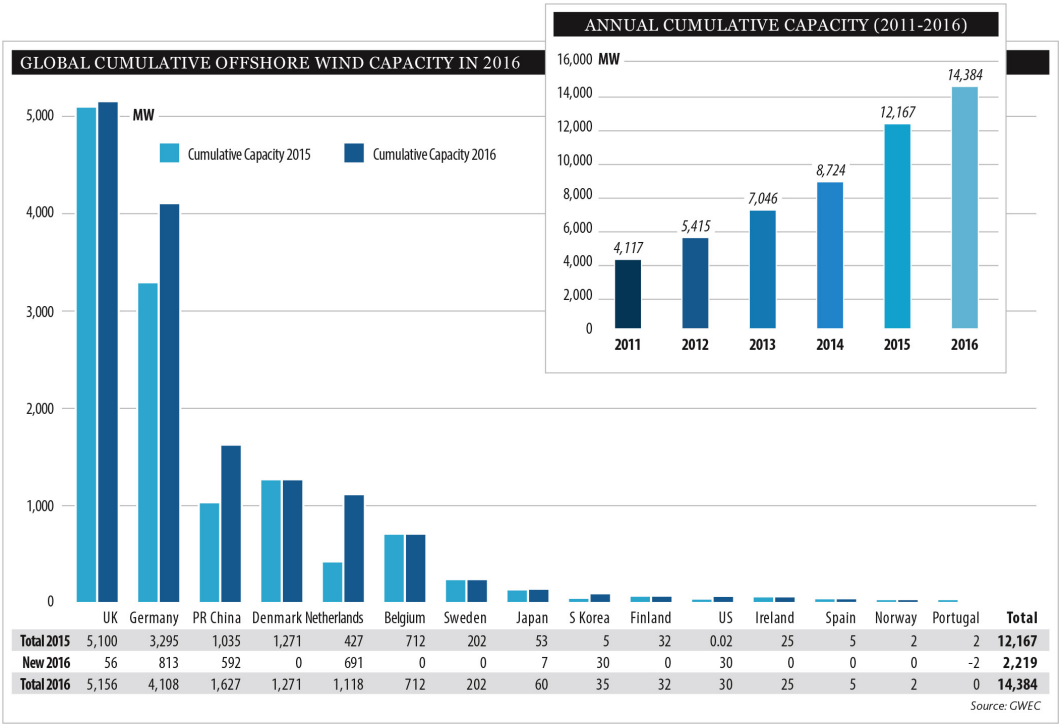

	UK	Germany	PR China	Denmark	Netherlands	Belgium	Sweden	Japan	S Korea	Finland	US	Ireland	Spain	Norway	Portugal	Total
Total 2015	5,100	3,295	1,035	1,271	427	712	202	53	5	32	0.02	25	5	2	2	**12,167**
New 2016	56	813	592	0	691	0	0	7	30	0	30	0	0	0	-2	**2,219**
Total 2016	5,156	4,108	1,627	1,271	1,118	712	202	60	35	32	30	25	5	2	0	**14,384**

Figure 1.5: Cumulative Global Offshore Wind Capacity from 2011 to 2016, and Cumulative Offshore Wind Capacity Growth in 2016 by Country

1.2 USA Wind Energy Market

1.2.1 Offshore Wind Potential

USA has the fortunate benefit of having great potential when it comes to Offshore wind energy. Offshore wind farms being located close to major coastal load centers provide an alternative to long-distance transmission of electricity in these land-constrained regions. Once built, these farms could

produce energy at low, long-term fixed costs, which can reduce electricity prices and improve energy security by providing a hedge against fossil fuel price volatility.

There are many factors which make offshore energy a lucrative opportunity for USA. The most important of these are presented here as stated by Gilman et al. (2016):

- **Offshore wind resources are abundant in USA** Today, a technical potential of 2,058 gigawatts (GW) of offshore wind resource capacity is accessible in the waters of USA using existing technology, enough to provide nearly double the total electric generation of USA in 2015. Figure 1.6 shows the regions in USA that have a strong potential for development of offshore wind energy. Figure 1.7 further gives an estimate on how much potential these locations have in terms of power generation with current technology.

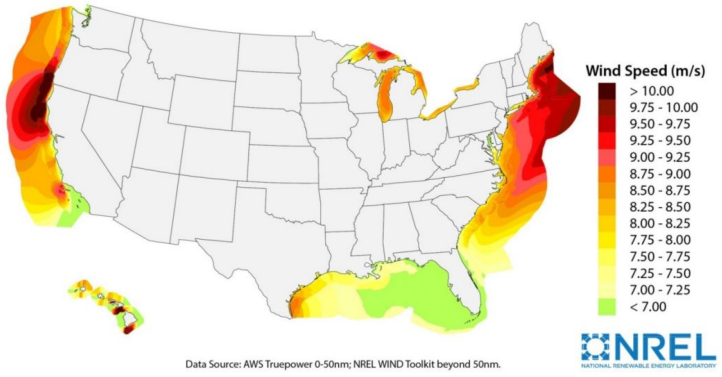

Figure 1.6: Offshore Wind Resource Data (100 m) used for the 2016 Offshore Wind Resource Assessment (Musial et al., 2016)

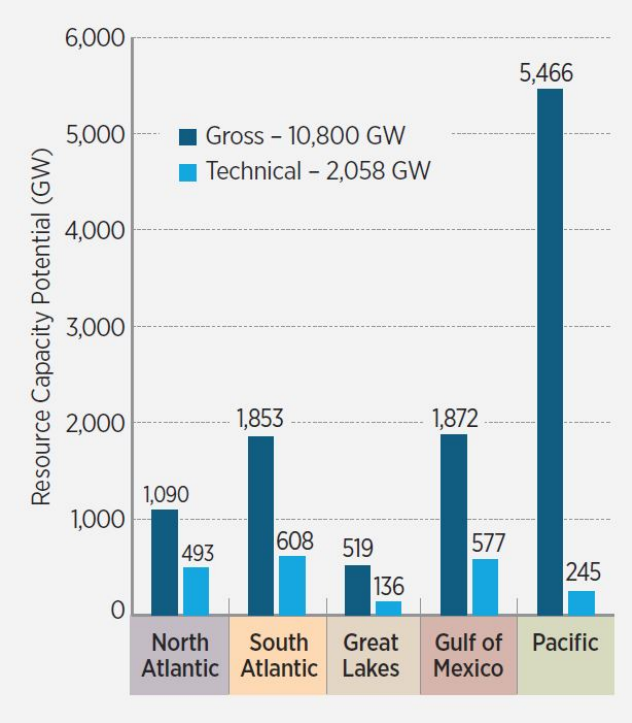

Figure 1.7: Capacity estimates for five U.S. offshore wind resource regions (Musial et al., 2016)

- **Decreased air pollution from other emissions.** The United States could save $2 billion in avoided mortality, morbidity, and economic damages from cumulative reductions in emissions of sulfur dioxide, nitrogen oxides, and fine particulates.

- **Reduced water consumption.** The electric power sector could reduce water consumption by 5% and water withdrawals by 3%.

- **Greater energy diversity and security.** Offshore wind could drive significant reductions in electricity price volatility associated with fossil

fuel costs.

- **Increased economic development and employment.** Deployment could support $440 million in annual lease payments into the U.S. Treasury and approximately $680 million in annual property tax payments, as well as support approximately 160,000 gross jobs in coastal regions and around the country

1.2.2 Current State of Development

Since the first national strategy for offshore wind which was released in 2011, there have been significant updates (Beaudry-Losique et al., 2011; Gilman et al., 2016):

- There are currently 11 active commercial leases for offshore wind farms along the Atlantic Coast.
- Coastal states have increased their demand for renewable energy deployment through renewable portfolio standards and other mandates.
- Land-based wind energy generation in the United States has increased nearly 60% and utility-scale solar generation increased more than 1,300% relative to 2011. Most of this renewable generation is located far from coastal load centers, and long-distance transmission infrastructure has not kept pace with this rapid deployment.
- At the same time, the offshore wind market has matured rapidly in Europe and costs are now falling.

These trends suggest that offshore wind has the opportunity to play a substantial role as a source of domestic, large-scale, affordable electricity for the nation.

1.2.3 Challenges to the Offshore Wind Market

There are certain challenges that need to be overcome before a strong future with offshore wind energy can become reality. The major aim of this research is to tackle these challenges. Some of the challenges are mentioned in the National Offshore Wind Strategy by the U.S. Department of Energy and Department of Interior (Gilman et al., 2016):

- **Reducing costs and technology risks.** Today, the cost of offshore wind energy is too high to compete in most U.S. markets without subsidies. However, continued global market growth and research and development investments are being made towards the areas of offshore site characterization, wind plant technology development and installation, operation, maintenance, and supply chain solutions. These could significantly reduce the costs of offshore wind toward competitive levels.

- **Offshore wind plant technology advancement.** Increasing turbine size and efficiency, reducing mass in substructures, and optimizing wind plants at a systems level for unique U.S. conditions can reduce capital costs and operating expenses and increase energy production at a given site.

- **Managing key environmental and human-use concerns.** More data need to be collected to verify and validate the impacts of offshore wind development on sensitive biological resources and existing human uses of ocean space. Improved understanding and further collaboration will allow for increased efficiency of environmental reviews and tighter focus on the most important issues.

This thesis attempts to tackle the first and second issue mentioned above by looking at ways to make the design of offshore monopile foundations in sandy soils more efficient so that the cost of production may be reduced.

1.3 Offshore Wind Turbine Foundations

One of the fundamental deterrents of offshore wind is its high cost. Offshore wind turbines are very large with rotor diameters and tower heights in excess of 100 m which makes them very expensive to install in marine environments. The foundation is a critical component of the structure both in terms of cost and the performance of the turbine. As given in a report to the to the Renewables Advisory Board of Great Britain (Blanco, 2009) the cost of construction and installation of foundations is about 25% (Figure 1.8) of the total project cost of an offshore wind farm. This shows that the economic feasibility of offshore wind options is significantly dependent on the foundation design optimization.

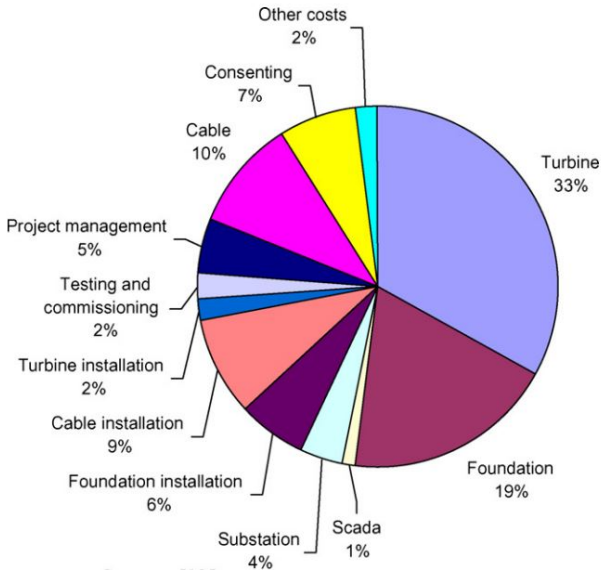

Figure 1.8: Cost Breakup of an Offshore Wind Farm (Blanco, 2009)

Support structures for offshore wind towers can be categorized based on their structural configurations into the following seven basic types (Malhotra, 2007)(Figure 1.9):

- Gravity structures
- Monopile structures
- Guyed Structures
- Tripod structures
- Braced frame lattice structures
- Suction Buckets

- Floating structures

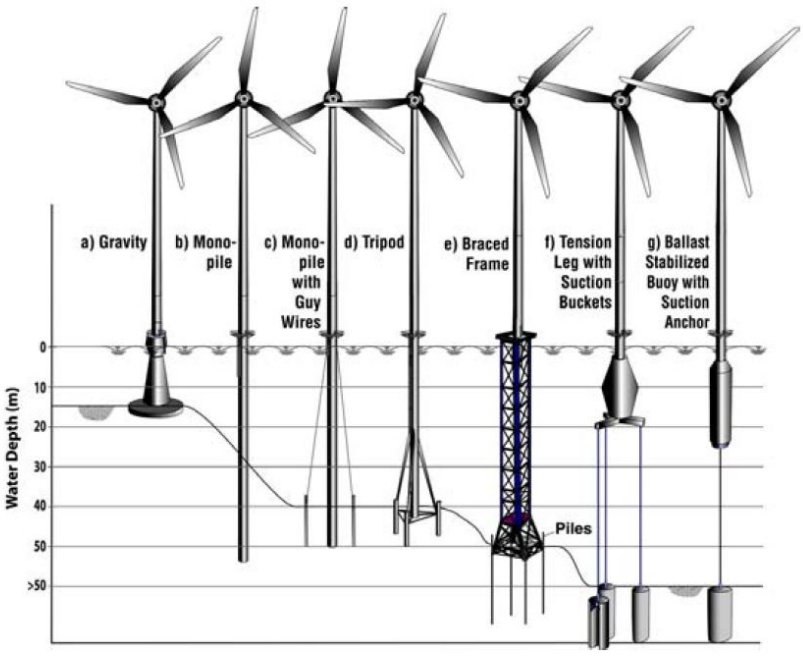

Figure 1.9: Different types of offshore foundations (Malhotra, 2007)

By far, the monopile is the most commonly used foundation for offshore wind turbines. The monopile consists of a large diameter steel pipe pile of up to 6 m in diameter with wall thicknesses as much as 150 mm. Depending on the subsurface conditions, the pile is typically driven into the seabed by either large impact or vibratory hammers, or the piles are grouted into sockets drilled into rock. These structures are well suited for shallow depths (20-30 m). The thickness and the depth the piling is driven depend on the design load, soil conditions, water depth, environmental conditions, and design codes. Pile

driving is more efficient and less expensive than drilling. Monopiles currently account for almost 80% of all offshore wind turbines (Figure 1.10.

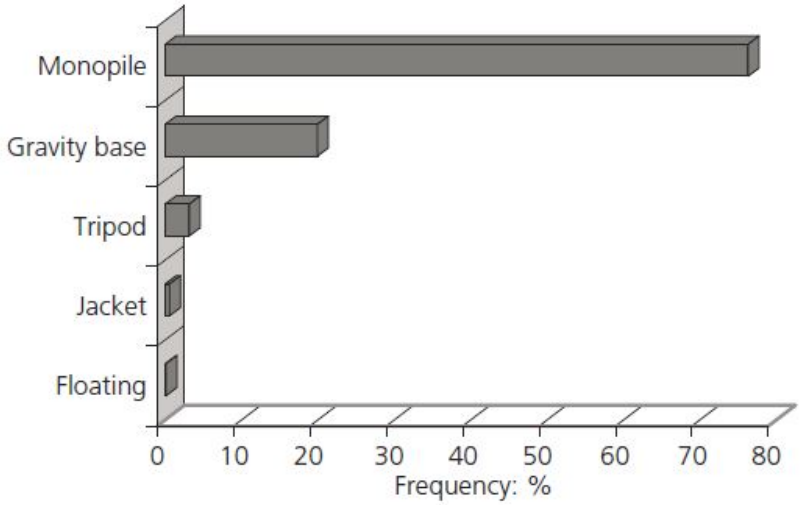

Figure 1.10: Foundation distribution for offshore wind turbines (Doherty and Gavin, 2011)

1.3.1 Monopile Foundations in Sands

Wind turbine monopiles predominantly carry lateral loads and moments as opposed to a typical deep foundation which mainly carries axial loads and moments. Most of the offshore continental shelf off of the Atlantic Coast of USA comprises of sands (Emery, 1966). Thus it is an important to understand the behavior of large diameter offshore monopiles in sands. There are many methods to analyze and design laterally loaded piles but the most widely used in practice is the "p-y method". It models the soil as a series of soil-springs and models the pile as an Euler-Bernoulli beam to obtain an ap-

proximate solution to the soil-structure interaction problem. The most popular design standard with regards to laterally loaded piles in sands is the American Petroleum Institute (API) RP 2GEO (2011). Chapter 2 goes in depth with regards to the derivation of the method and how it is used in design.

1.4 Research Motivation, Objectives and Methodology

This section describes the motivation, the objectives and the methodology for this research.

1.4.1 Motivation

The current design methods for laterally loaded offshore foundation, API RP 2A/2GEO are unverified for the large diameter, relatively short monopiles used for offshore wind turbines. These monopiles have a significantly larger diameter and smaller length to diameter ratio than typical piles used for offshore structures; and these piles are subjected to significant cycles of lateral loading and their design is governed by strict tolerance on rotation. Monopiles also behave differently in that they tend to rotate and translate, instead of the conventional bending of long, slender piles. The strict restriction on rotation also merits the study of these piles at small strain levels. Conventionally, load tests are performed to describe the behavior of the piles at failure, but in the special case of wind turbine foundations, low strain levels govern the behavior. Therefore methods that are based on load tests calibrated for long, slender piles that were loaded all the way to failure may not

provide the best prediction of behavior. An important aspect to consider is that conventional site characterization, such as SPT and CPT, are based on shearing the soil to failure. Soil characteristics such as friction angle obtained from such tests may not truly represent small strain properties of the soil.

1.4.2 Objectives

The objectives that this research attempts to achieve are as follows:

1. To synthesize the research literature on the subject of laterally loaded offshore monopiles in sands.

2. To develop a database of lateral load test results for field scale and model scale piles that was compiled for this research.

3. To analyze the most relevant field test results in detail.

4. To compare predictions from the API RP 2A (2010) with the five field test results chosen. The API RP 2A is chosen as it is the most descriptive design standard and the one that LPILE v 9.0 uses.

5. To perform a sensitivity study with respect to the k (initial stiffness modulus) and the effect it has on the pile response.

6. To evaluate whether the L/D ratio has an effect on the pile response when focusing on low strain levels.

1.4.3 Methodology

The research methodology consists of collection of published literature and presenting a review. Next, a database of lateral load tests on piles in sand is compiled and some important tests were chosen for further analysis. The analysis involves comparison of measured data against the API predictions. The API p-y method calculations were done in LPILE by ENSOFT. A sensitivity study is done on the effect of initial stiffness modulus (k) on the small strain response of the pile for both monotonic and cyclic tests. Additionally, the effect of base shear is investigated for the short-rigid piles.

1.5 Organization of Thesis

This thesis is organized into the following chapters:

1. **Introduction:** The background of the renewables market with wind in particular (globally and U.S. based), basics of offshore foundations, research motivation, research objectives, and the methodology for this study is presented in this chapter.

2. **Literature Review:** A concise review of the literature on analysis of laterally loaded pile foundations in sands is provided in this chapter. The p-y method is explained briefly with the derivation of the governing differential equation for a laterally loaded pile. After that, published p-y curves for sands are listed. The different components of p-y curves, the ultimate soil resistance and the initial modulus of subgrade reaction,

are also discussed. Next, the typical design standards are compared for differences. Finally, a summary is presented for research studies involving field tests, 1-g scale model tests, centrifuge model tests, and finite element models.

3. **Database for Lateral Load Tests on Monopiles in Sand:** This chapter presents a lateral load test database of monopiles in sand that is compiled as part of the research. The chapter mentions the method of data collection and organization. Finally it presents some summary statistics about the tests in the database and the tests chosen for closer study.

4. **Site Descriptions:** This chapter discusses the site characterization of the different test sites chosen for further analysis. Details about soil stratigraphy, in-situ testing, and pile installation are provided. his chapter details the steps involved in collecting disturbed sand samples from Mustang Island, TX. The potential for future testing is discussed.

5. **Analysis:** The chapter on analysis deals with looking at the measured versus the API predicted response of a few important load tests. A sensitivity study is done on the effect of initial stiffness modulus (k) on the small strain response of the pile for both monotonic and cyclic tests. Additionally, the effect of base shear is investigated for the short-rigid behaving piles. For the cyclic tests, results from their original literature source is included and discussed in this chapter.

6. **Conclusions:** The conclusions based on observations and analyses presented in the previous chapters are presented in this chapter. A short section on the recommended future work is presented.

Chapter 2

Literature Review

Before any ideas can be had about an efficient foundation design, a thorough review of the past research about laterally loaded piles is important. This section reviews the p-y method for analyzing laterally loaded piles as well as the codes and standards that are currently based on it for the design of laterally loaded piles in sands - the American Petroleum Institute (API) and the Det Norske Veritas (DNV)standards . Slight differences between older versions of the codes and the latest versions are highlighted.

2.1 p-y Method

There are many methods with which to analyze the behavior of laterally loaded piles. Some of the more widely used ones are limit analyses, theories of elasticity and plasticity, the p-y method and finite-element (FE). This thesis focuses only on the p-y method for sands.

The p-y method is the most commonly used method of analyzing laterally loaded piles in practice. The method was first suggested by McClelland and Focht (1958). The p-y method was developed originally from proprietary research sponsored by the petroleum industry in the 1950s and 1960s. At the

time, large piles were being designed for to support offshore oil production platforms that were to be subjected to exceptionally large horizontal forces from storm waves and wind. Rules and recommendations for the use of the p-y method for design of such piles are presented by the API (2011) and DNV-GL (2016).

The model shown in Figure 2.1 represents a generic representation of the p-y method. The loading on the pile is two-dimensional consisting of shear, overturning moment, and axial thrust. The soil around the pile is replaced by a set of nonlinear springs that represent the soil resistance p as a nonlinear function of pile deflection y. The nonlinear springs and the corresponding curves that model their behavior are widely spaced in the figure, but are actually spaced at every nodal point on the pile. The p-y curves are nonlinear with respect to depth x along the pile and lateral deflection y.

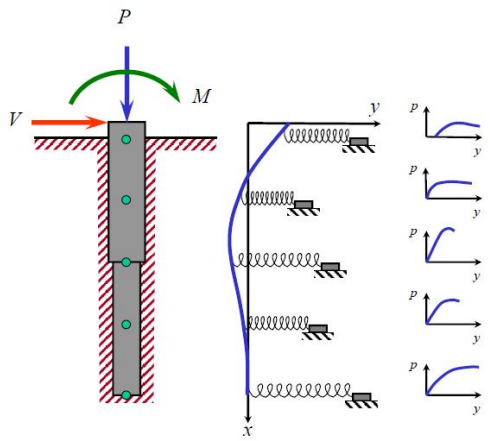

Figure 2.1: Example of a laterally loaded pile and corresponding p-y curves (Isenhower and Wang, 2016a)

The sketch in Figure 2.2a shows a uniform distribution of radial stresses normal to the wall of a non-displaced cylindrical pile. This distribution of stresses is correct for a pile that has been installed without bending. If the pile is displaced a distance y (the amount of the displacement is exaggerated in the sketch for clarity), the distribution of stresses becomes non-uniform and will be similar to that shown in Figure 2.2.b. The stresses will have decreased on the backside of the pile and increased on the front side. Integration of the unit stresses around the perimeter of the pile results in the lateral load intensity p, which acts opposite to the direction of pile displacement y. The dimensions of p are force per unit length of the pile. These definitions of p and y are convenient in the solution of the differential equation and are consistent with those used in the solution of the elastic beam equation (Isenhower and Wang, 2016a).

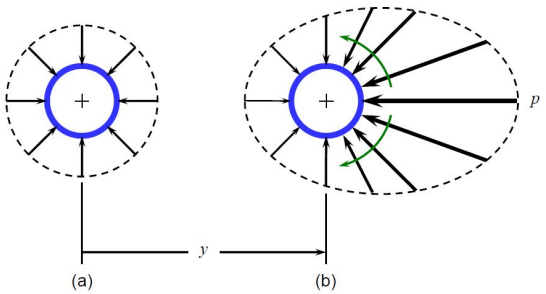

Figure 2.2: Distribution of Stresses Acting on a Laterally Loaded Pile, (a) Before Deflection and (b) After Deflection y (Isenhower and Wang, 2016a)

2.1.1 Derivation of the p-y Model

To understand the p-y method it is important to understand the governing differential equation that it attempts to solve. The derivation of that equation is described in this section as given in the LPILE Technical Manual (Isenhower and Wang, 2016a):

The derivation of the differential equation for a beam-column foundation was presented by Hetényi (1946). There is an assumption that a bar on an elastic foundation is subjected not only to the vertical loading, but also to the pair of compressive forces P_x acting at the centroid of the end cross-sections of the bar. From the equilibrium of moments (ignoring second-order terms), we get the equation (Figure 2.3):

$$(M + dM) - M + P_x\ dy - V_v\ dx = 0 \tag{2.1}$$

where: P_x = axial thrust load in the pile,

y = lateral deflection of the pile at a point x along the length of the pile,

p = soil reaction per unit length,

EI = flexural rigidity

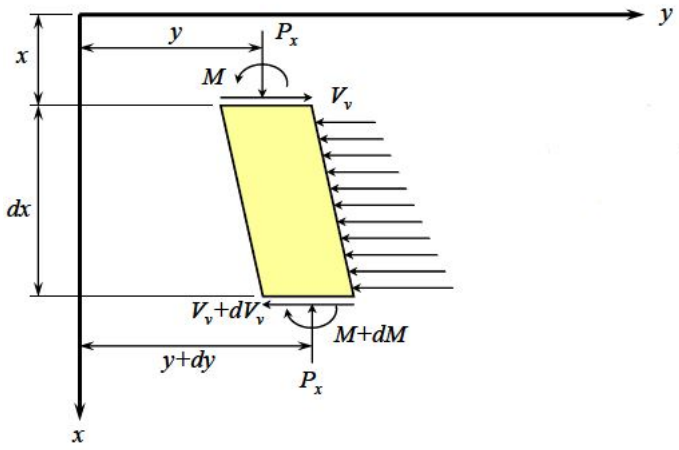

Figure 2.3: Element of Beam Column after Hetényi (1946) as presented in Isenhower and Wang (2016a)

Differentiating Equation 2.1 with respect to x, the following equation is obtained:

$$\frac{dM}{dx} + P_x \frac{dy}{dx} - V_v = 0 \tag{2.2}$$

The following definitions are important and substituted into the above equation (2.2):

$$\frac{d^2M}{dx^2} + P_x \frac{d^2y}{dx^2} - \frac{dV_v}{dx} = 0 \tag{2.3}$$

$$\frac{d^2M}{dx^2} = EI \frac{d^4y}{dx^4} \tag{2.4}$$

$$\frac{dV_v}{dx} = p \tag{2.5}$$

$$p = -E_s \, y \tag{2.6}$$

where E_s is equal to the secant modulus of the soil-response curve. On substitution into Equation (2.2) we get:

$$EI\ \frac{d^4y}{dx^4} + P_x\ \frac{d^2y}{dx^2} + E_s\ y = 0 \tag{2.7}$$

This is the general differential equation for a p-y analysis. An analytical solution is possible upon making some assumptions, but a more general solution can be obtained by using the Finite-Difference numerical technique to solve it. This is the method that is employed by LPILE (Isenhower and Wang, 2016a).

2.2 p-y Models for Sands

For the p-y method to produce accurate results, it is necessary to accurately represent the mobilization of soil resistance against a laterally loaded pile. Ideally, mobilized soil resistance versus lateral displacement curves or p-y curves should be obtained by carrying out a load test on an instrumented pile. Since the p-y curves are functions of the pile-soil system rather than a property of the soil alone, these test piles would have to be of the same scale as the production piles and they should be installed at the same site in the same way. In situ tests on instrumented piles are expensive and not financially feasible for relatively small construction projects. Therefore, models of p-y curves that can be adapted for use with different types of soils based on more readily measurable soil properties are available as design guidelines. The Reese et al. (1974) and Murchison and O'Neill (1984) models are some p-y models that have been widely accepted and used in the industry for sands.

Most of the published p-y curves have these three common attributes, which are discussed in further detail in the next sections:

1. Initial stiffness or the initial slope of the curve.

2. Ultimate capacity. which is asymptotic to the p-y curve or is an upper bound.

3. Shape of the curve between the initial response and the ultimate capacity.

2.2.1 Reese et al. (1974) Model

The Reese et al. (1974) method of analyzing laterally loaded piles is presented here. This was the original method that the future API method stemmed from and has a historical significance. This model was based on the Mustang Island Field Tests performed in 1974 as described in Cox et al. (1974).

The shape of the p-y curves computed using this procedure is shown in Figure 2.4.

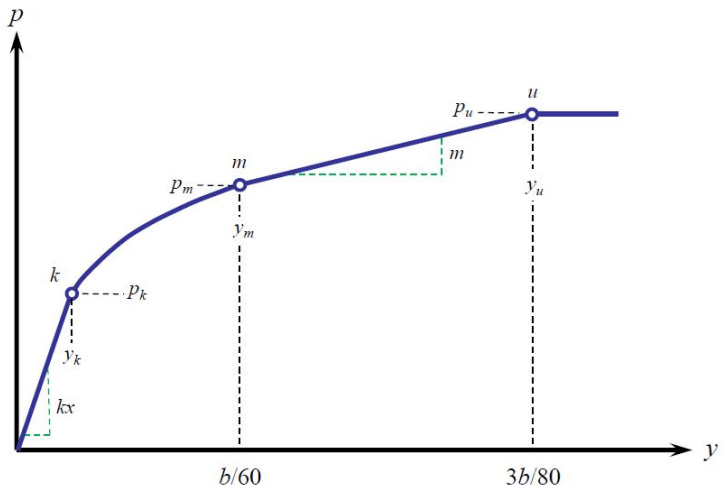

Figure 2.4: Characteristic Shape of p-y Curves for Static and Cyclic Loading Sand as per Reese et al. (1974) procedure

The procedure is as follows (Isenhower and Wang, 2016a; Reese et al., 1974):

1. Obtain values for the depth of the p-y curve x, angle of internal friction, effective unit weight of soil γ, and pile diameter b (Note: use effective unit weight for sand below the water table and total unit weight for sand above the water table).

2. Compute the following parameters:

$$\alpha = \frac{\phi}{2}, \beta = 45^o + \frac{\phi}{2}, K_o = 0.4, K_A = tan^2\left(45^o - \frac{\phi}{2}\right) \tag{2.8}$$

3. Compute the ultimate soil resistance per unit length of pile, p_s, using the smaller of p_{st} or p_{sd}:

$$p_s = min[p_{st}, p_{sd}] \tag{2.9}$$

where:

$$p_{st} = \gamma x \left[\frac{K_o x tan\phi sin\beta}{tan(\beta - \phi)cos\alpha} + \frac{tan\beta}{tan(\beta - \phi)}(b + x tan\beta tan\alpha) + K_o x tan\beta(tan\phi sin\beta - tan\alpha) - K_A b \right] \tag{2.10}$$

$$p_{sd} = K_A b\gamma x(tan^8\beta - 1) + K_o b\gamma x tan\phi tan^4\beta \tag{2.11}$$

4. Compute the y value defining point u using

$$y_u = \frac{3b}{80} \tag{2.12}$$

5. Compute p_u defining point u for static loading conditions using

$$p_u = \overline{A_s}\, p_s \tag{2.13}$$

or for cyclic loading conditions using

$$p_u = \overline{A_c}\, p_s \tag{2.14}$$

6. Obtain the appropriate value of $\overline{A_s}$ or $\overline{A_c}$ from Figure 2.5 as a function of the nondimensional depth and type of loading (either static or cyclic). Compute p_s using the appropriate equation, either Equation 2.10 or Equation 2.11.

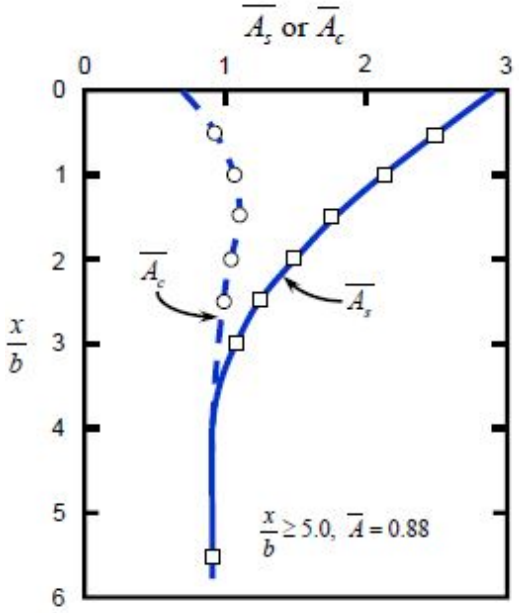

Figure 2.5: Values of Coefficients $\overline{A_s}$ and $\overline{A_c}$ for Cohesionless Soils (Isenhower and Wang, 2016a)

7. Compute the y-value at point m using

$$y_m = \frac{b}{60} \tag{2.15}$$

   Compute p_m at point m for static loading conditions using

$$p_m = B_s\, p_s \tag{2.16}$$

   or for cyclic loading conditions using

$$p_m = B_c\, p_s \tag{2.17}$$

8. Obtain the appropriate value of B_s or B_c from Figure 2.6 as a function of the nondimensional depth and the type of loading (either the static

or cyclic). Use the appropriate equation for p_s. The two straight-line portions of the p-y curve, beyond the point where y is equal to b/60, can now be determined.

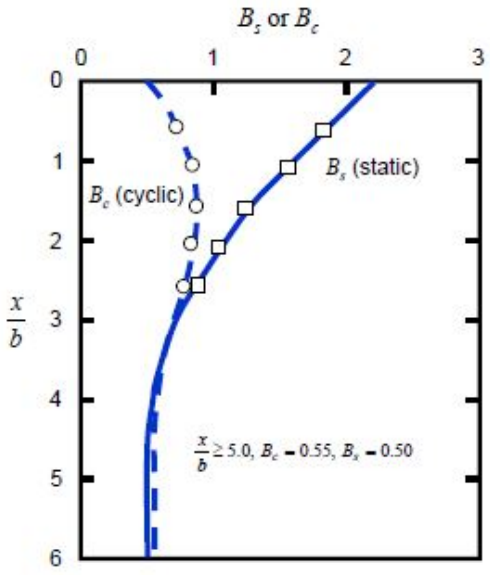

Figure 2.6: Values of Coefficients B_s and B_c for Cohesionless Soils (Isenhower and Wang, 2016a)

9. Establish the initial straight-line portion of the p-y curve,

$$p = (k\,x)\,y \tag{2.18}$$

Use the appropriate value of k from Table 2.2 or Table 2.1.

10. Fit the parabola between point k and point m as follows: a. Compute the slope of the p-y curve between point m and point u using

$$m = \frac{p_u - p_m}{y_u - y_m} \tag{2.19}$$

Table 2.1: Representative Values of k for Fine Sand Below the Water Table for Static and Cyclic Loading (Isenhower and Wang, 2016a)

Recommended k	Relative Density		
	Loose	Medium	Dense
MN/m^3 (pci)	5.4 (20.0)	16.3 (60.0)	34.0 (125.0)

Table 2.2: Representative Values of k for Fine Sand Above the Water Table for Static and Cyclic Loading (Isenhower and Wang, 2016a)

Recommended k	Relative Density		
	Loose	Medium	Dense
MN/m^3 (pci)	6.8 (25.0)	24.4 (90.0)	61.0 (225.0)

b. Compute the power of the parabolic section using

$$n = \frac{p_m}{m y_m} \tag{2.20}$$

c. Compute the coefficient C using

$$\overline{C} = \frac{p_m}{y_m^{\frac{1}{n}}} \tag{2.21}$$

11. Compute the y value defining point k using

$$y_k = \left(\frac{\overline{C}}{kx} \right)^{\frac{n}{n-1}} \tag{2.22}$$

Compute the p value defining point k using

$$p_k = k\, x\, y_k \tag{2.23}$$

12. Compute p-values along the parabolic section of the p-y curve between points k and m using

$$p = \overline{C}\, y^{\frac{1}{n}} \tag{2.24}$$

Note that the curve in Figure 2.4 is drawn as if there is an intersection between the initial straight-line portion of the p-y curve and the parabolic portion of the curve at point k. However, in some instances there may be no intersection with the parabola. Equation 3-61 defines the p-y curve until there is an intersection with another portion of the p-y curve or if no intersection occurs, Equation 2.18 defines the complete p-y curve. If y_k is in between points y_m and y_u, the curve is tri-linear and if y_k is greater than y_u, the curve is bilinear as shown in Figure 2.7.

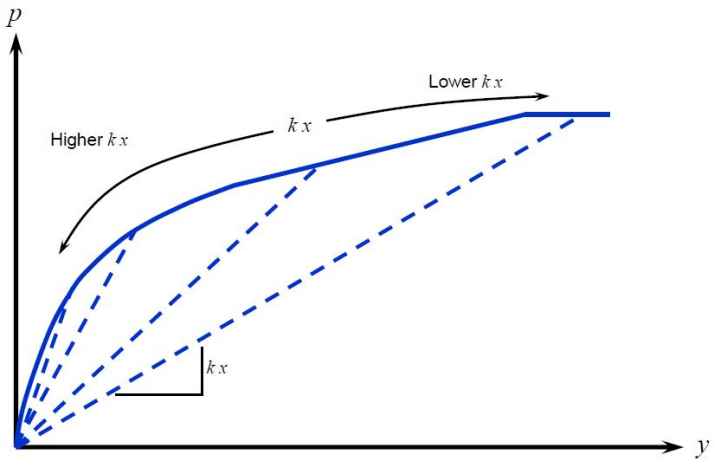

Figure 2.7: Effect of k on p-y curve in Sand (Isenhower and Wang, 2016a)

2.2.2 API RP 2A Model

This procedure is recommended by the American Petroleum Institute in its manual for recommended practice for designing fixed offshore platforms (API RP 2A, 2010).

The API procedure for p-y curves in sand was based on a number of field experiments. A survey of the available information of p-y curves for sand was made by ONeill and Murchison (1983), and some changes were suggested in the procedure given in the Reese et al. method. Their suggestions were submitted to the American Petroleum Institute and modifications were adopted by the API review committee.

A point to note would be that there is no difference for ultimate resistance (p_u) between the Reese et al. criteria and the API procedure. The API method uses a hyperbolic tangent function for computation of the curve. The main difference between those two criteria will be the initial modulus of subgrade reaction and the shapes of the curves.

The following procedure is for both short-term static loading and for cyclic loading as described in API RP2A (2010):

1. Obtain values for the angle of internal friction ϕ , the effective unit weight of soil, γ, and the pile diameter b.

2. Compute the ultimate soil resistance at a selected depth x. The ultimate lateral bearing capacity (ultimate lateral resistance p_u) for sand has been

found to vary from a value at shallow depths determined by Equation 2.25 to a value at deep depths determined by Equation 2.26. At a given depth, the equation giving the smallest value of p_u should be used as the ultimate bearing capacity. The value of p_u is the lesser of p_u at shallow depths, p_{us}, or p_u at great depth, p_{ud} , where:

$$p_{us} = (C_1 x + C_2 b)\gamma' x \tag{2.25}$$

$$p_{ud} = C_3 b \gamma' x \tag{2.26}$$

where p_u = ultimate resistance (force/unit length), lb./in. (kN/m),

γ' = effective unit weight, pci (kN/m3),

x = depth, in. (m),

b = average pile diameter from surface to depth, in. (m).

ϕ' = angle of internal friction of sand, degrees,

C_1, C_2, C_3 = coefficients determined from Figure 2.8 as a function of ϕ':

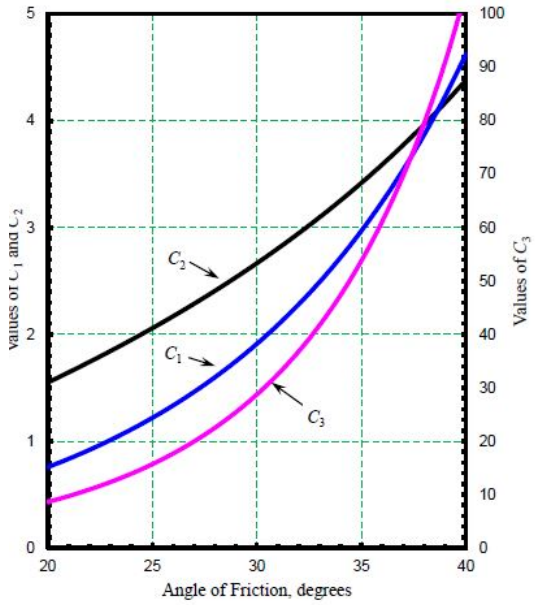

Figure 2.8: Effect of k on p-y curve in Sand (Isenhower and Wang, 2016a)

3. Compute the load-deflection curve based on the ultimate soil resistance p_u which is the minimum value of p_u calculated previously. The lateral soil resistance-deflection (p-y) relationships for sand are nonlinear and, in the absence of more definitive information, may be approximated at any specific depth x by the following expression:

$$p = Ap_u tanh\left(\frac{kx}{Ap_u}y\right) \tag{2.27}$$

where A = factor to account for cyclic or static loading. Evaluated by:

$$A = 0.9 \quad \text{for cyclic loading} \tag{2.28}$$

$$A = \left(3.0 - 0.8\frac{x}{b}\right) \quad \text{for static loading} \tag{2.29}$$

p_u = smaller of values computed from Equation 2.25 or 2.26, lb./in. (kN/m), k = initial modulus of subgrade reaction, pci (kN/m3). Determine k from Figure 2.9 as a function of angle of internal friction, ϕ' y = lateral deflection, in. (m), and x = depth, inches (m).

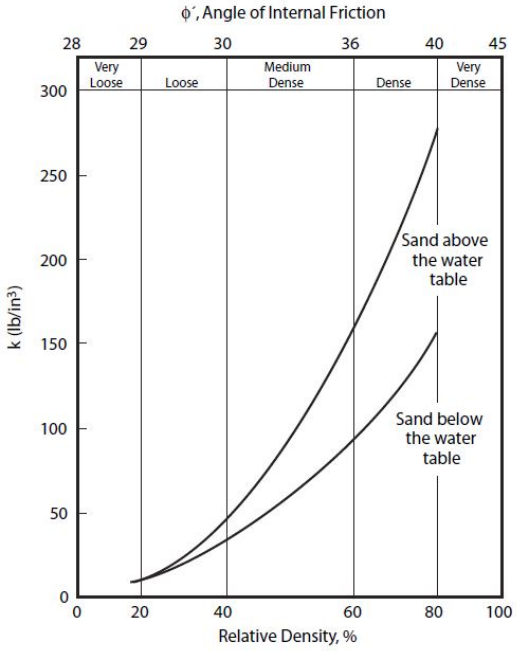

Figure 2.9: Value of k for API Sand Procedure (API, 2010)

2.2.3 API RP 2GEO

The API RP 2GEO (2011) is the latest improvement on the API code. With regard to lateral capacity of piles in sand there were two key differences from the API RP 2A (2010):

1. The curves giving the C_1, C_2 and C_3 coefficients are extended upto 42

degrees (Figure 2.10). In the previous version, these could be taken from the chart only upto 40 degrees (Figure 2.8).

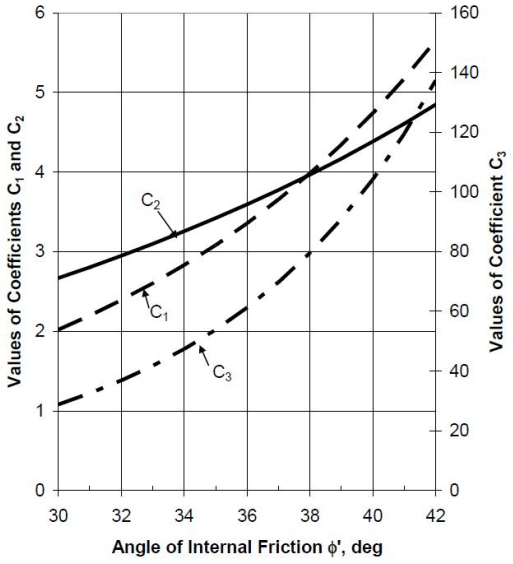

Figure 2.10: Coefficients C_1, C_2 and C_3 as function of $\phi^{'}$ (API, 2011)

2. The other major difference between API (2010) and API (2011) is that the newer version removed the curve to calculate the k using internal angle of friction $\phi^{'}$ (Figure 2.9) and replaced it with Table 2.3 which gives the value of k at discrete friction angles with no specification of the role of ground water table. Judging from the values, the water table is assumed to be high.

Table 2.3: k values as specified by API (2011)

ϕ'	k	
$degrees$	MN/m^3	lb/in^3
25	5.4	20
30	11	40
35	22	80
40	45	165

2.2.4 DNV GL - ST - 0126 - 2016

The other major design standard for laterally loaded piles in sands is the DNV-GL (2016). In its most updated form, the following specifications are given:

1. The exact procedure to obtain the p-y curves matches the one given in the API RP 2A (2010).

2. Use of p-y curves for design of piles with diameters of more than 1.0 m (for example monopiles) is recommended to be validated for such use, e.g. by means of FE analysis.

3. For offshore monopiles, in addition, another tolerance is usually specified which is an upper limit for the accumulated permanent rotation of the pile head due to the history of Serviceability Limit State loads applied to the monopile throughout the design life. The accumulated permanent rotation subject to meeting this tolerance usually results from permanent

accumulated soil deformations caused by cyclic wave and wind loads about a non-zero mean.

2.2.5 LPILE ver 9.0 2016 (Isenhower and Wang, 2016a)

On going through the LPILE technical manual (Isenhower and Wang, 2016a), certain differences and additional information were found with regards to the methods of analysis. These points are summarized here briefly -

1. Figure 2.11 which gives the k for different friction angles and relative densities has been corrected and differs from a similar figure presented in API RP-2A (Figure 2.9).

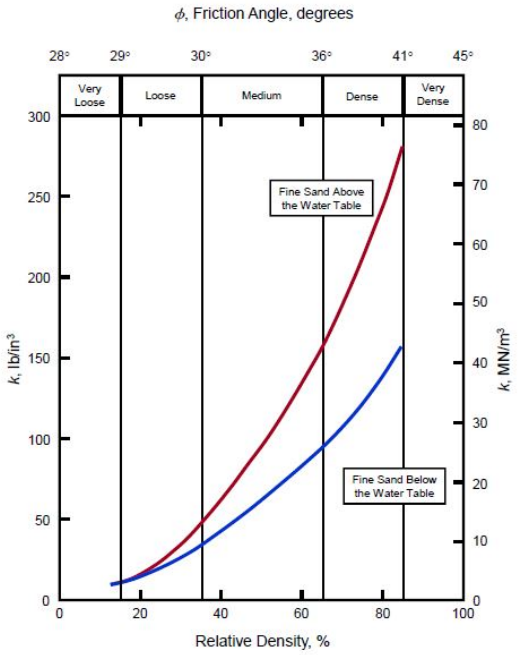

Figure 2.11: Value of k for API Sand Procedure as per Isenhower and Wang (2016a)

The positions of the labels for relative density on the bottom axis have moved to their correct positions, the label for friction angle at the division line between dense and very dense sand has be corrected to the correct value of 41 degrees, and the scale in SI units has been added.

2. The value of k is determined from the angle of friction and it is assumed that the sand is fine. The equations used by LPILE to determine k as a function of friction angle for fine sand are shown in Figure 2.12. "Whether the sand is above or below the water table will be determined from the input value of effective unit weight. If the effective unit weight is less than 77.76 pcf (12.225 kN/m3) the sand is considered to be below the water table. If the input value of is greater than 45 degrees, a k value corresponding to 45 degrees is used by LPILE. The two correlation lines intersect at a friction angle value of 27.6423 degrees and a k value of 10.2068 pci. If the input value of is less than 27.6423 degrees, the value of k linearly varies from a value of zero at zero degrees to a value of 10.2068 pci at 27.6423 degrees." (Isenhower and Wang, 2016a)

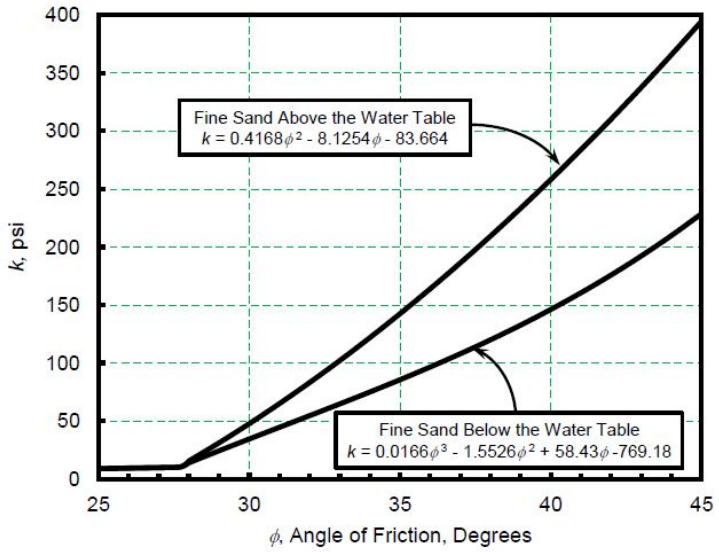

Figure 2.12: Equations for k for the API Sand Procedure as defined by LPILE Isenhower and Wang (2016a)

3. A comment about using a higher k value is mentioned. "If the sand profile is coarse or well-graded sand, the user may consider using a higher value of k that those suggested in the tables above. While experimental data for k in well graded sands is poorly documented, use of values 10 to 50 percent higher may be appropriate in dense and very dense well-graded sands that do not contain any compressible minerals such as mica." (Isenhower and Wang, 2016a)

4. The original equations for C1, C2 and C3 are given in the technical manual along with the graph. These equations have not been mentioned in any of the design standards. Only the curve is mentioned (Figure 2.8).

   These factors were developed as follows (Isenhower and Wang, 2016a):

Two models are used for computing the ultimate resistance for piles in sand. The first of the models for the soil resistance near the ground surface is shown in Figure 2.13. The total lateral force F_{pt} (Figure 2.13c) may be computed by subtracting the active force F_a, computed by use of Rankine theory, from the passive force F_p, computed for the model by assuming that the Mohr-Coulomb failure condition is satisfied on vertical wedge side planes defined by ADE and BCF, and on the sloping wedge surface defined by AEFB in Figure 2.13a. The directions of the resultant forces are shown in Figure 2.13b. Solutions other than the ones shown here have been developed by assuming a friction force on the pile-soil interface surface defined by DEFC (assumed to be zero in the analysis shown here) and by assuming the water table to be within the wedge (the unit weight is assumed to be constant in the analysis shown here).

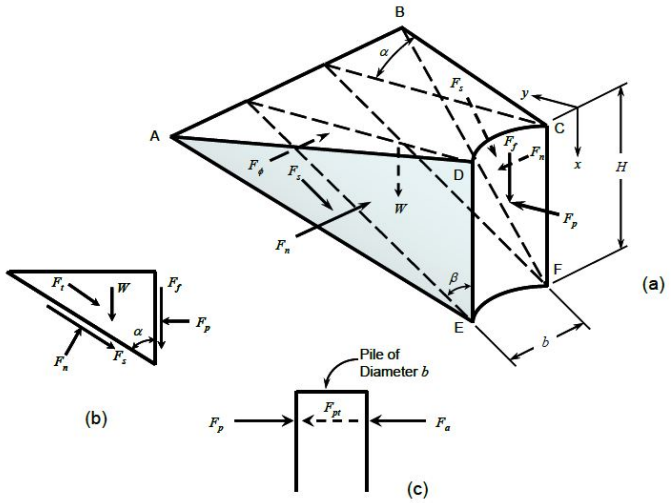

Figure 2.13: Geometry Assumed for Passive Wedge Failure for Pile in Sand (Isenhower and Wang, 2016a)

Summing the forces in the vertical direction yields:

$$F_n sin\alpha = W + F_s cos\alpha + 2F_t cos\alpha + F_f \tag{2.30}$$

where:

α = angle of the inclined plane with the vertical,

W = Weight of the wedge,

F_s = resultant shear force on the inclined plane

F_t = resultant shear force on a side plane

F_f = frictional force between the wedge and the pile The expression for W is

$$W = \gamma \frac{bH^2}{2} tan\alpha \tag{2.31}$$

where:

γ = unit weight of soil,

b = diameter of pile,

H = depth of wedge.

On proper substitution, F_{pt} is:

$$F_{pt} = \gamma H^2 \left[\frac{K_o H tan\phi tan\beta}{3tan(\beta - \phi)cos\alpha} + \frac{tan\beta}{tan(\beta - \phi)} \left(\frac{\beta}{2} + \frac{H}{3} tan\beta tan\alpha \right) \right] + \gamma H^2 \left[\frac{K_o H tan\beta}{3} (tan\phi sin\beta - tan\alpha) - \frac{K_A}{2} \right] \tag{2.32}$$

where:

β = angle of the wedge with the ground surface,

K_o = coefficient of earth pressure at rest,

K_A = coefficient of active earth pressure.

The ultimate soil resistance near the ground surface per unit length of the pile is obtained by differentiating Equation 2.32 with respect to depth.

$$p_{us} = \gamma H \left[\frac{K_o H tan\phi sin\beta}{tan(\beta - \phi) cos\alpha} + \frac{tan\beta}{tan(\beta - \phi)} (b + Htab\beta tan\alpha) \right] + \gamma H [K_o H tan\beta (tan\phi sin\beta - tan\alpha) - K_A b] \quad (2.33)$$

Bowman (1958) performed laboratory experiments with careful measurements and suggested values of α from $\phi/3$ to $\phi/2$ for loose sand and up to ϕ for dense sand. The value of β is approximated by $45^o + \phi/2$

The model for computing the ultimate soil resistance at some distance below the ground surface is shown in Figure 2.13a. The stress 1 at the back of the pile must be equal or larger than the minimum active earth pressure; if not, the soil could fail by slumping. The assumption is based on two-dimensional behavior; thus, it is subject to some uncertainty. If the states of stress shown in Figure 2.14b are assumed, the ultimate soil resistance for horizontal movement of the soil is

$$p_{ud} = K_A b \gamma H (tan^8\beta - 1) + K_o b \gamma H tan\phi tan^4\beta \quad (2.34)$$

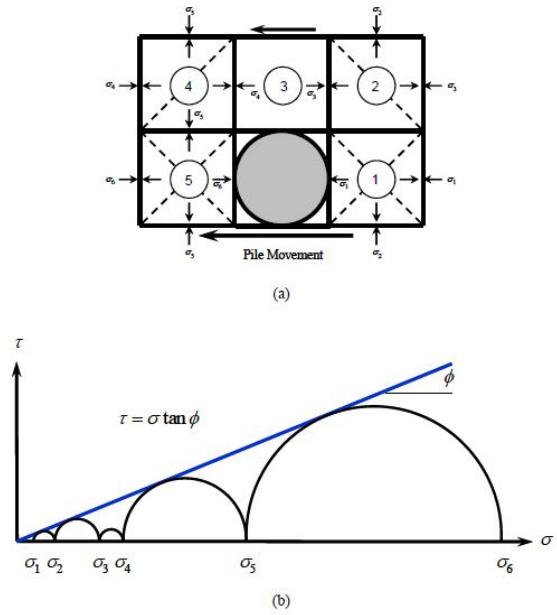

Figure 2.14: Assumed Mode of Soil Failure by Lateral Flow Around Pile in Sand, (a) Section Though Pile, (b) Mohr-Coulomb Diagram (Isenhower and Wang, 2016a)

Comparing with the equations for p_{us} and p_{ud} given in Section 2.2.2 we get:

$$C_1 = tan\beta\left\{K_p tan\alpha + K_o\left[tan\phi sin\beta\left(\frac{1}{cos\alpha}+1\right) - tan\alpha\right]\right\} \tag{2.35}$$

$$C_2 = K_p - K_A \tag{2.36}$$

$$C_3 = {K_p}^2(K_p + K_o tan\phi) - K_A \tag{2.37}$$

where:

$$K_p = tan^2\left(45^o + \frac{\phi}{2}\right) \tag{2.38}$$

$$K_o = 0.4 \tag{2.39}$$

2.2.6 Summary of Methods

A short summary of the different methods and standards of p-y analysis are given here:

1. **Reese et al. (1974)** - The original basis for the present design standard. This method is calibrated for long slender piles of relatively short diameters. The initial stiffness is modelled as linear.

2. **API (2010)** - An older version of the current design standard for laterally loaded piles. This is based on the research done by Murchison and O'Neill (1984). The curve follows a hyperbolic tangent function. A chart is provided to obtain the initial stiffness based on the friction angle of the sand (limited to 40 degrees) (Figure 2.9).

3. **API (2011)** - The latest version of the API design standard - the API RP 2GEO. The chart previously mentioned has been replaced with a table of discrete friction angles and k values. There is also no mention of the change of k due to presence of the water table.

4. **DNV-GL (2016)** - Another popular design standard. It follows the same procedure as the API RP 2A (2010). There are a few comments about large diameter piles and advanced analysis such as finite element modeling is recommended. No other descriptive information is provided towards design.

5. **LPILE ver 9.0 2016 (Isenhower and Wang, 2016a)** - The p-y analysis is done using a finite difference solver LPILE by ENSOFT. The technical manual for the software is highly descriptive with additional equations (such as for coefficients C1, C2 and C3; and the k value correlated to friction angle). Some comments about taking a higher k value for granular dense sands is mentioned. It is valuable to note that LPILE computes k values upto 45 degrees unlike the other standards. This is vital for sites with highly dense sand sites.

2.3 Overview of Offshore Monopile Research in Sands

A considerable amount of literature is reviewed to attempt to understand how the current API standard for laterally loaded piles in sands performs for the design of large diameter relatively short monopiles. Many types of analyses were performed in the literature and these have been characterized into 4 categories Field Load Tests, 1-g Model Laboratory Tests, Centrifuge Model Tests, Finite Element Analyses. Depending on the type of analyses, various inferences are drawn. These are summarized in the following subsections for each type of research methodology.

2.3.1 Field Testing

There are not many field tests that have been documented in published literature for studying offshore monopiles in sands. An important test series that is available is the one done in Ireland by the University College Dublin

(UCD). Through multiple publications (Doherty et al., 2012b,a; Doherty and Gavin, 2011; Murphy et al., 2016, 2012; Li et al., 2015) the two test sites (Blessington and Garryhesta) have been well characterized in terms of geotechnical properties. Also, a variety of load tests on small-diameter but low L/D ratio steel pipe piles have been conducted. These include both monotonic and cyclic load testing. Tests were also run to check the effect of wings on monopiles to increase the stiffness of the response. The monotonic tests find that the conventional API approach overestimates the stiffness of the piles initially and underestimates the ultimate load resistance. The cyclic tests find that there is a stiffening of the response as the cycles are run, with greater stiffening of response if the cycles are run at a higher amplitude.

In Europe, to develop a new design method for offshore wind turbine monopiles, a large joint industry project, PISA (PIle Soil Analysis) was established. The project involves three sections of work including (a) the development of a new design methodology (Byrne et al., 2015b) (b) numerical modeling from which the design method is developed (Zdravković et al., 2015) and finally (c) field testing (Byrne et al., 2015a) to provide data against which new methods can be assessed and validated. The focus of the work is for monotonic loading, but future phases is said to explore design for cyclic loading. For the lateral load tests, Dunkirk, a dense sand site is considered in northern France.

2.3.2 1-g Model Testing

A large quantity of research has been published on 1-g model testing of offshore monopiles in sands.

Yan and Byrne (1992) talks about a testing method similar to the centrifugal testing called Hydraulic Gradient Similitude (HGS). It is a way to increase the soil stress level in a model to simulate field stress condition by using the seepage forces rather than the centripetal forces. Comparison between the experimental p-y curves and those recommended by the API shows that the API code gives a stiffer P-y curve than observed at small deflections, whereas at large deflection the API curve reaches an ultimate soil resistance that is lower than the experimental data.

Lada et al. (2014) says that contrary to the recommended practice, where the ultimate capacity is degraded, the results of small scale tests show that the soil become stronger due to the cyclic loading.

Nicolai et al. (2015) provides the results of an experimental investigation aimed at studying the long-term variation of the stiffness of a soil-pile system in dense sand. The setup used for carrying out the tests was a 1g testing rig at Aalborg University, Denmark. There is an increase of stiffness with increase in number of cycles with almost half of the total stiffness increase occurring within the first hundred cycles

The paper by Abadie et al. (2015) presents a series of laboratory floor model tests exploring pile response under multi amplitude cyclic loading, rep-

resenting storm loading on the pile. It was observed that the pile rotation appears to reach a limiting value following a series of maximum storm type loads.

A series of tests performed on a model monopile to understand its response under long-term repeated lateral loading is described by Arshad and OKelly (2016). The test results show that the cyclic stiffness of the soilpile system always increased under repeated lateral loading, whereas the absolute secant stiffness always has a decreasing trend due to the continuous accumulating rotation of the pile.

LeBlanc et al. (2010) describes a series of tests that were conducted on small-scale driven piles subjected to long-term cyclic loading. A complete non-dimensional framework for stiff piles in sand is presented and applied to interpret the test results. The accumulated rotation of a stiff pile is largely affected by the characteristics of the applied cyclic load. For example, results for one-way loading were found to differ by a factor of four as compared with two-way loading. A very significant result is that the most onerous loading condition was found to be between one-way and two-way loading. The tests showed that cyclic loading always increased the pile stiffness, and the increase is found to be independent of relative density.

Chen et al. (2015) describes six model tests on an instrumented rigid model pile in Qiantang River silt that was subjected to lateral cyclic loading with different cyclic ratios for 5000-10000 cycles. The accumulated displacement is said to be closely related to the cyclic load ratio and has no obvious

relationship with soil density. The first 10 cycles (of shearing stage) has the largest influence on the cyclic responses of the rigid monopile under cyclic loading, rather than the subsequent densification stage.

Lin et al. (2014) describes advanced sensors, including thin tactile pressure sensors, shape acceleration arrays, and in-soil null pressure sensors to analyze the pressure around a model steel-pipe pile as it is laterally loaded. The measurement-based p-y curves at different depths along the pile length shows nonlinear behavior, with the initial slope (initial stiffness) and ultimate soil reaction increasing as the depth increases. Also, the changes in soil horizontal stresses measured using the in-soil null pressure sensors shows that the pressure contours formed a pressure wedge with a bulb shape around the pile.

Hanssen and Eiksund (2014) describes a model pile test using a dynamic frequency analysis. The soil stiffness contribution to the pile-soil interaction stiffness is indicated to be underestimated by a factor of 2.2 by the API p-y curves.

Static and cyclic behavior of laterally loaded piles in dry sand is investigated by Qin and Guo (2016), through instrumented model tests,and theoretical analysis using elastic-plastic solutions.The accumulated pile displacement increases with increasing numbers of cycles but at a decreasing rate during the cyclic loading.

2.3.3 Centrifuge Model Testing

This subsection lists out the relevant past literature on offshore monopiles in sands conducted using centrifuge model testing.

Klinkvort et al. (2010) describes centrifuge model tests at the Technical University of Denmark. They talk about both monotonic as well as cyclic load tests in the centrifuge. The monotonic tests reveal a relationship between the lateral bearing capacity of the pile and the load eccentricity. This In practice this may be of importance for offshore wind turbines subjected to a combination of wind load from the rotor acting 60 - 100 m above seabed level and wave forces acting relatively closer to the seabed. The centrifuge modeling indicates that using the design code recommendations to generate p-y curves led to an overestimation of the pile - soil stiffness. From all the cyclic tests, accumulations of deflections were seen. The secant stiffness of every cycle reveals that the cyclic loading leads to an increase in secant stiffness. From the centrifuge tests it is said that no reduction of the bearing capacity of dry sand occurs due to cyclic loading.

Zakeri et al. (2016b) describes an extensive study involving physical model testing of a pile in a centrifuge. Soil p-y models for conductors installed in medium-dense sands are shown. The model relies on the cyclic response of degraded soil at the steady-state condition and provides the fatigue life predictions with high accuracy.

Georgiadis et al. (1992) talks about centrifuge tests on steel piles under monotonic loading. The measured pile responses demonstrates that existing p-y curves underestimated the bending moments developed along the pile and especially the pile head displacement.

Kirkwood and Haigh (2014) talks about how the cyclic loading ratio of lateral loads applied to the monopile can change the stiffness of the soil surrounding the pile. According to their results, this change of stiffness can allow for increasing pile head displacement and rotation as the cyclic loading ratio falls below zero due to the reduction of locked in stresses caused by a reversal in the loading direction. A considerable change in system stiffness and therefore natural frequency was observed.

Alderlieste (2011) and Alderlieste et al. (2011) describe a series of centrifuge model tests run on offshore monopiles in sands at Delft University, Netherlands. They say that the pile response is affected by both pile diameter as well as load eccentricity. An increase in pile diameter leads to an increase in static capacity. The secant and tangent stiffness from cyclic load tests also increase significantly with increasing pile diameter.

Li et al. (2010) describes a series of force-controlled one-way cyclic lateral load tests conducted on a model of a large diameter mono-pile in the centrifuge at Cambridge University. The force-controlled one-way cyclic lateral loads induce significant accumulated permanent pile lateral displacements. There is a dramatic increase in the pile lateral secant cyclic stiffness (Ks) in the first cycle, and thereafter Ks increases slightly with the increasing number

of load cycles.

In the study by Bae et al. (2015), a static and cyclic loading test conducted laterally by varying the relative density of the sands is described. The tests are performed in a centrifuge. For the higher relative densities, the API (2010) method overpredicts the initial stiffness for monotonic loading. It is shown that the initial slope and ultimate soil resistance of test results tend to be larger than that of API (2010) cyclic p-y curve predictions.

Choo et al. (2013) and Choo and Kim (2015) describe the lateral response of large diameter monopiles in the centrifuge tests. According to their results, the lateral load - lateral displacement relationship estimated by API (2010) and Reese et al. (1974) py analyses underestimates the lateral displacement and moments for a given lateral load i.e. overestimate the initial stiffness of the pile.

2.3.4 Finite Element Modeling

Multiple studies have been published which present finite element models for analyzing the response of a large diameter OWT monopile foundation in sands.

Yang et al. (2016) describes a numerical study to simulate the monotonic lateral response of a monopile driven in dense sands and found that the API p-y model overestimates the initial stiffness of ground soil at deeper depth for larger diameter monopiles.

According to Versteijlen et al. (2014), when using the in situ measured

(Seismic Cone Penetration Tests) small-strain shear modulus in a global 3D model, the monotonic analyses indicated smaller mudline displacements than the ‘p-y curve approach dictated by the API method.

Sahasakkul et al. (2016) also says that using the API relations results in an overestimation of the initial lateral loading stiffness and an underestimation of the peak lateral load when comparing the values to the finite element model for the case of monotonic loading.

Ahmed and Hawlader (2016) and Ahmed et al. (2015) mention that according to their numerical model,the initial stiffness increases with increases in the size of the pile, and the increases are very significant at low eccentricities.

Edgers et al. (2013) and Ebin (2012) include the results of finite element analyses done at Tufts University with regard to offshore wind turbine monopiles. The analysis incorporates an implicit method to model the soil modulus degradation and increased strain as a function of the number of loading cycles. The results show that the monopile displacements and rotations accumulate with additional cycles of loading, almost doubling after 10^7 cycles.

Recent finite element studies by the Institute for Geotechnical Engineering, Leibniz University of Hannover, Germany (Achmus et al., 2007, 2005, 2014) consider the accumulation of displacements of monopiles under cyclic loading needs to be taken into account in the design. The proposed method called the soil degradation model is based on numerical simulations in combination with an evaluation of cyclic triaxial tests. For small head displacements,

the foundation stiffness is larger than it results from the approach by the API (2010).

Velarde (2016) mention finite element studies in PLAXIS and find that the API method, by overestimating soil stiffness, generally underestimates lateral deflection at both seabed and pile toe.

Bekken (2009) shows that the initial stiffness increases with an increase in pile diameter. It is also shown that the horizontal shear at the tip contributed 32% pf the horizontal load in resistance.

Wichtmann et al. (2008) discusses a finite element model based on a high-cycle accumulation (HCA) model for the purpose of analyzing cyclic loading in offshore monopiles. The lateral deflections of the monopile increased with increasing amplitude and with increasing average value of the cyclic loading.

Lesny and Wiemann (2006) reports results using finite element analyses that the standard p-y method overestimates the pile-soil-stiffness of large diameter monopiles at great depths which leads to insufficient pile length.

Chapter 3

Database for Lateral Load Tests on Monopiles in Sands

A database is compiled of all the lateral load tests in sands through accessible literature to summarize recent results with particular focus on the effects of pile diameter and slenderness on the pile response. This chapter is divided into four sections - to explain how the database is compiled, what the format of the database is, a summary of the tests in the database and to describe the tests chosen for further analysis. The table of contents of the database listing all the tests and some of their important attributes is included at the end of the thesis in Appendix A.

3.1 Data Collection

A literature review is carried out to find lateral load tests on deep foundations in predominantly sandy soils. Sources from which test data is obtained included text books, journal papers, conference papers, technical reports submitted to government agencies (e.g., state Departments of Transportation, US Army Corp of Engineers, Naval Facilities Engineering Command etc.), previously published databases on deep foundation testing, and unpublished data

from tests carried out at The University of Texas at Austin. The major portion of the load test results in this database is obtained from papers and/or reports published by the original researchers who conducted the tests. These data were supplemented by load test results extracted from the Deep Foundation Load Test Database (DFLTD) by the Federal Highway Administration (FHWA) and from the Laterally Loaded Pile Database by the University of Florida. The database maintained by UC Irvine, DFI and ADSC (www.findapile.com) is also utilized. Data from over 150 lateral load tests is obtained, out of which 82 tests were chosen to be included in this database. Key criteria used in the selection process were soil stratigraphy, shape of foundation, and diameter of foundation. For soil stratigraphy only tests with sandy or silty sandy sites are included. Sites with a lot of inter-layering of sands and clays are not considered for this database. Only circular shaped piles are chosen as the piles installed offshore are always circular piles. A wide range of diameters of piles are considered so as to notice the effect a small versus large diameter pile on the load-displacement response.

3.2 Format of Database

This database is compiled in the form of an MS Excel spreadsheet. Each test result is saved in a numbered worksheet and in some cases multiple test results are held in a single worksheet. The worksheet named "Contents" provides a table of all the test results together with some key attributes of the load tests and the numbered worksheet in which each test result can be

found. This table can sorted as required by the user via the "Sort & Filter" option in Excel, however, the order of worksheet tabs will not change. In general, each test record contains two pages of data. The first page contains qualitative information about the load test such as source, type of lateral load test (monotonic and/or cyclic loading), pile head constraints (rotational fixity at pile head), date of installation and testing. Information regarding method of installation, soil stratigraphy, loading sequence, test results, and references has been provided in greater detail. A schematic diagram of the pile setup including a simplified soil stratigraphy is also provided. The second page contains quantitative data such as foundation dimensions, structural properties, soil properties, and load-deflection data. A graph of Load versus Deflection is shown at the bottom of the page. In the cases where the results are not directly presented by the literature in the form of a Load versus Deflection curve, the curve as presented by the author replaces the position for the Load versus Deflection Curve at the bottom of the page. In the cases, where multiple results need to be shown, a third page of results is added. A worksheet named "Template" is included for the purpose of adding new data in the future. Figure 3.1 and Figure 3.2 below shows the template utilized in the database. Figures 3.3 and 3.4 show an example of the database test for the Mustang Island tests.

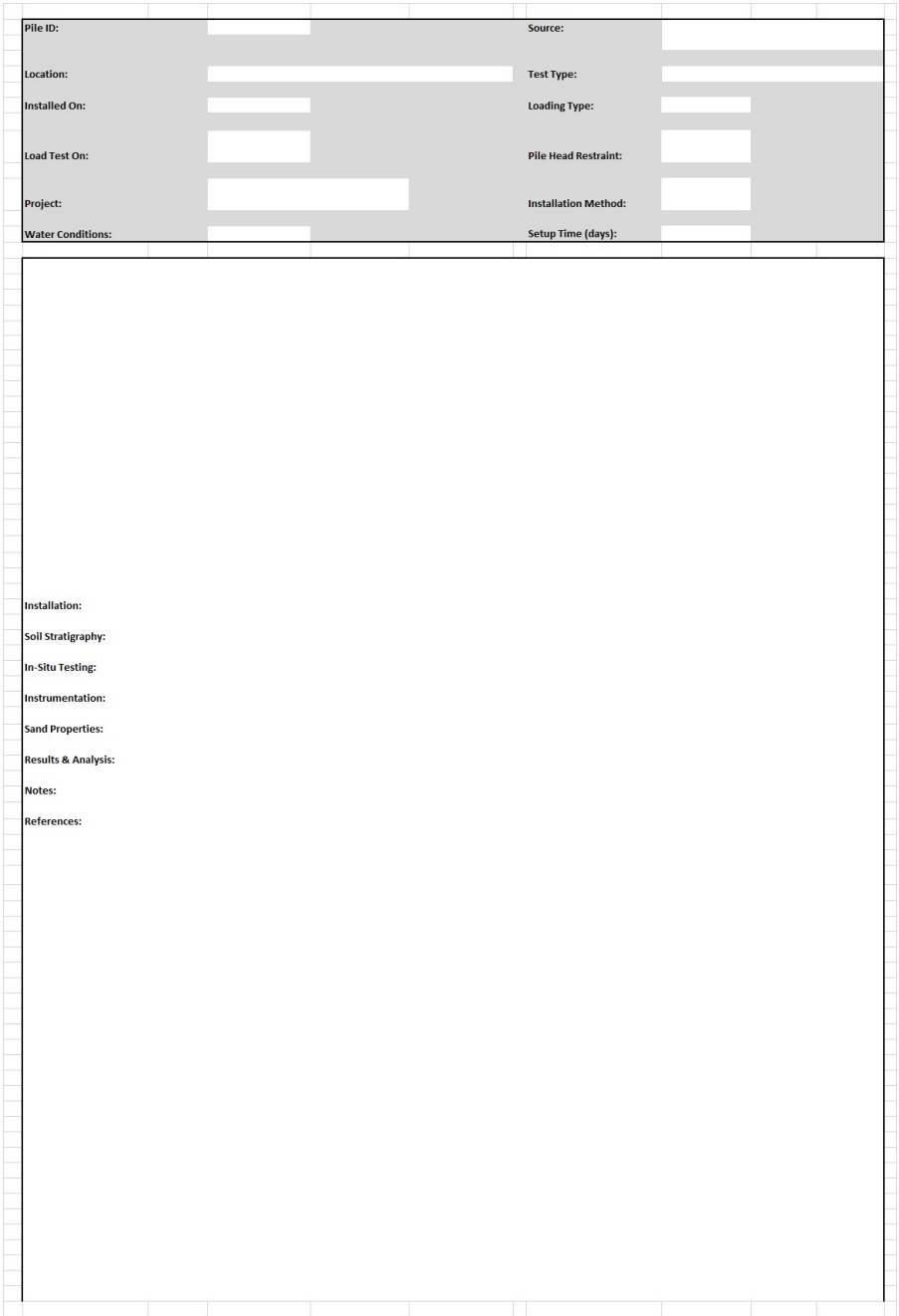

Figure 3.1: Database Template Sheet Pg 1 of 2

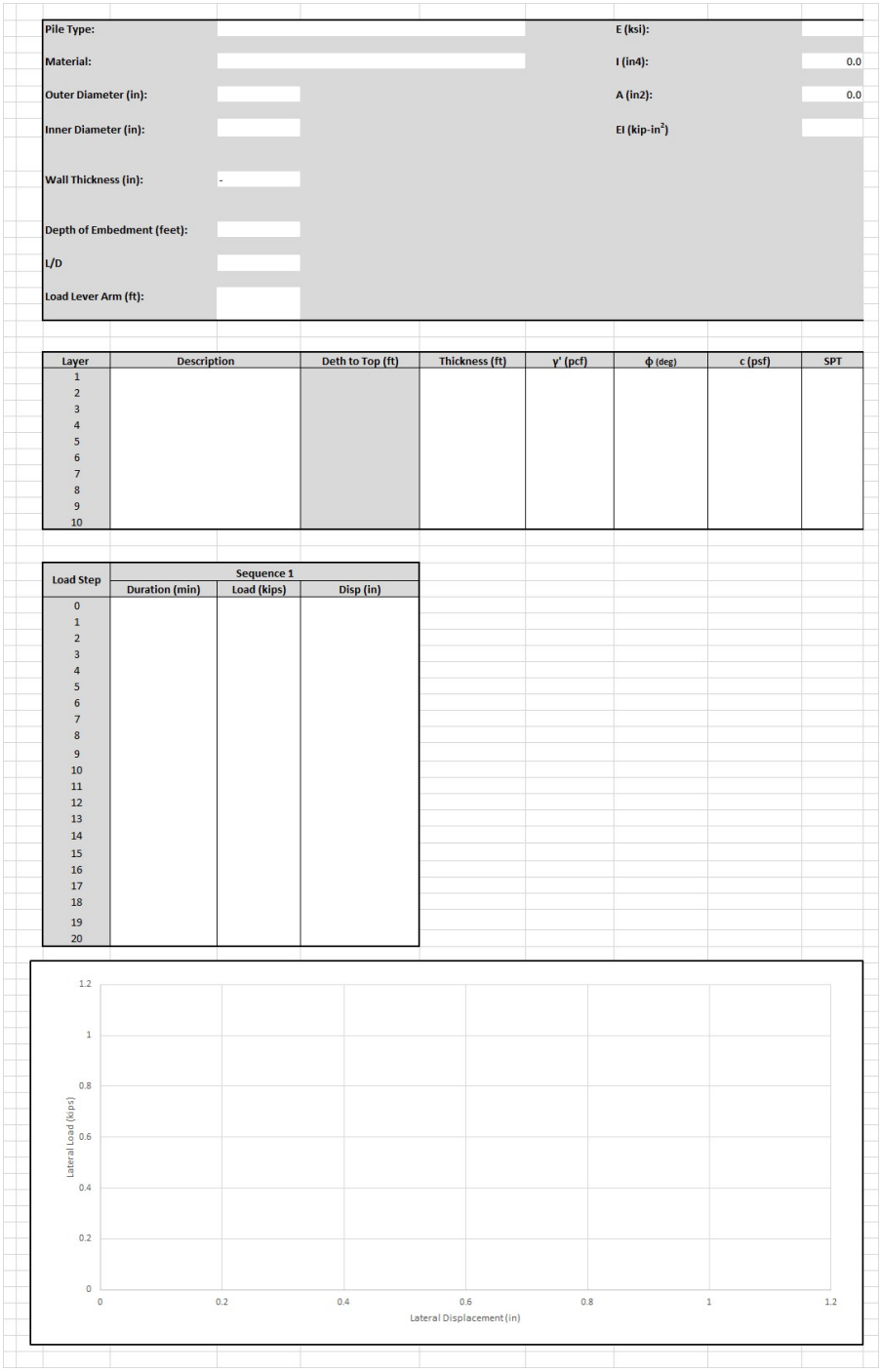

Figure 3.2: Database Template Sheet Pg 2 of 2

Pile ID:	1	**Source:**	OTC 2079 Cox et al. (1974), Compilation of Benchmark Tests by Reese (1996), Reese & Van Impe (2001)
Location:	Mustang Island, TX	**Test Type:**	Field
Installed On:	2/10/1966	**Loading Type:**	Cyclic and Monotonic
Load Test On:	2/26/1966	**Pile Head Restraint:**	Free
Project:		**Installation Method:**	Driven (Delmag-12 diesel hammer)
Water Conditions:	Submerged	**Setup Time (days):**	16

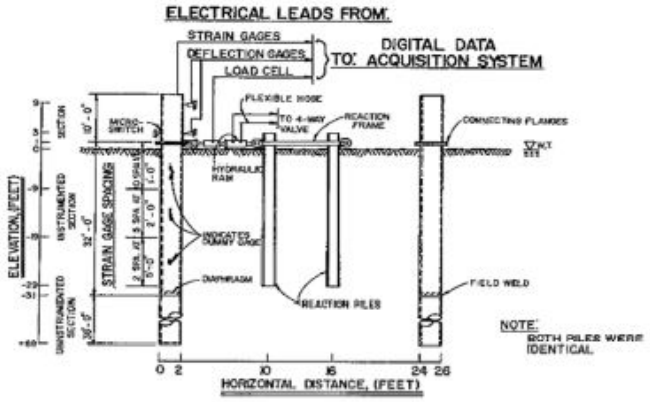

Installation:
The two test piles were driven with a Delmag- 12 diesel hammer in the excavated pit during the period from February 9 to Feb- ruary 14, 1966. Driving records for both test piles are shown in Fig. 10 of Cox et al. (1974).

Soil Stratigraphy:
In the top 40 ft, the sand strata at hole 2 had enough silt particles to be classified as a silty fine sand while the soil in hole 1 in the top 40 ft was classified as fine sand. The sand from 0 to 20 ft would be classified as medium dense, 20 to 40 ft as dense, and 50 to 70 ft as dense. The water surface was maintained at 6" (150mm) above the mudline throughout the test program.

In-Situ Testing:
Wire Line Sampler and Split-spoon sampler were used. Standard Penetration Tests were conducted along with the sampling and a piston sampler was used to obtain relative density values

Instrumentation:
Two piles were driven and both were instrumented internally with strain gauges for the measurement of bending moments. Pile 1 was subjected to static loading and Pile 2 to cyclic loading.

Sand Properties:
The soil at the site was uniformly graded fine sand with a friction angle of 39 degrees. The submerged unit weight was 62.6 pcf (10.4 kN/m3) and the relative density averaged about 90%. The sand particles by inspection through a microscope were found to be subangular with a large percentage of flaky grains.

Results & Analysis:
Elastic Moment Capacity = 472 kip-ft (640 kNm)
Plastic Moment Capacity = 611 kip-ft (828 kNm)

Notes:

References:
Cox, W., Reese, L., and Grubbs, B. (1974). "Field testing of laterally loaded piles in sand."
Figure 8 - Load Test Setup
Figure 5 - Results of standard and wire-line penetration test and relative density values from piston samples

Reese & Van Impe (2001). "Single Piles and Pile Groups under Lateral Loading"
Figure 7.17 and Figure 7.19 -- Load deflection curves
Reese, L. C. (1996). Compilation of Benchmark Lateral Load Tests on Piles in Sand and Clay. REESE (LYMAN C) AUSTIN TX

Figure 3.3: Database Example Sheet - Mustang Island - Pg 1 of 2

Pile Type:	Open Ended Pipe Pile	E (ksi):	29000
Material:	Steel	I (in4):	1942.3
Outer Diameter (in):	24	A (in2):	27.8
Inner Diameter (in):	23.25	EI (kip-in^2)	5.63E+07
Wall Thickness (in):	0.375		
Depth of Embedment (feet):	69		
L/D	35		
Load Lever Arm (ft):	1		

Layer	Description	Depth to Top (ft)	Thickness (ft)	γ' (pcf)	Su,top (psf)	Su,bot (psf)	ϕ (deg)	SPT
1	Tan Fine Sand, Light Gray Silty Fine Sand	0	40	66.3			39	
2	Gray Clay	40	10	66.3			39	
3	Gray Silty Fine Sand	50	20	66.3			39	
4	Firm Gray Clay Laminated with Sand and Sandy Clay	70	10	66.3			39	
5		80						
6								
7								
8								
9								
10								

Load Step	Static			Cyclic		
	Duration (min)	Load (kips)	Disp (in)	Duration (min)	Load (kips)	Disp (in)
0		0	0		0.0	0.00
1		5	0.02		4.5	0.02
2		10	0.06		6.8	0.04
3		15	0.13		9.0	0.06
4		20	0.22		11.3	0.10
5		25	0.32		18.0	0.20
6		30	0.4		22.5	0.31
7		35	0.5		28.1	0.39
8		40	0.62		33.8	0.51
9		45	0.75		39.4	0.63
10		50	0.9		45.0	0.79
11		55	1.02		50.6	0.94
12		60	1.2		56.3	1.26
13						
14						
15						
16						
17						
18						
19						
20						

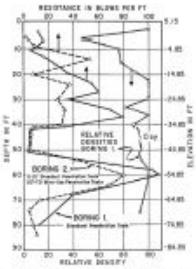

Fig. 5 - Results of standard and wire-line penetration test and relative density values from piston samples.

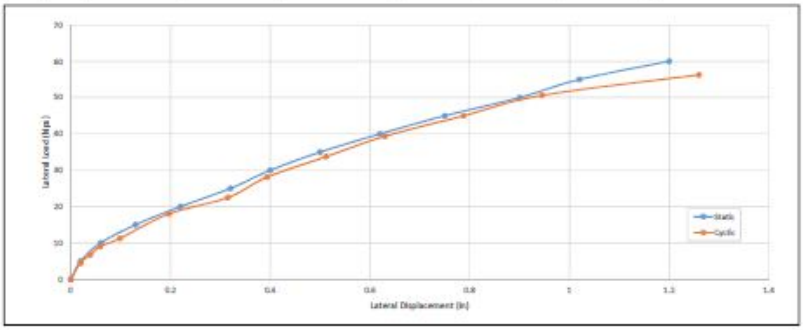

Figure 3.4: Database Example Sheet - Mustang Island - Pg 2 of 2

3.3 Statistics from Database

A summary of the statistics from the database are compiled in this section. The database has the following attributes:

- Total of 82 tests on laterally loaded deep foundations
- Tests conducted in Clean Sands (51 tests), Silty Sands (19), Gravelly Sand (1) and Layered Clay-Sand Stratigraphy (11)
- Steel Pipe Piles, Steel Solid Piles, Reinforced Concrete Drilled Shafts, Winged Monopiles and Prestressed Concrete Piles/Shafts
- Field tests, and laboratory tests (including one-g and centrifuge) on models
- Pile/Shaft diameters ranging from 2 inches to 173 inches (Prototype Model in Centrifuges)
- Pile/Shaft aspect ratios (Length/Diameter) ranging from 1 to 81

3.4 Tests Chosen for Analysis

Since the objective of this research project is to develop design methods for large diameter monopile foundations, the selected test results were limited to piles/shafts with circular cross-sections. Tests performed at sites with soils stratigraphies consisting of materials other than sands or stratified mixtures

(e.g., clays or rock) were excluded since this study mainly deals with monopile response in sands.

For the purpose of the study of steel monopiles driven in sands, the field tests fitting these criteria were closely examined. These tests are few in number but the most essential ones due to them closely depicting the true behavior of the piles. Also, since these monopiles are meant for wind turbine applications where the strain levels are low, only those tests were considered where there were load-displacement measurements at low displacements (within 0.0025 times the pile diameter). This level of displacement is around the maximum displacement seen in a representative field test for monopiles in sand as given in Pan et al. (2016). These tests are highlighted in Table 3.1.

Table 3.1: Tests Chosen for Further Analysis

No.	Location	Material	Diameter (in)	Length (ft)	L/D	Source
1	Mustang Island, TX	Steel Pipe	24	69	35	Cox et al. (1974), Reese (1996), Reese & Van Impe (2001)
2	Houston, TX	Steel Pipe	24	100	50	Little & Briaud (1988)
3	Blessington, Ireland (Pile 1)	Steel Pipe	13.39	7.22	6.5	Doherty & Gavin (2010)
4	Blessington, Ireland (Pile 2)	Steel Pipe	9.65	4.9	6	Murphy et al. (2016)
5	Garryhesta, Ireland	Steel Pipe	9.65	4.9	6	Murphy et al. (2016)

Chapter 4

Site Descriptions

This chapter provides the descriptions of the soils at the sites chosen for further analysis along with comments about pile properties and installation. Supplemental information such as boring logs and CPT profiles are provided at the end of the thesis in Appendix B.

4.1 Mustang Island, TX

The Mustang Island tests are the historic tests that led to the formation of the API code for sands. These tests are very well described in Cox et al. (1974) with an abundance of data and information. There is also data measurement at smaller strains and hence it would be fruitful to take a closer look at the load-test information for our purposes.

4.1.1 Test Location

As indicated in Figure 4.1, a test site was selected at the Shell Oil Company tank battery on Mustang Island, near Port Aransas, Texas.

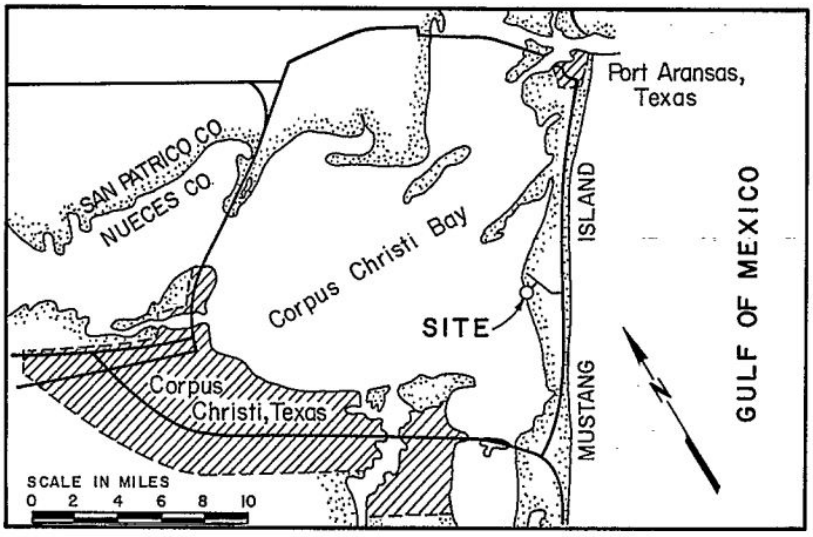

Figure 4.1: Location of test site at Mustang Island as given in Cox et al. (1974)

4.1.2 Sampling and In-Situ Testing

Two soil borings were made at the test site. Soil samples were taken from one hole by continuously alternating a 2 -inch split- spoon sampler with a 3-inch piston sampler. Samples from the second hole were taken at 5 foot intervals with a 2-inch split-spoon to 15 feet. Below 15 feet, samples were taken at 5 feet intervals with a wireline sampler. Logs of the two borings are shown in Appendix B. It should be noted in the logs that the depth as shown relates to original ground surface, and elevation relates to the bottom of the test pit. In conjunction with disturbed sampling by the split-spoon sampler and wire-line sampler, standard penetration tests were also run. Results from standard penetration tests are expressed as the number of blows, N , required

to advance the sampler 1 feet into the soil are given in the Appendix B.

4.1.3 Soil Properties

The schematic of the pile and soil strata is given in Figure 4.2.

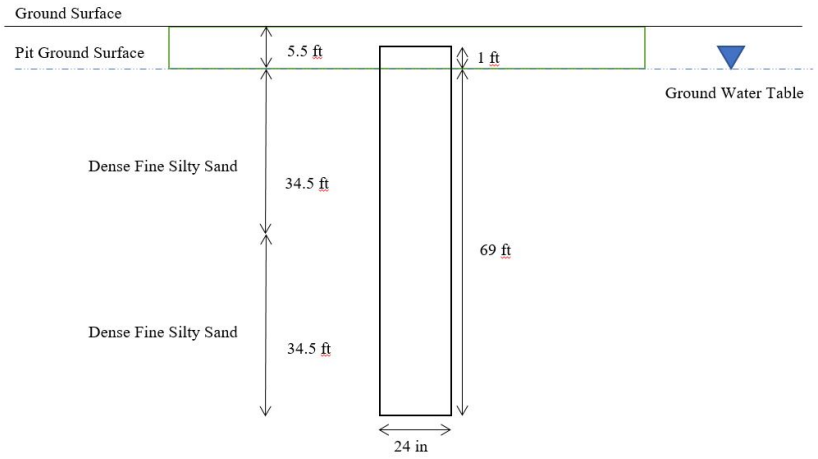

Figure 4.2: Schematic of Pile and Soil Strata at Mustang Island as described in Cox et al. (1974)

In the top 40 ft, the sand was characterized as silty fine to fine sand. The SPT N values were correlated with relative density of sands using the chart given in Peck et al. (1974) (Figure 4.3).

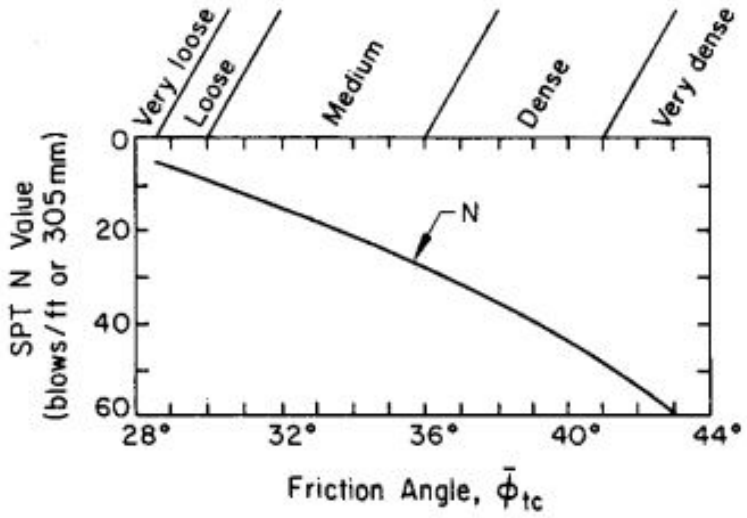

Figure 4.3: Chart for correlation between SPT N value and Internal Angle of Friction (Peck et al., 1974)

The sand from 0 to 20 feet is classified as medium dense, from 20 to 40 feet as dense, and from 50 to 70 feet as dense. The angle of internal friction is taken to be 39 degrees (Corresponding to an average SPT N value of around 40). Soil properties determined from laboratory tests included grain-size distribution, in-situ densities, and minimum and maximum densities. These test results are included in the Appendix B. The cohesionless materials were uniformly graded sands with the percentage of fines passing the number 200 sieve varying from 0 to 15 percent. The sand particles by inspection through a microscope were found to be subangular with a large percentage of flaky grains. The relative density of the soils in situ is about 90%.

4.1.4 Pile Properties and Installation

Before the test piles were installed at the site, it was necessary to excavate about 5 and a 1/2 feet of material to reach the water table. In addition, further excavation was required to remove a 2-1/2 feet layer of clay just below the water table. The layer of clay was removed and sand filled in to bring the soil surface back up to the water table. It is believed that the sand fill assumed an in-situ character similar to clean sands near the surface of marine floors. The area excavated was approximately 40 feet wide by 60 feet long.

The two test piles were 24-in. diameter with a wall thickness of 3/8 inch. The material was A-53 grade-B seamless steel. The embedment length was chosen to be 69 feet. Each test pile consisted of a 38-feet uninstrumented section, a 32 -feet instrumented section, and a 10-feet uninstrumented section. Connecting flanges, 36 x 20 x 1-1/2 inches, were welded to the instrumented section and to the 10-feet section. During driving and testing, the 10-ft section was bolted to the 32-feet section at the flange by seven 1-inch diameter bolts.

The test piles were driven with a Delmag- 12 diesel hammer in the excavated pit. A point to note would be that during driving of the last 10 feet of pile 1, excessive rotation of the pile occurred. A torque was applied to the flange of the pile and driving was resumed. This torque returned the pile to its original orientation so that the diameter on which strain gages were located would be in line with lateral loads. Loads to the free-head piles were applied at 1 ft above the mudline.

4.1.5 Instrumentation

A total of 40 strain gages, 34 active gages and 6 dummy gages, were placed in each pile. Dummy gages were to be used to complete the circuits where active gages might become inoperative.

A 20-channel digital-data-acquisition system was used for recording the output of the strain gages, deflection gages, and the load cell.

Loads were measured in the calibration and field tests by a universal load cell of 100,000-lb capacity. The gages used were linear-displacement transducers with 6-inch strokes capable of measuring displacements to one micro-inch. For these tests, however, the resolution was reduced to 0.001 inch.

4.1.6 Sample Collection at Mustang Island

4.1.6.1 Site of Collection

Disturbed samples were collected using a hand auger apparatus at a site about 5 miles from the original test site of the Mustang Island Tests. Cox et al. (1974) specified that the test site was located at a Shell Oil Company tank battery on Mustang Island, near Port Aransas, Texas. On comparison of distances in the Figure 4.4a and the scaled map shown in Figure 4.4c, a fair sense of the original location of the test site is asserted. Additionally, the plausible site has a tank battery as shown in Figure 4.4b which provides evidence to the assertion that it is the original site.

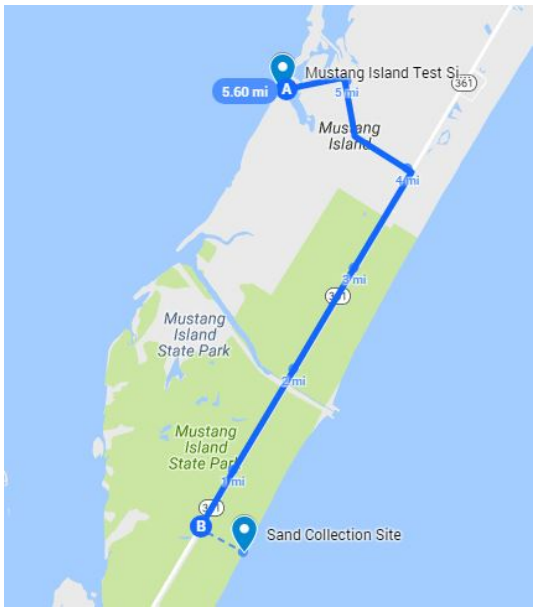

(a) Mustang Island with Sample Collection Site and Test Site (Google Maps)

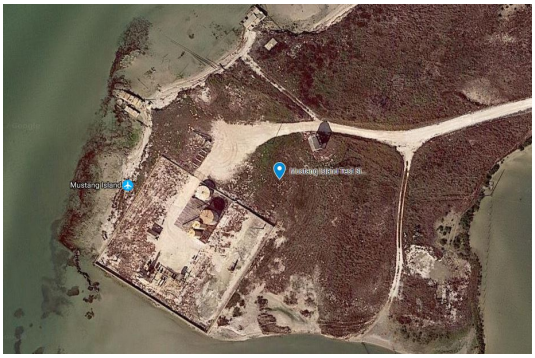

(b) Mustang Island Test Site (Google Maps Satellite View)

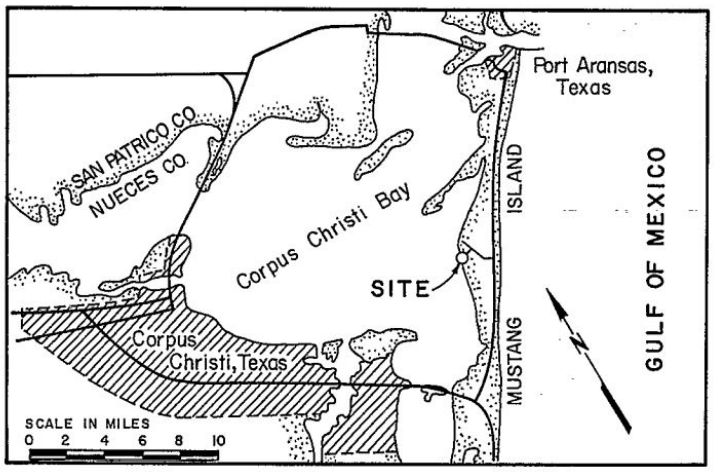

(c) Mustang Island Test Site Map (Cox et al., 1974)

Figure 4.4: Mustang Island Sample Collection and Test Sites

4.1.6.2 Apparatus

Figure 4.5a and Figure 4.5b show the various equipment that was used to collect the disturbed samples. These included a soil hand augering setup, bucket, shovel, and ziplock bags to store the samples. The hand auger consisted of connection rods, a pair of wrenches, a rubber handle, and a 5-in sand sampler. The screws on the rods were 5/8 in threaded.

(a) Hand Auger with Rods and 5 Gallon Bucket

(b) 5-inch Hand Auger for Sands

Figure 4.5: Soil Collection Equipment Utilized at Mustang Island

4.1.6.3 Procedure

The following procedure was employed in excavation and collection of the disturbed sample:

1. The area under consideration was leveled using the shovel.
2. A standard reference was established to be regarded as the ground surface elevation.
3. A preliminary hole was dug using the shovel.
4. A 5-in hand auger was used to core a hole and obtain sample at 3-4 ft below ground surface (Right at the Ground Water Table)
5. It was not possible to go any deeper as the borehole under the water table would collapse over the auger, thereby jamming it in the ground.
6. The soil was carefully removed from the auger and kept in air tight 1 gallon zip lock bags.
7. A 5 gallon bucket's worth of samples were collected.
8. Care was taken to avoid organics such as seaweed in the soil samples.
9. Picture were obtained to supplement the data and are given below in Figure 4.7a, 4.7b and 4.7c

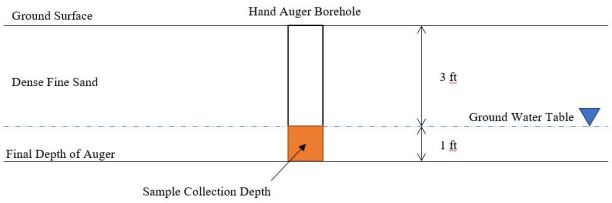

Figure 4.6: Schematic of Borehole dug with Hand Auger

(a) Mustang Island Sample Collection Site

(b) Start of Borehole Augering

(c) End of Borehole Augering

Figure 4.7: Sample Collection Site and Boreholes

4.1.6.4 Grain Size Distribution

The grain size distribution of the samples collected was done using sieve analysis and compared with the original distribution.

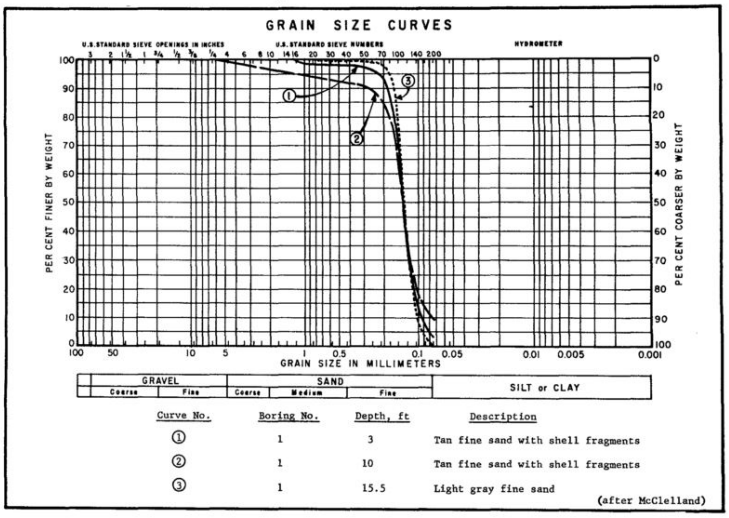

Figure 4.8: Grain Size Curves for Mustang Island Sands (Cox et al., 1974)

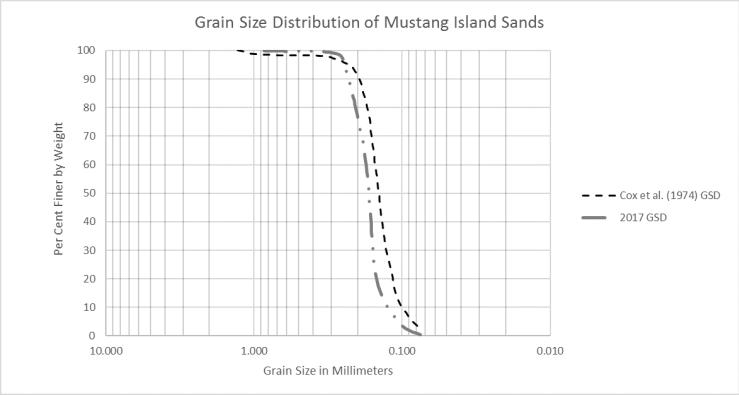

Figure 4.9: Grain Size Distribution of Mustang Island Soil Collected compared to Cox et al. (1974)

4.1.6.5 Discussion

Disturbed sand samples were obtained at Mustang Island. After running sieve analysis, the grain size distribution was obtained. From the figure above (Figure 4.9) it can be said that the grain size distributions match closely with the historic data. This opens up options for further research, where the collected samples can be tested for its seismic characteristics (shear wave velocity). Characterizing the soil using resonant column and torsional shear testing, coupled with a robust numerical model and lab scale model testing, would be the best approach to understand the behavior of large diameter monopiles at small strains. Since the mustang island site has been heavily studied and has ample data, it could serve useful for validation of a finite element model.

4.2 Houston, TX

This test is well described in a report to the US Army Engineer District, St.Louis by the faculty at Texas A & M University. Six existing piles were readily available for lateral load testing. The purpose of the project was to subject those six piles to cyclic horizontal loads and study the corresponding accumulation of horizontal displacement. A major part of the study was to look at the effectiveness of the pressuremeter to predict the lateral response, but in this thesis we only consider the measured test results and how those compare to the API method. The description of the test site is included in the following sections. Only one of the test piles is considered for the analysis (the 24-in steel pipe pile).

4.2.1 Test Location

The pile load test site was located on property under the authority of the Texas State Department of Highways and Public Transportation at the northern end of the Baytown-La Porte tunnel on State Highway 146 near Houston, Texas (Figure 4.10).

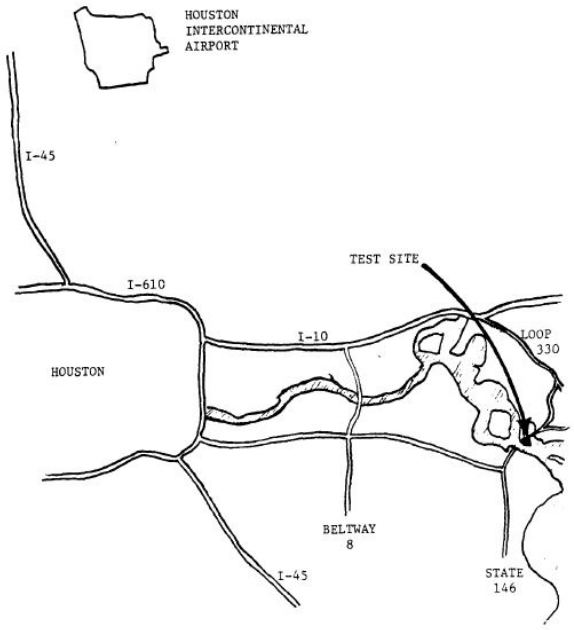

Figure 4.10: Location of Test Site at Houston as given in Little and Briaud (1988)

4.2.2 Sampling and In-Situ Testing

A boring log with Standard Penetration Test (SPT) results, grain size analysis curves and cone penetrometer test results are available in the original report and are given in Appendix B. The average SPT value for the site was

taken to be 21.

4.2.3 Soil Properties

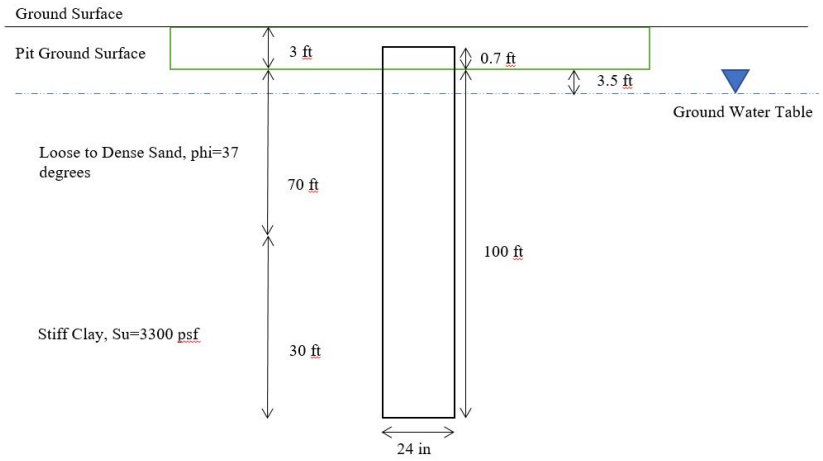

Figure 4.11: Simplified Schematic of Pile and Soil Strata at Houston as described in Little and Briaud (1988)

The soil was primarily composed of loose to medium dense fine sand in the upper 73 ft underlain by stiff to very stiff clay. The water table was at 3.5 ft below excavated ground level. This is illustrated in the simplified schematic given in Figure 4.11. Using the Peck et al. (1974) (Figure 4.3) correlation between SPT and friction angle, we obtain a friction angle of 34 degrees for the site. The undrained shear strength of the stiff clay was specified as 3300 psf.

4.2.4 Pile Properties and Installation

The site had been backfilled following completion of vertical load tests done at the site previously, necessitating excavation before conducting the lateral load tests. The depth of the excavation was approximately 3 ft. Each pile was cored horizontally to allow a length of 1-3/8 in, 150 ksi Dywidag threadbar to be passed through the pile's central axis. A 200-kip load cell was used to measure the loads during the load test.

The 24-in pipe pile was assumed to have an elastic modulus of 29,000 ksi. It was driven to a depth of 100 ft below groundline. So, the L/D ratio comes out to be 50. The moment of inertia selected for the prediction process was based on the pile being completely empty of any soil throughout its length due to the soil plug being drilled out after driving.

4.2.5 Instrumentation

Dial gages were securely attached to an independently supported displacement measuring frame. Deflections were measured at two points on each pile: one point below the axis of loading close to the groundline and one above the axis of loading. This allowed the deflection and the slope at the groundline to be obtained. In all of the load displacement curves in this thesis, the displacement readings at the lower LVDT are considered. This point was 0.41 in below the head of the pile i.e. 0.3 in above the ground line.

4.3 Ireland

4.3.1 Blessington

4.3.1.1 Test Location

The field test presented in this paper was conducted at a dense sand research site in Blessington, a small village located 25km to the south-west of Dublin, Ireland as shown in Figure 4.12. The test area is a dedicated research site within an active quarry, where the underlying deposits of uniform sand have been confirmed by extensive excavations.

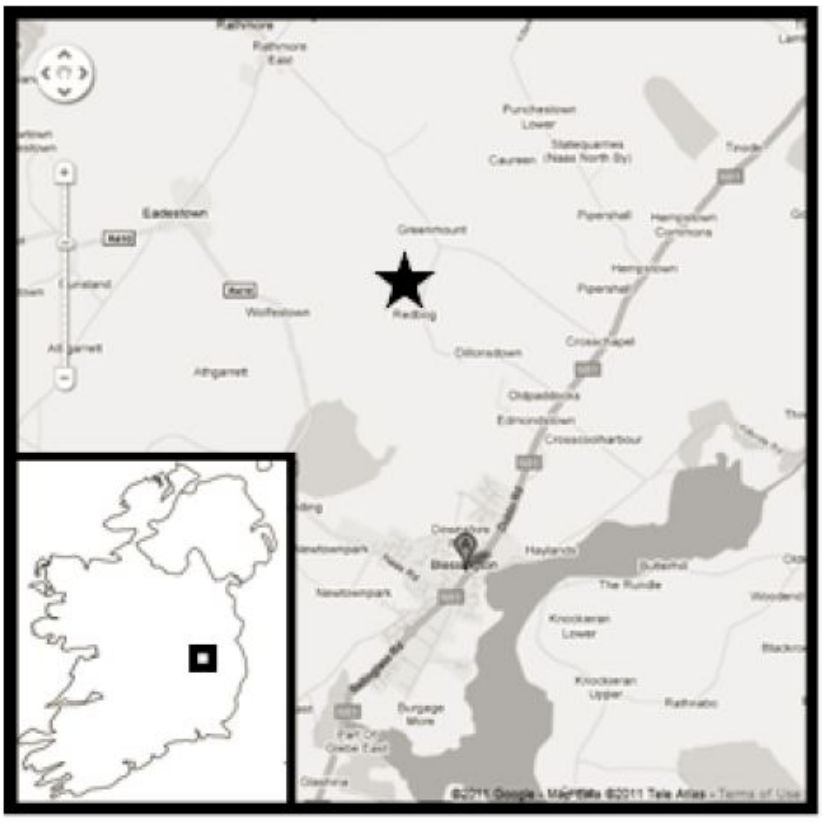

Figure 4.12: Test Site Location at Blessington (Doherty and Gavin, 2011)

4.3.1.2 Soil Properties

The dense sand at this site was formed by combined glacial and fluvio-glacial action that has impacted the engineering properties of the deposit. The interbedded sand layers have a particle grading from silty sand to coarser sand, depending on the lake level at the time of deposition. The site is heavily overconsolidated from a combination of post-depositional glacial processes and more recent excavations at the quarry, resulting in a maximum pre-consolidation pressure in the range of 8001400kPa at ground surface. The sand is fine with D_{50} ranging from 0.10.15mm. The moisture content measured in a series of boreholes has a range of 10 $\pm$ 2%. The relative density of the deposit was determined to be close to 100%.

4.3.1.3 Sampling and In-Situ Testing

Cone penetration tests (CPT) were conducted adjacent to the test pile and are shown in Figure 2. The cone tip resistance (qc) was found to increase from approximately 10 MPa at ground surface, to 25 MPa at 10m depth. From Doherty and Gavin (2011), the friction angle at the site is taken to be 42 degrees and the unit weight as $20KN/m^3$. The water table was deeper than the pile tip.

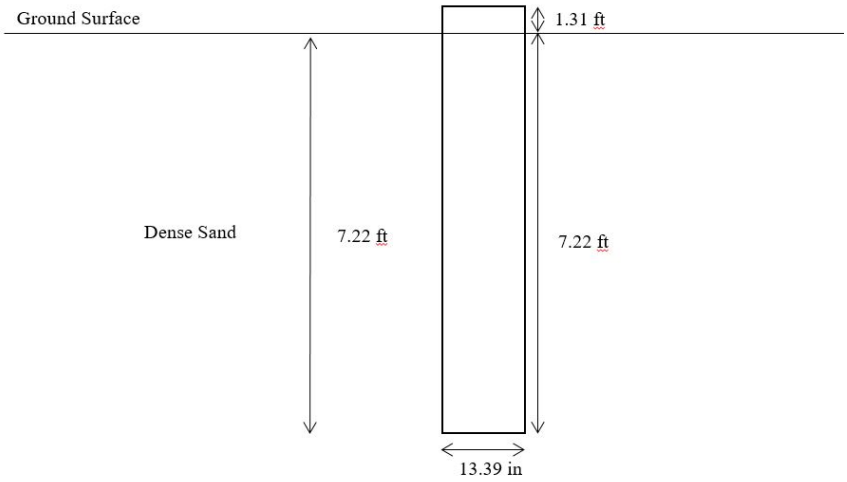

Figure 4.13: Simplified Schematic of Pile and Soil Strata at Blessington as described in Doherty and Gavin (2011)

4.3.1.4 Pile Properties and Installation

A 3m-long open-ended steel pile was manufactured from an offshore conductor pipe. The pile had an outer diameter (OD) of 340mm and a wall thickness (t) of 13mm. The pile was then driven to an embedment (L) of 2.2m using a 5-tonne Juntann hammer, which resulted in an aspect ratio (L/D) of 6.5. Strain gauges were bonded in diametrically opposite pairs externally on the pile shaft. This was to provide an indication of the load transfer and the moments mobilised during load testing. Two mild steel channels were welded to the outside of the pile shafts to protect the instrumentation; this increased the bending stiffness (EI) to 390,000 kNm^2.

4.3.1.5 Instrumentation

The static load was applied using a hydraulic jack connected to a pump, with the load control provided by an electronic loadcell mounted in-line with the loading point 0.4m above the ground level. The displacements and pile head rotation were measured using linear variable displacement transducers connected to the pile head. The resolution of the measurements were such that a continuous profile was obtained instead of just discrete data points. The strain gauges, load cell and displacement transducers were all logged on a Vishay system 5000 data logger system at a sampling rate of 1Hz. The pile was loaded until lateral displacements greater than 10% of the pile diameter were achieved. Reaction was provided by concrete blocks, which were stacked vertically adjacent to the pile.

4.3.2 Garryhesta

4.3.2.1 Test Location

The model pile tests were conducted in the Roadstone Wood sand pit in Garryhesta, which is located approximately three kilometers west of Ballincollig in Co. Cork. The site has a large supply of dense fine-grained silty sands and gravels.

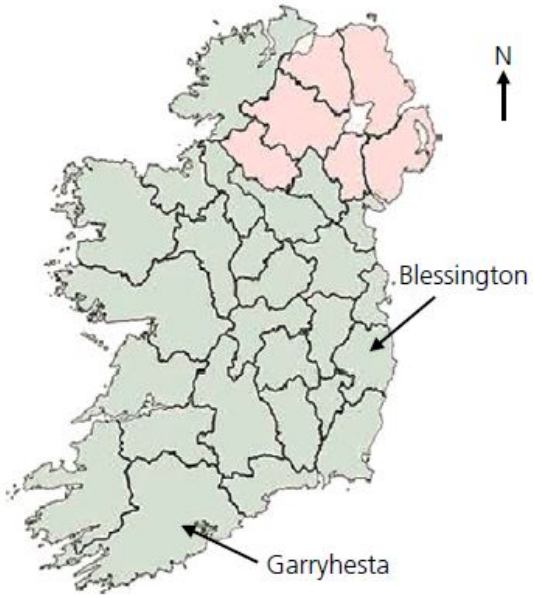

Figure 4.14: Test Site Location (Murphy et al., 2016)

4.3.2.2 In-Situ Testing

CPT and Dilatometer results for the Garryhesta site are presented in Appendix B. The shear wave velocity (Vs) of the soil was measured using Multi-Channel Analysis of Surface Waves (MASW) equipment, with the data as presented in Appendix B.

4.3.2.3 Soil Properties

Prior to pile testing, a series of laboratory and field tests were conducted to determine the in-situ soil properties on site. The results of a series of cone penetrometer (CPT) tests yielded a relatively consistent CPT profile, with the

tip resistance, qc, around 6.5 MPa shown in Appendix B. The peak friction angle is found to be around 45 degrees. The bulk unit weight was 18.6 KN/m^3.

The Initial Shear Stiffness (G_o) at Garryhesta is found to be 200 MPa. to be The natural water content of the samples was found to be approximately 12%. Soil classification tests were also conducted and the soil was deemed to be "very silty sand SM" with 15% fines and a uniformity coefficient of 2.5, suggesting that the soil is well graded.

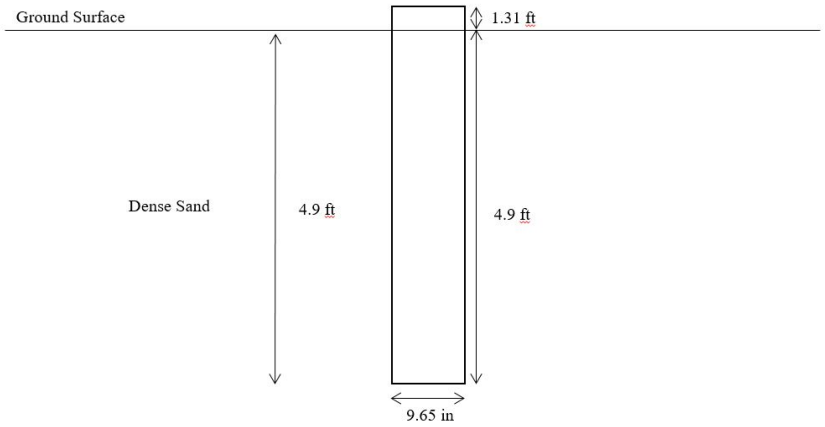

Figure 4.15: Simplified Schematic of Pile and Soil Strata at Garryhesta as described in Murphy et al. (2016)

4.3.2.4 Pile Properties and Installation

The model piles were installed at the test site, using a heavy tracked excavator to push them into the ground and the guide frame to maintain verticality. The piles were laterally-loaded using a 25-tonne hydraulic jack and employing a 30-tonne excavator for reaction.

4.3.2.5 Instrumentation

The static load was applied using a hydraulic jack connected to a pump, with the load control provided by an electronic loadcell mounted in-line with the loading point 0.4 m above the ground level. The strain gauges, load cell and displacement transducers were all logged on a Vishay system 5000 data logger system at a sampling rate of 1Hz. The pile was loaded until lateral displacements greater than 10% of the pile diameter were achieved. Reaction was provided by concrete blocks, which were stacked vertically adjacent to the pile.The displacements and pile head rotation were measured using linear variable displacement transducers connected to the pile head. The resolution of the measurements were such that a continuous profile was obtained instead of just discrete data points.

Chapter 5

Analysis

This chapter looks at the analysis of the small strain response of the chosen tests using the 2D finite difference software LPILE, which is produced and distributed by ENSOFT Inc. There are two aspects of the lateral load response being considered - monotonic and cyclic. In both cases, the effect of initial stiffness modulus, k, is considered through a sensitivity study. Another important problem looked into is the effect of the L/D ratio on the prediction of the response using the API (2010) procedure. The API (2010) procedure is the most prescriptive of the different models and the one utilized in LPILE. Hence it is chosen for this study. Finally, a study with respect to the influence of base shear on the response of the stiff monopiles is presented.

For this analysis, an emphasis is laid on the initial stiffness of the lateral load-displacement curve and a displacement level (strain) of 0.0025 times the diameter is chosen as a reference for small strain. This level is chosen as it is the level of maximum strain obtained in a field load test on a OWT monopile as given in Pan et al. (2016). It is valuable to note that the k values chosen in the sensitivity study can be related to an equivalent friction angle using Figure 2.12.

5.1 Mustang Island

The following tables (Table 5.1 and Table 5.2) contain the input parameters for the LPILE model. This was the original test that was utilized to calibrate the Reese model for the p-y method, so it was expected to obtain a good fit. Both the static and cyclic load tests are considered in the next two subsections.

Table 5.1: Mustang Island Pile Properties in LPILE

Mustang Island	
Property	**Value**
Section Type	Elastic Section (Non-yielding)
Total Length (ft)	70
Embedded Length, L (ft)	69
Shape	pipe
Section Diameter (in)	24
L/D	35
Wall Thickness (in)	0.375
Area (in^2)	27.83
Moment of Inertia (in^4)	1942.3
Elastic Modulus, E (psi)	29000000
Flexural Rigidity, EI (lbs-in^2)	5.63E+10

Table 5.2: Mustang Island Soil Strata Properties in LPILE

Layer	**Model**	**Vertical Depth Below Pile Head of Top of Soil Layer (ft)**	**Vertical Depth Below Pile Head of Bottom of Soil Layer (ft)**	γ' **(pcf)**	ϕ' **(degrees)**	**k (pci)**
1	API Sand (O'Neill)	1	70	66.2	35	Variable
1	Sand (Reese)	1	70	66.2	39	Variable

5.1.1 Monotonic Response

The monotonic response is plotted against the API (2010) predictions by LPILE. A point to note would be that for the Reese model, a friction angle of 39 (Value found from SPT Correlations) degrees did a very good job at prediction, but for the API model, a lower friction angle of 35 degrees was able to predict the overall response (See Figure 5.1a). The 35 degree angle for the API model was back calculated by matching the the curve to the data. This gives an idea that model input depends on the model chosen and it is important to consider how the models were calibrated. On zooming into the curve, the API prediction with 39 degrees input matches closely with the Reese model (Figure 5.1b). But in our further analysis the 35 degree input for friction angle is taken in the API model, because it gives a better overall fit for the curve. For either of the models, the prediction underpredicts the

initial stiffness.

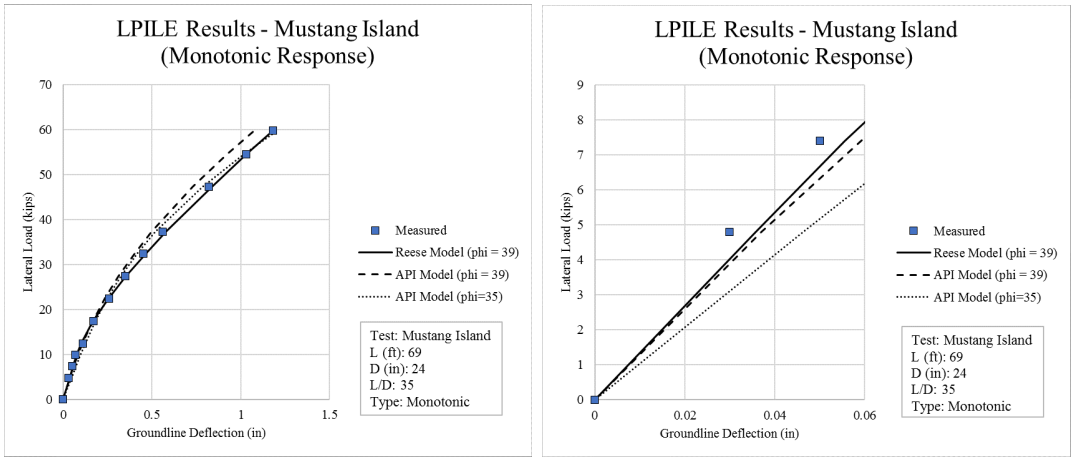

(a) Full range of results (b) Range upto 0.0025 of Diameter

Figure 5.1: LPILE Results - Mustang Island (Monotonic Response)

A sensitivity study is also conducted by varying the initial stiffness modulus (k) from the default value assigned as a function of friction angle. At a low strain level (Figure 5.4b), as k increases, the initial stiffness of the prediction increases with a better match for a k lying between 150 and 200 pci.

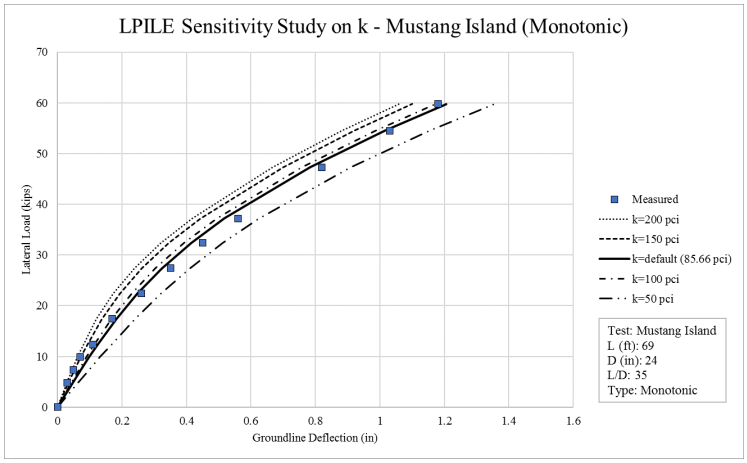

(a) Full range of results

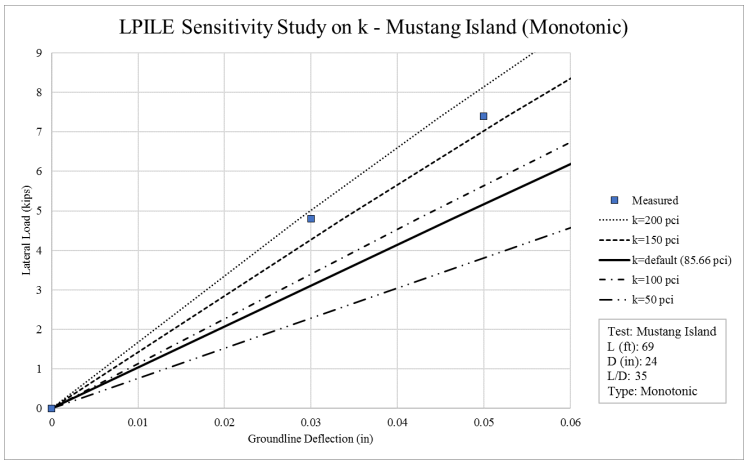

(b) Range upto 0.0025 of Diameter

Figure 5.2: LPILE Sensitivity Study on k - Mustang Island (Monotonic Response)

5.1.2 Cyclic Response

Cyclic tests were also run on the piles at Mustang Island, and the procedure of softening the response was implemented as suggested by Reese et al. (1974). The number of cycles was set to 1000. Once again, the data

matches well for the Reese model for a friction angle of 39 degrees. But for the API model, this angle is 35 degrees. Figures 5.3a and 5.3b, demonstrate that the predictions underpredict the initial stiffness even further. This could be because the emphasis of the method is to better match the ultimate resistance rather than the initial part of the load-displacement curve. Therefore, it can be asserted that the API method isn't well suited for small-strain problems until it has been calibrated for it.

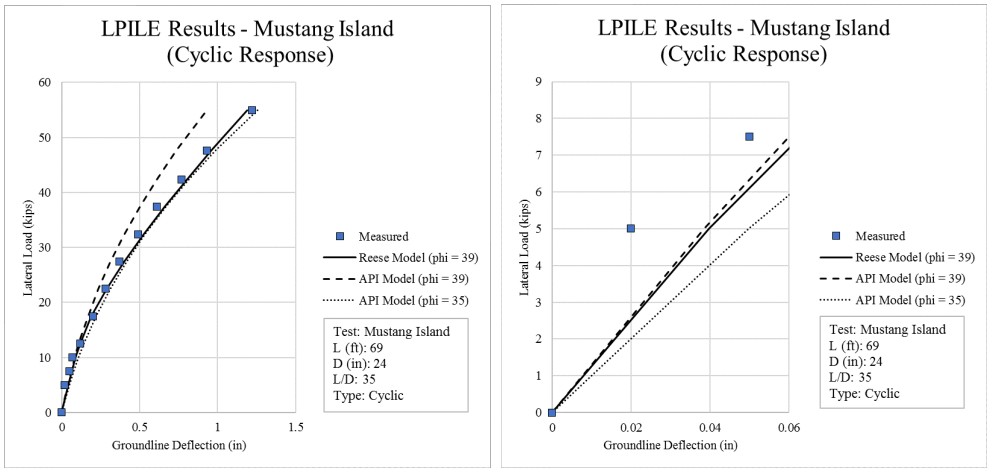

(a) Full range of results (b) Range upto 0.0025 of Diameter

Figure 5.3: LPILE Results - Mustang Island (Cyclic Response)

A sensitivity study is also conducted by varying the initial stiffness modulus (k) from the default value assigned as a function of friction angle. At a low strain level (Figure 5.4b), as k increases, the initial stiffness of the prediction increases. The prediction does not fit the data well even for even higher k values.

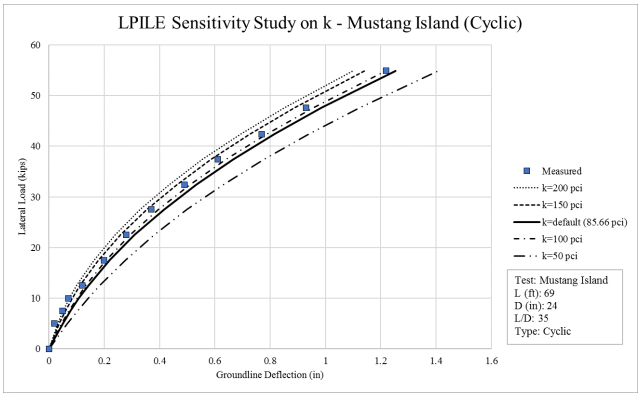

(a) Full range of results

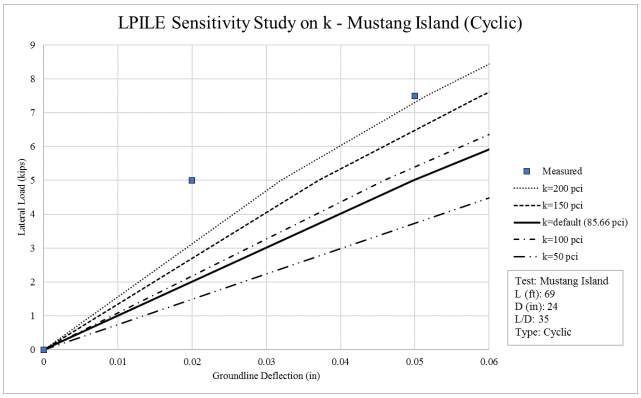

(b) Range upto 0.0025 of Diameter

Figure 5.4: LPILE Sensitivity Study on k - Mustang Island (Cyclic Response)

5.2 Houston

Both monotonic and cyclic tests were run at Houston, TX as given in Little and Briaud (1988). The following subsections cover the monotonic and cyclic response of the tests along with the analysis in LPILE. The Tables 5.3 and 5.4 contain the input parameters for the LPILE model.

Table 5.3: Houston Pile Properties in LPILE

Houston	
Property	**Value**
Section Type	Elastic Section (Non-yielding)
Total Length (ft)	100.7
Embedded Length, L (ft)	100
Shape	pipe
Section Diameter (in)	24
L/D	50
Wall Thickness (in)	0.625
Area (in^2)	45.9
Moment of Inertia (in^4)	3136.93
Elastic Modulus, E (psi)	29000000
Flexural Rigidity, EI (lbs-in^2)	9.10E+10

Table 5.4: Houston Soil Strata Properties in LPILE

Layer	**Model**	**Vertical Depth Below Pile Head of Top of Soil Layer (ft)**	**Vertical Depth Below Pile Head of Bottom of Soil Layer (ft)**	γ' **(pcf)**	ϕ' **(degrees)**	S_u **(psf)**	**k (pci)**
1	API Sand (O'Neill)	0.7	4.2	120	34	-	Variable
2	API Sand (O'Neill)	4.2	70.7	57.6	34	-	Variable
3	Stiff Clay w/o Free Water (Reese)	70.7	113	57.6	-	3300	Default

There are three layers considered in this analysis - a sand layer above the water table, a sand layer below the water table and a stiff clay layer without access to free water. In the subsequent sensitivity studies, k1 refers to the k value assigned to the upper sand layer above the water table and k2 refers to the k values assigned to the lower sand layer below the water table.

5.2.1 Monotonic Response

The friction angle found using the correlation between SPT N value and friction angle as given by Peck et al. (1974) (See Figure 4.3) is 34 degrees.

The monotonic response data for the piles is given upto a load level of 40 kips. Beyond that, two stages of cyclic loading were done and the monotonic backbone curve is given. There is a good fit for the monotonic portion of the curve. On zooming in to a low strain level (Figure 5.5b), the API method underpredicts the response.

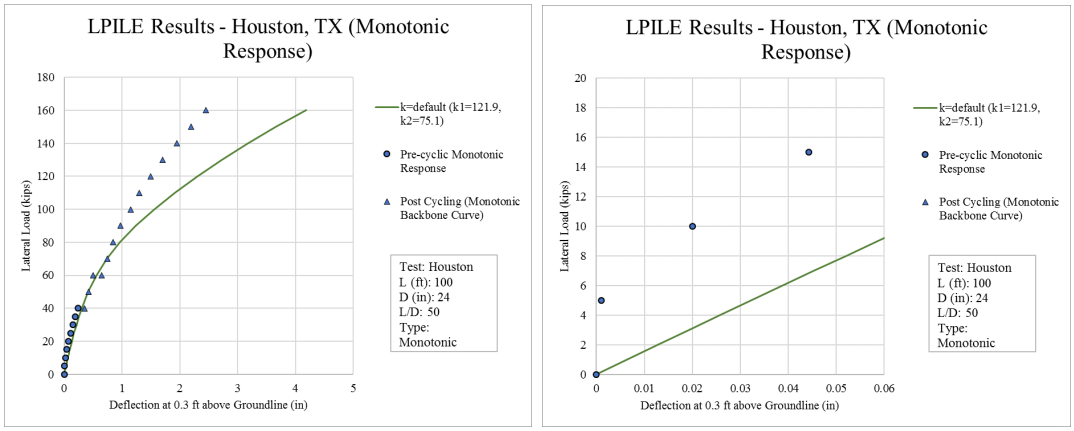

(a) Full range of results (b) Range upto 0.0025 of Diameter

Figure 5.5: LPILE Results - Houston (Monotonic Response)

A sensitivity study is also conducted by varying the initial stiffness modulus (k) from the default value assigned as a function of friction angle. Since there are two layers of sand, the k1 and k2 values are varied proportionately according to different friction angles. At a low strain level (Figure 5.6b), as k increases, the initial stiffness of the prediction increases. But even with a higher k value, the response is underpredicted and there isn't a good fit with the data.

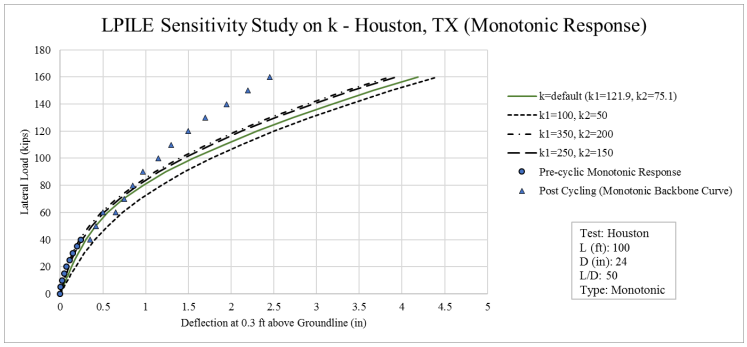

(a) Full range of results

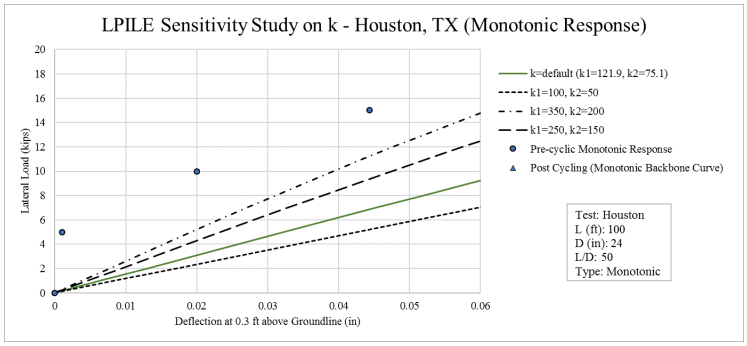

(b) Range upto 0.0025 of Diameter

Figure 5.6: LPILE Sensitivity Study on k - Houston (Monotonic Response)

5.2.2 Cyclic Response

Cyclic tests were also run on the piles at Houston, and the procedure of softening the response was implemented as suggested by Reese et al. (1974). The number of cycles was set to 200 as in the original tests. Direct comparisons with the data could not be made as the post-cyclic monotonic measurements were made at a high strain and load level. But, a comparison is made between the change in stiffness between the LPILE predictions. Figures 5.7a and 5.7b, demonstrate that at a small strain level, there isn't much difference between

the predicted monotonic and cyclic response. The stiffness degradation is observed for the higher strain levels, keeping the ultimate resistance in mind.

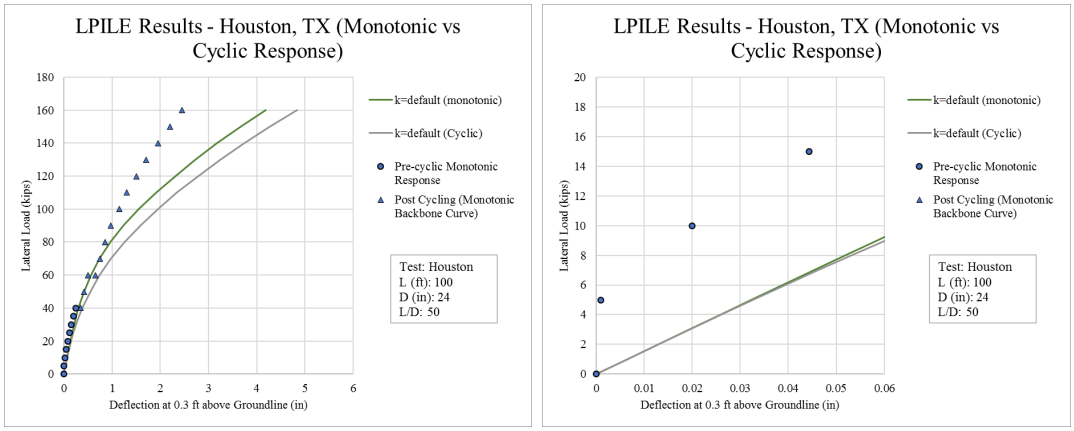

(a) Full range of results (b) Range upto 0.0025 of Diameter

Figure 5.7: LPILE Monotonic vs Cyclic Response - Houston

The original analysis as given in Little and Briaud (1988) are also presented here.

A method used to evaluate the effect of cyclic loading on the pile-soil stiffness was to evaluate the degradation of the piles secant stiffness K_S(N) as described in Figure 5.8a. The cyclic degradation parameter "a" is defined as the negative slope of the best fit line through the points plotted on the graph of the relative secant stiffness k_S(N)/K_s(1) , versus the cycle number, N, on a log-log scale (Figure 5.8a).

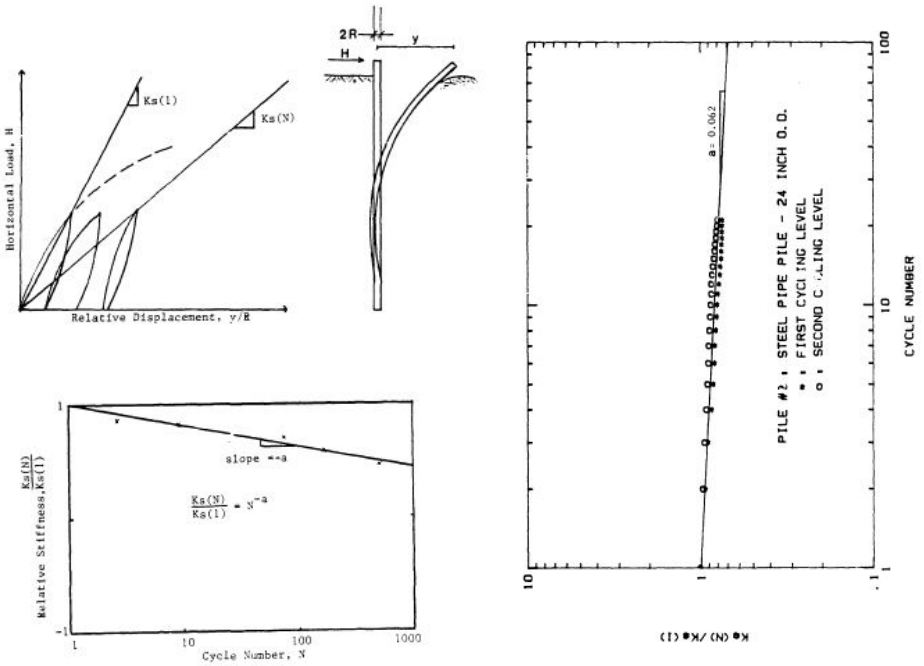

(a) Definitions of Cyclic Parameters (b) Results for 24-in Steel Pipe Pile

Figure 5.8: Original Results on Secant Stiffness Degradation with number of cycles as given in Little and Briaud (1988) - Houston (Cyclic Response)

When comparing the "a" values, cycling with total unloading causes greater degradation than cycling with only partial unloading (one-half of the top load). The steel pipe pile also had less degradation during the second series of cycles with "a" values of 0.065 and 0.059 respectively.

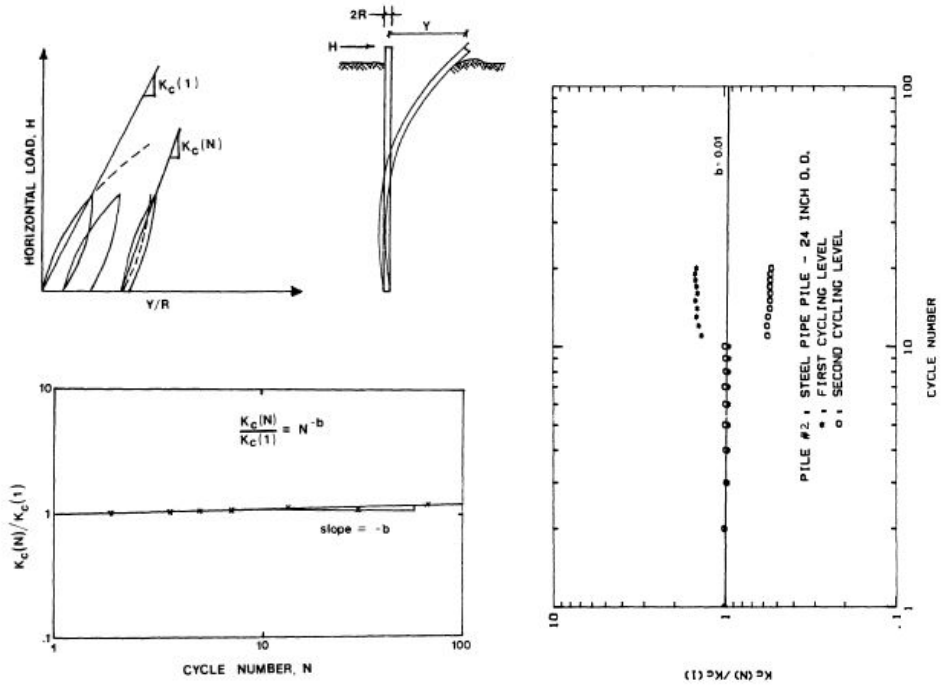

(a) Full range of results (b) Range upto 0.0025 of Diameter

Figure 5.9: Original Results on Tangential Stiffness Degradation with number of cycles as given in Little and Briaud (1988) - Houston (Cyclic Response)

The cyclic stiffness for the pile K_C(N), as defined in Figure 5.8b, showed little or no degradation within each portion of the cyclic loading where the difference between the upper and lower loads was constant (Figure 5.9b). The first series of cycles may have caused a slight densification of the soil in front of the pile.

5.3 Blessington

Two series of tests were run at Blessington, Ireland. One was a part of a study by Doherty and Gavin (2011), and another was a part of a study to understand winged monopile behavior (Murphy et al., 2016). For the second study, reference monotonic tests were done on a pile without wings. This data has been considered for further analysis.

5.3.1 Pile 1

Both monotonic and cyclic tests were run at Blessington as given in Doherty and Gavin (2011) and Li et al. (2015). The following subsections cover the monotonic and cyclic response of the tests along with the analysis in LPILE. The Tables 5.5 and 5.6 contain the input parameters for the LPILE model.

Table 5.5: Blessington (Pile 1) Pile Properties in LPILE

Blessington (Pile 1)	
Property	**Value**
Section Type	Elastic Section (Non-yielding)
Total Length (ft)	8.53
Embedded Length, L (ft)	7.22
Shape	pipe
Section Diameter (in)	13.39
L/D	6.5
Wall Thickness (in)	0.51
Area (in^2)	20.8
Moment of Inertia (in^4)	432.3
Elastic Modulus, E (psi)	314346000
Flexural Rigidity, EI (lbs-in^2)	1.36E+11

Table 5.6: Blessington (Pile 1) Soil Strata Properties in LPILE

Layer	**Model**	**Vertical Depth Below Pile Head of Top of Soil Layer (ft)**	**Vertical Depth Below Pile Head of Bottom of Soil Layer (ft)**	γ' **(pcf)**	ϕ' **(degrees)**	**k (pci)**
1	API Sand (O'Neill)	1.31	8.53	127.31	42	Variable

5.3.1.1 Monotonic Response

The monotonic response results were obtained from Doherty and Gavin (2011). A sensitivity study is also conducted by varying the initial stiffness

modulus (k) from the default value assigned as a function of friction angle. Looking at Figures 5.10a and 5.10b, the default design criteria leads to an overestimation of stiffness at low strains. Overall also there isn't a good fit the data, where the ultimate load is underestimated. But, the initial stiffness of the response matches well with the data for k= 150 pci (corresponds to an angle of 35 degrees) as compared to the default k value for the friction angle of 42 degrees (310.3 pci).

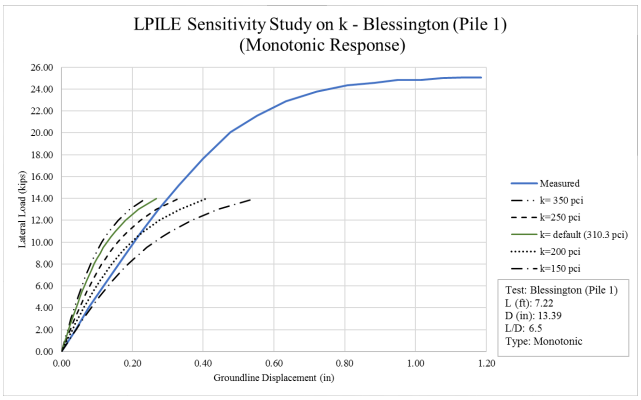

(a) Full range of results

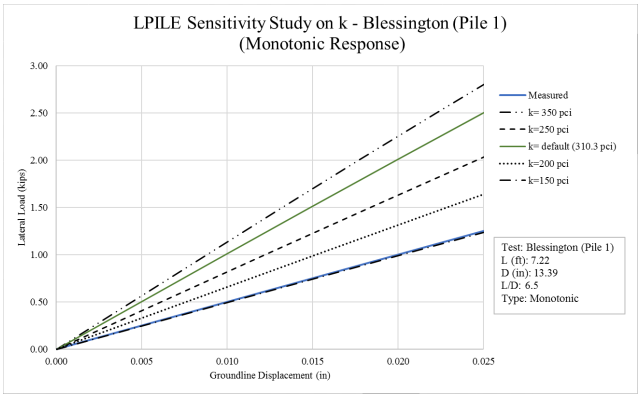

(b) Range upto 0.0025 of Diameter

Figure 5.10: LPILE Sensitivity Analysis on k - Blessington (Pile 1) (Monotonic Response)

5.3.1.2 Cyclic Response

The cyclic test results on two model piles are presented here as given in Li et al. (2015). PS2 refers to the static pile response, whereas PC1 and PC2 refer to the post cyclic monotonic backbone curves. From Figure 5.11, the cyclic initial stiffness is greater than the observed initial stiffness for the static case.

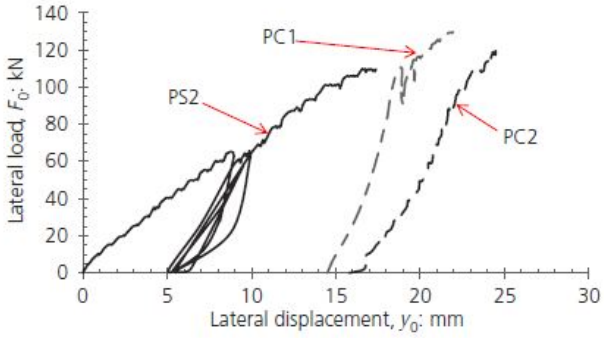

Figure 5.11: Cyclic Test Results - Blessington (Pile 1) (Li et al., 2015)

An LPILE analysis was run considering the effect of 5000 cycles on the monotonic response. There is a reduction in the response of the pile at large strains, but not much difference at small strains (Figures 5.12a and 5.12b).

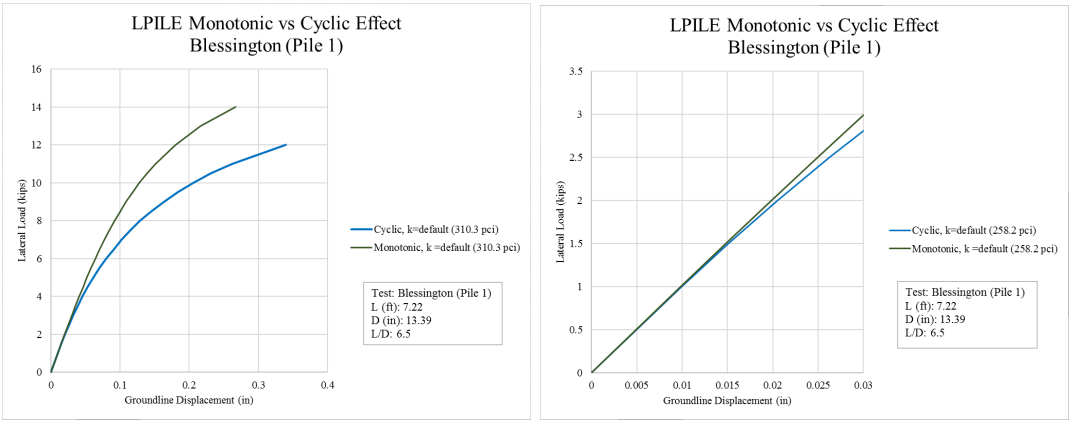

(a) Full range of results (b) Range upto 0.0025 of Diameter

Figure 5.12: LPILE Monotonic vs Cyclic - Blessington (Pile 1)

This prediction contradicts the true post-cycling response where there was an actual increase in initial stiffness. Thus the API method does not do a good job at predicting the cyclic response. To quote the original conclusion as per Li et al. (2015), "Even though, generally, the pile head load displacement became stiffer as the number of load cycles (and the accumulated displacement) increased, a relatively softer load displacement response was noted over the first 34 mm of lateral displacement. This response is suggested to be caused by induced gapping over the upper portion of the pile shaft."

A sensitivity study was run on k for the cyclic API predictions. As the k is increased the initial stiffness increases as expected. No further inferences are drawn, as the prediction does not match the measured load response at all.

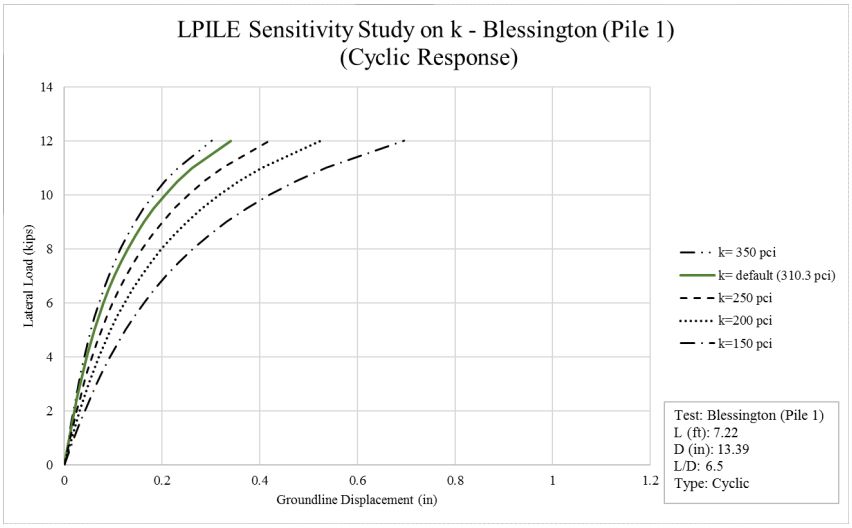

(a) Full range of results

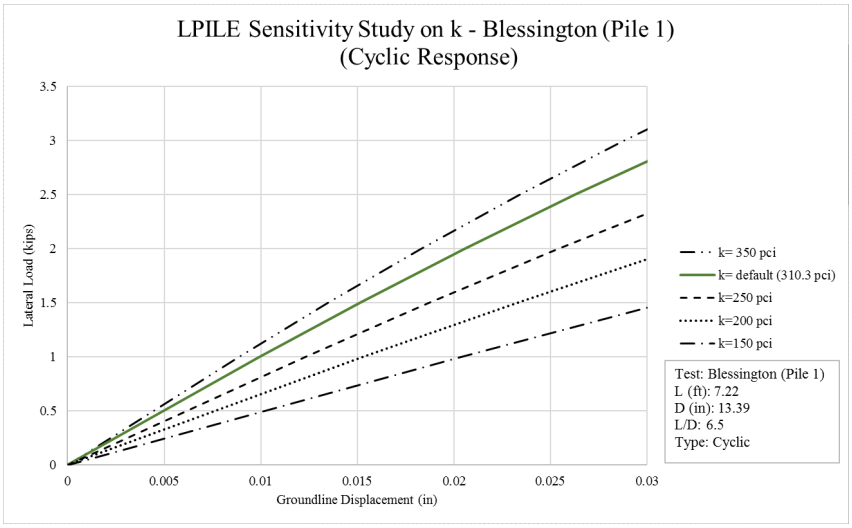

(b) Range upto 0.0025 of Diameter

Figure 5.13: LPILE Sensitivity Analysis on k - Blessington (Pile 1) (Cyclic Response)

5.3.2 Pile 2

A second pile load test was run at Blessington as part of a study to understand the effects of wings on the response of a monopile (Murphy et al., 2016). The Tables 5.7 and 5.8 contain the input parameters for the LPILE model.

Table 5.7: Blessington (Pile 2) Pile Properties in LPILE

Blessington (Pile 2)	
Property	**Value**
Section Type	Elastic Section (Non-yielding)
Total Length (ft)	6.23
Embedded Length, L (ft)	4.90
Shape	pipe
Section Diameter (in)	9.65
L/D	6
Wall Thickness (in)	0.31
Area (in^2)	9.10
Moment of Inertia (in^4)	99.30
Elastic Modulus, E (psi)	29000000
Flexural Rigidity, EI (lbs-in^2)	2.88E+09

Table 5.8: Blessington (Pile 2) Soil Strata Properties in LPILE

Layer	**Model**	**Vertical Depth Below Pile Head of Top of Soil Layer (ft)**	**Vertical Depth Below Pile Head of Bottom of Soil Layer (ft)**	γ' **(pcf)**	ϕ' **(degrees)**	**k (pci)**
1	API Sand (O'Neill)	1.31	6.23	127.31	42	Variable

5.3.2.1 Monotonic Response

The monotonic response results were obtained from Murphy et al. (2016). A sensitivity study is also conducted by varying the initial stiffness modulus (k) from the default value assigned as a function of friction angle. Looking at Figures 5.14a and 5.14b, the default design criteria leads to an overestimation of stiffness at low strains. Overall also there isn't a good fit the data, where the ultimate load is greatly underestimated. But, the initial stiffness of the response matches well with the data for k= 250 pci (corresponds to an angle of 40 degrees) as compared to the default k value for the friction angle of 42 degrees (310.3 pci).

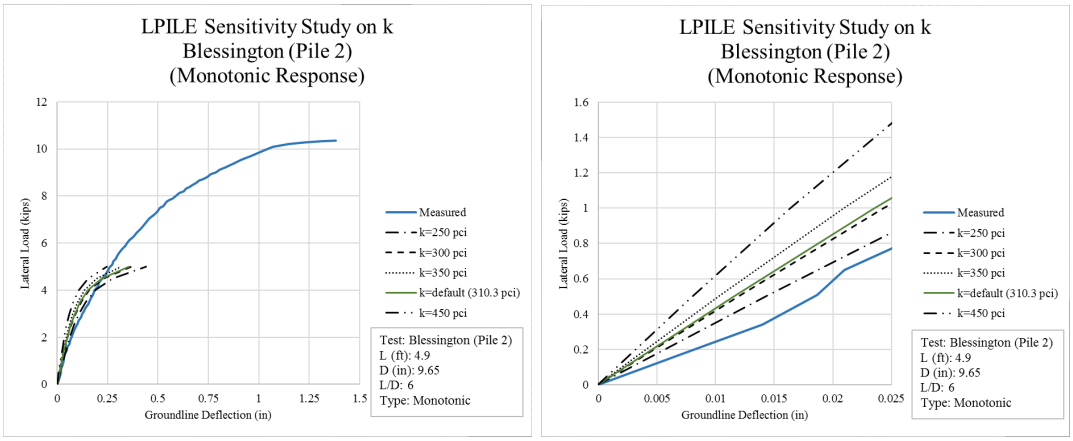

(a) Full range of results (b) Range upto 0.0025 of Diameter

Figure 5.14: LPILE Sensitivity Analysis on k - Blessington (Pile 2) (Monotonic Response)

5.4 Garryhesta

A pile load test was run at Garryhesta as part of a study to understand the effects of wings on the response of a monopile (Murphy et al., 2016). The Tables 5.9 and 5.10 contain the input parameters for the LPILE model.

Table 5.9: Garryhesta Pile Properties in LPILE

Garryhesta	
Property	**Value**
Section Type	Elastic Section (Non-yielding)
Total Length (ft)	6.23
Embedded Length, L (ft)	4.90
Shape	pipe
Section Diameter (in)	9.65
L/D	6
Wall Thickness (in)	0.31
Area (in^2)	9.10
Moment of Inertia (in^4)	99.40
Elastic Modulus, E (psi)	29000000
Flexural Rigidity, EI (lbs-in^2)	2.88E+09

Table 5.10: Garryhesta Soil Strata Properties in LPILE

Layer	**Model**	**Vertical Depth Below Pile Head of Top of Soil Layer (ft)**	**Vertical Depth Below Pile Head of Bottom of Soil Layer (ft)**	γ' **(pcf)**	ϕ' **(degrees)**	**k (pci)**
1	API Sand (O'Neill)	1	1.31	6.23	45	Variable

5.4.1 Monotonic Response

The monotonic response results were obtained from Murphy et al. (2016). A sensitivity study is also conducted by varying the initial stiffness

modulus (k) from the default value assigned as a function of friction angle. Looking at Figures 5.15a and 5.15b, the default design criteria leads to an overestimation of stiffness at low strains. Overall also there isn't a good fit the data, where the ultimate load is greatly underestimated. But, the initial stiffness of the response matches well with the data for k=250 pci (corresponds to an angle of 40 degrees) as compared to the default k value for the friction angle of 45 degrees (394.71 pci).

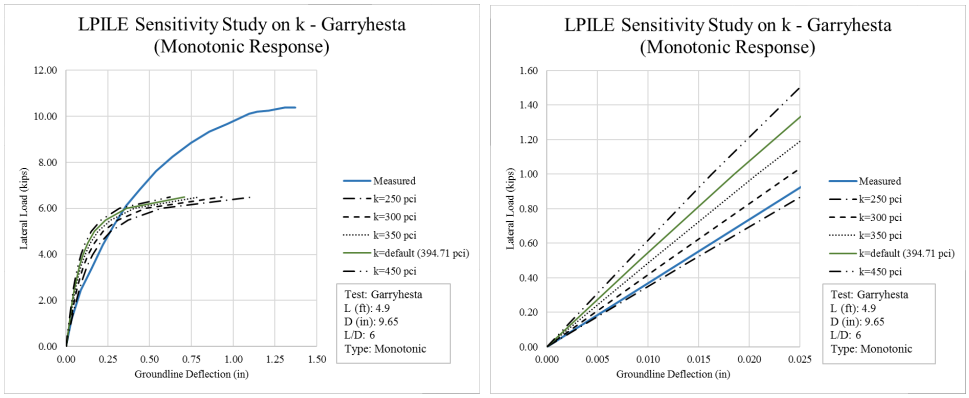

(a) Full range of results (b) Range upto 0.0025 of Diameter

Figure 5.15: LPILE Sensitivity Analysis on k - Garryhesta (Monotonic Response)

5.5 Effect of L/D on Response

Looking at the results together, in the piles that behave rigidly, the initial stiffness of the pile is overestimated by the API method. Whereas, in the long and slender piles, this stiffness is underestimated. The behavior of rigid vs flexible is verified by the displacement versus depth profiles of the

tests.

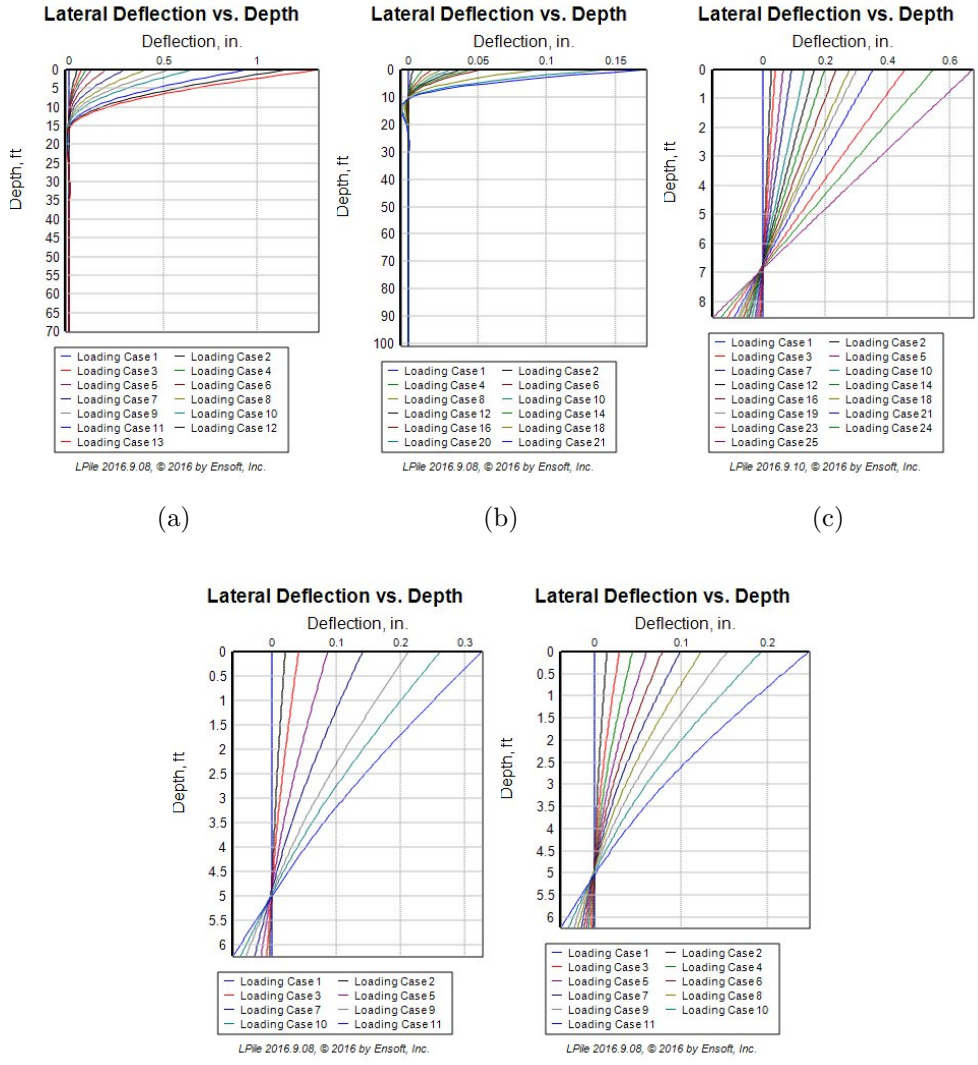

(a) (b) (c)

(d) (e)

Figure 5.16: Lateral Deflection vs Depth profiles at (a) Mustang Island (b) Houston (c) Blessington (Pile 1) (d) Blessington (Pile 2) (e) Garryhesta

5.6 Consideration of Base Shear at Tip in Ireland Tests

Looking at the profile of displacement vs depth of the piles in the previous section (Figure 5.16), by basic mechanics it is possible that the translation of the pile tip would result in a component of shear along it. This effect has been discussed previously in the literature (LeBlanc et al., 2010) but there isn't an exact procedure as to how base shear is to be accounted for in the design standards. In the API comparison with measured results as given in Doherty and Gavin (2011), this effect is not discussed. Version 9 of LPILE has the capability to account for base shear in piles that tend to rotate and translate instead of bending. A procedure based on using the frictional resistance as calculated by a shear resistance based on the vertical stresses at the base and using a t-z curve form the API RP 2GEO code. This method is considered here in this section for the Ireland tests, and the effect is observed for the monotonic response at the default initial stiffness (k) values.

5.6.1 Calculation of Base Shear using t-z analysis

Figure 5.17 demonstrates the development of base shear in a short rigid pile. As the pile tends to rotate or translate, there is a shearing of the soil at the tip of the pile and a frictional resistance develops.

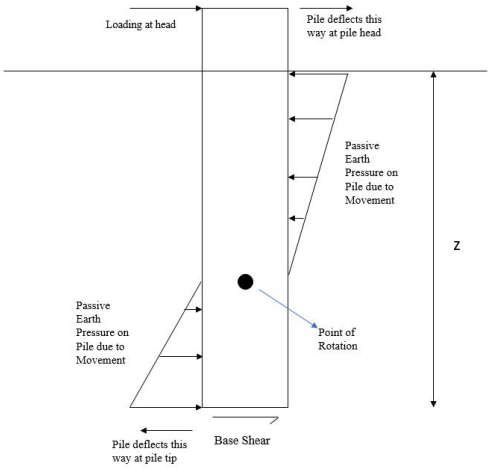

Figure 5.17: Schematic of Base Shear in Short Rigid Pile

The base shear calculations are done using the following equation:

$$f = \sigma_v{}' tan\phi' \tag{5.1}$$

where:

f = Unit skin friction (at the tip of pile) at a certain depth (psf)

$\sigma_v{}' = \gamma' z$ = In-Situ Vertical effective stress (psf) at a depth z(ft)

$\gamma' z$ = Effective unit weight of the sand (pcf)

ϕ' = Internal angle of friction (degrees) for soil-soil interface

$$\tau = fA \tag{5.2}$$

where:

τ = Base shear force (lbs)

A = Area of cross section of tip of pile (ft^2)

z/z_{peak}	t/t_{max}	
	Clays	Sands
0.16	0.30	0.30
0.31	0.50	0.50
0.57	0.75	0.75
0.80	0.90	0.90
1.0	1.00	1.00
2.0	0.70 to 0.90	1.00
∞	0.70 to 0.90	1.00

Key

z is the local pile axial deflection;

z_{peak} is the displacement to maximum soil pile adhesion or unit skin friction;

D is the outside diameter;

t is the mobilized soil-pile adhesion;

t_{max} = $f(z)$ = maximum soil-pile adhesion or unit shaft friction, computed according to 8.1.

Figure 5.18: t-z analysis as per API RP 2GEO (2011)

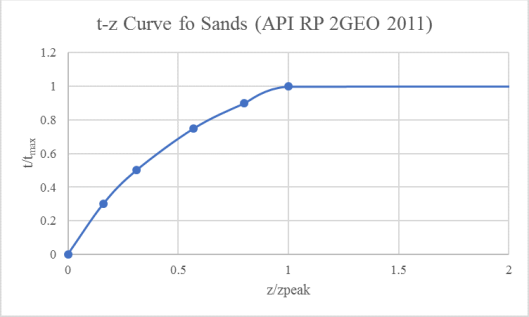

Figure 5.19: t-z curve plotted as per API RP 2GEO (2011)

Figures 5.18 and 5.19 give the recommended values for the side-shear vs displacement curves i.e. t-z analysis as per the API RP 2GEO (2011). Although the mobilization of shear force is not vertical, it should still theoretically follow the same relationship to mobilize. The difference is in the stresses. A typical value for z_{peak} of one percent of the pile outer diameter (i.e. z_{peak} /D = 0.01) is recommended for routine design purposes. Also, the t_{max} here refers to f or the unit skin friction as defined previously.

5.6.2 LPILE Results

In LPILE, base shear can be introduced in the form of a load-displacement curve. The displacement needed to mobilize the shear strength is inputed as a curve. The curve is inputted as calculated in Section 5.6.1. The shear force mobilized is given by Equations 5.1 and 5.2. The displacement needed to mobilize the shear force is given using the values in Figures 5.18 and 5.19. Here the displacement needed to mobilize the maximum shear force is taken to be 0.01 times the pile diameter. The base shear-displacement curves are thus calculated for each of the Ireland test piles and tabulated in Tables 5.11, 5.12, and 5.13.

Table 5.11: Base Shear Input into LPILE for Blessington (Pile 1)

Displacement (in)	**Base Shear Mobilized (lbs)**
0.00	0.00
0.02	242.80
0.04	404.67
0.08	607.00
0.11	728.40
0.13	809.33
0.27	809.33

Table 5.12: Base Shear Input into LPILE for Blessington (Pile 2)

Displacement (in)	**Base Shear Mobilized (lbs)**
0.00	0.00
0.02	85.59
0.03	142.64
0.06	213.96
0.08	256.76
0.10	285.28
0.19	285.28

Table 5.13: Base Shear Input into LPILE for Garryhesta

Displacement (in)	Base Shear Mobilized (lbs)
0.00	0.00
0.02	88.40
0.03	147.33
0.06	221.00
0.08	265.20
0.10	294.67
0.19	294.67

The results for the three pile load tests in Ireland are included as follows in Figures 5.20a, 5.20b, and 5.20c.

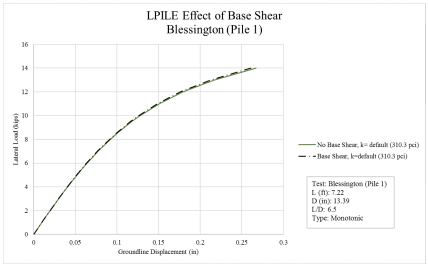

(a) Effect of Base Shear - Blessington (Pile 1)

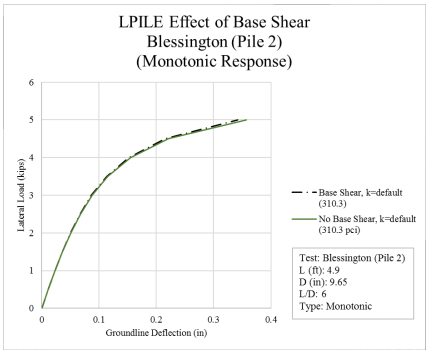

(b) Effect of Base Shear - Blessington (Pile 2)

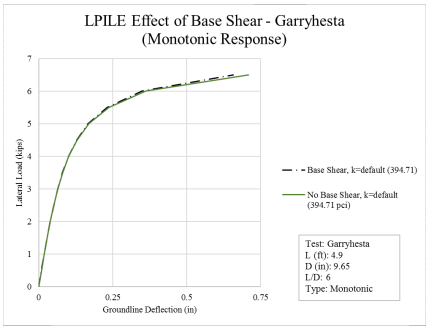

(c) Effect of Base Shear - Garryhesta

Figure 5.20: LPILE Sensitivity Analysis on Base Shear - Ireland Pile Load Tests (Monotonic Response)

It is found that the base shear has a very slight to negligible effect on the response of the piles. This could be due to the lower magnitude of force that is mobilized relative to the forces applied to the piles. While not producing much effect for the smaller diameter piles, it would be unwise to not consider the effect, especially when larger diameter piles are to be considered. With larger diameters, the area that is sheared is much larger and proportionately, the base shear would be much higher even for the same length of pile. Another

point worth considering is that the stresses in the base of the pile might not be the in-situ vertical stresses, but a much higher value locked in due to pile driving. If the stresses are high enough, the resulting base shear might have an effect on the response of the pile.

5.7 Summary

The results presented in this section are summarized as follows:

1. The low strain response is dependent on the subgrade modulus (k) which is dependent on the friction angle by conventional design standards (API RP 2GEO).

2. For the Mustang Island Tests, the initial stiffness fits quite well for the Reese model, but API model underestimates it. This is the case for both monotonic and cyclic tests. There is a stiffness reduction at higher strains when cyclic considerations are taken in the model.

3. For the Houston test, a higher k value gives a closer fit than when k values suggested by LPILE are used, with the data at small strain, but even then API underestimates the value.

4. The API method does not do well at predicting the behavior of the initial part of the curve when it is highly non-linear such as in the Houston test.

5. For the Ireland tests the design overestimates the stiffness and a lower k value fits the data very well across all the sites. There isn't a good fit for

the ultimate resistance though, and the API consistently underpredicts it.

6. From the cyclic tests at Blessington, there isn't a good fit with the inital stiffness of the prediction with the data. The API method considers a reduction in stiffness at large strains, whereas there is an increase in stiffness as per the data.

7. The cyclic consideration in LPILE, does not affect the initial stiffness much at small strains. The difference becomes apparent at larger strains.

8. There is a possible correlation between L/D ratio and initial stiffness of the piles. Lower L/D ratios give an overprediction of the initial stiffness using the API Method while the higher L/D ratios give an underprediction of initial stiffness using the API Method.

9. The effect of base shear is analyzed using a conventional t-z analysis to obtain the frictional resistance. Not much effect is seen on the response for the piles considered. This is thought to be because of the relatively low magnitude of base shear compared to the loading. It might be important to consider the effect in larger diameter piles, where the base area will be much larger.

Chapter 6

Conclusions

6.1 Conclusions

The conclusions from the analysis and observations in this thesis are summarized as follows:

1. There are subtle differences between the different codes utilized for p-y analysis, especially with the latest version API RP 2GEP (2011), where the procedure is less descriptive than the API RP 2A (2010).

2. The low strain response is dependent on the subgrade modulus (k) which is dependent on the friction angle by conventional design standards (API RP 2A/2GEO).

3. For the Mustang Island Tests, the initial stiffness fits quite well for the Reese model, but API model underestimates it. This is the case for both monotonic and cyclic tests. There is a stiffness reduction at higher strains when cyclic considerations are taken in the model.

4. The soil samples collected from Mustang Island show a match with the original soil at the site. This promotes the possibility of seismic site char-

acterization, and getting a better understanding of the initial stiffness at low strain levels.

5. For the Houston test, a higher k value gives a closer fit than when k values suggested by LPILE are used, with the data at small strain, but even then API underestimates the value.

6. The API method does not do well at predicting the behavior of the initial part of the curve when it is highly non-linear such as in the Houston test.

7. For the Ireland tests the design overestimates the stiffness and a lower k value fits the data very well across all the sites. There isn't a good fit for the ultimate resistance though, and the API consistently underpredicts it.

8. From the cyclic tests at Blessington, there isn't a good fit with the inital stiffness of the prediction with the data. The API method considers a reduction in stiffness at large strains, whereas there is an increase in stiffness as per the data.

9. The cyclic consideration in LPILE, does not affect the initial stiffness much at small strains. The difference becomes apparent at larger strains.

10. There is a possible correlation between L/D ratio and initial stiffness of the piles. Lower L/D ratios give an overprediction of the initial stiffness using the API Method while the higher L/D ratios give an underprediction of initial stiffness using the API Method.

11. The effect of base shear is analyzed using the frictional resistance at the tip of the pile. Not much effect is seen on the response for the piles considered. This is thought to be because of the relatively low magnitude of base shear compared to the loading. It might be important to consider the effect in larger diameter piles, where the base area will be much larger. Another consideration could be that the higher stresses from pile driving are locked in at the tip and these bearing stresses are contributing to the base friction.

6.2 Recommended Future Work

These results show merit in being able to choose better fitting k values to predict the response of the pile. The best approach to understanding the behavior of large diameter relatively short rigid piles is to run full scale model tests and calibrate the p-y curves accordingly. But that is a highly expensive method and might not be feasible at this stage of research. Another approach would be creating a better soil constitutive model through finite element analysis that takes into account changing shear stiffness at small strains. If validated by lab scale testing that inputs fundamental soil properties (shear wave velocity), it seems possible to establish k value that predicts the response well and can be used in design directly. The Mustang Island sand samples would be crucial in understanding the small strain behavior of the piles. Further study will involve analyzing centrifuge data and field data for cyclic loading, and investigating non-linear models for the initial stiffness.

Appendices

Appendix A

Lateral Load Test Database

The compiled lateral load test database for monopiles in sand is contained in a spreadsheet "Database of Lateral Load Test of Monopiles in Sands.xlsx" which is available with this thesis as a supplemental file. The table of contents of the database are shown in Table A.1.

Table A.1: Table of Contents of Lateral Load Test Database

No.	Field/ Lab	Cyclic Loading	Location	Soil	Diameter (in)	Length(ft)	L/D	Type	Source
1	F	Y	Mustang Island, TX	Sand	24	69.0	34.5	Steel Pipe Pile	Cox et al. (1974), Reese (1996), Reese & Van Impe (2001)
2	F	N	Building Research Establishment, Garston	Sand and Gravel	59.1	41.0	8.3	RC Solid Circular	Price & Wardle (1987), Reese (1996), Reese & Van Impe (2001)
3	F	N	Pine Bluff, Arkansas	Sand	16	49.2	36.9	Steel Pipe Pile	Alizadeh & Davisson (1970), Reese (1996), Reese & Van Impe (2001), Mansur & Hunter (1970), Meyer & Reese (1979)
4	F	N	Pine Bluff, Arkansas	Sand	16	49.2	36.9	Steel Pipe Pile	Alizadeh & Davisson (1970), Reese (1996), Reese & Van Impe (2001), Mansur & Hunter (1970), Meyer & Reese (1979)
5	F	N	Alcacer do Sol	Layered Clay and Sand	47.2	131.2	33.4	RC Drilled Shaft	Portugal & Seco e Pinto (1993), Reese & Van Impe (2001)
6	F	N	Miami, FL	Layered Clay and Sand	56	26.0	5.6	Steel Pipe Pile (with a portion concrete filled)	Davis (1977), Reese & Van Impe (2001), Reese & Meyer (1979)
7	F	N	South Surra, Kuwait	Sand (Cemented)	11.8	16.4	16.7	RC Drilled Shaft	Ismael (1990), Reese & Van Impe (2001), FindAPile.com by the DFI, ADSC and UC Irvine
8	F	N	Jleeb Al-Shuyoukh, Kuwait	Sand	12	16.4	16.4	RC Drilled Shaft	Ismael (2007), FindAPile.com by the DFI, ADSC and UC Irvine
9	F	N	Jleeb Al-Shuyoukh, Kuwait	Sand	12	16.4	16.4	RC Drilled Shaft	Ismael (2007), FindAPile.com by the DFI, ADSC and UC Irvine

Continued on next page

No.	Field/ Lab	Cyclic Loading	Location	Soil	Diameter (in)	Length(ft)	L/D	Type	Source
10	F	N	Oregon Inlet, NC	Sand	66	106.0	19.3	Prestressed Concrete Pile	Keaney & Batts (2007), UFlorida Database
11	F	N	Oregon Inlet, NC	Sand	54	71.0	15.8	RC Drilled Shaft	Keaney & Batts (2007), UFlorida Database
12	F	N	Onslow, NC	Sand	48	57.0	14.3	RC Drilled Shaft	UFlorida Database, NCDOT
13	F	N	New Bern, NC	Sand	48	44.0	11.0	RC Drilled Shaft	UFlorida Database, NCDOT
14	F	N	Nevada	Sand	96	32.0	4.0	RC Drilled Shaft	UFlorida Database
15	F	N	Skyway Bridge Site	Sand	48	51.0	12.8	RC Drilled Shaft	UFlorida Database, FDOT
16	F	N	Skyway Bridge Site	Sand	48	51.0	12.8	RC Drilled Shaft	UFlorida Database, FDOT
17	F	N	California	Layered Clay, Silt and Sand	96	62.0	7.8	RC Drilled Shaft	UFlorida Database, Caltrans
18	F	N	Jacksonville, FL	Marl	72	114.0	19.0	RC Drilled Shaft	UFlorida Database, Castelli & Fan (2002)
19	F	N	Jacksonville, FL	Marl	72	114.0	19.0	RC Drilled Shaft	UFlorida Database, Castelli & Fan (2002)
20	F	N	Century Freeway, California	Layered Clay and Sand	96	56.0	7.0	RC Drilled Shaft	UFlorida Database, Caltrans, Naramore & Feng (1990)
21	F	N	Century Freeway, California	Layered Clay and Sand	48	51.0	12.8	RC Drilled Shaft	UFlorida Database, Caltrans, Naramore & Feng (1990)
22	F	N	Century Freeway, California	Layered Clay and Sand	50.4	50.0	11.9	RC Drilled Shaft	UFlorida Database, Caltrans, Naramore & Feng (1990)
23	F	N	Century Freeway, California	Layered Clay and Sand	97.2	59.0	7.3	RC Drilled Shaft	UFlorida Database, Caltrans, Naramore & Feng (1990)
24	F	N	Daytona Broadway Bridge, FL	Layered Clay and Sand	60	93.0	18.6	RC Drilled Shaft	UFlorida Database
25	F	N	Boston	Sand (Silty)	48	173.0	43.3	Drilled Shaft with Casing	FHWA Database
26	F	N	Boston	Sand (Silty)	54	171.0	38.0	Drilled Shaft with Casing	FHWA Database
27	F	N	Boston	Sand (Silty)	48	156.0	39.0	Drilled Shaft with Casing	FHWA Database
28	F	N	Boston	Sand (Silty)	54	144.3	32.1	Drilled Shaft with Casing	FHWA Database
29	F	Y	UC San Diego, CA	Sand (Silty)	16	15.0	11.3	RC Drilled Shaft	Juirnarongrit and Ashford (2004), FindAPile.com by the DFI, ADSC and UC Irvine
30	F	Y	UC San Diego, CA	Sand (Silty)	24	39.0	19.5	RC Drilled Shaft	Juirnarongrit and Ashford (2004), FindAPile.com by the DFI, ADSC and UC Irvine
31	F	Y	UC San Diego, CA	Sand (Silty)	35	39.0	13.4	RC Drilled Shaft	Juirnarongrit and Ashford (2004), FindAPile.com by the DFI, ADSC and UC Irvine

Continued on next page

No.	Field/ Lab	Cyclic Loading	Location	Soil	Diameter (in)	Length(ft)	L/D	Type	Source
32	F	Y	UC San Diego, CA	Sand (Silty)	47	39.0	10.0	RC Drilled Shaft	Juirnarongrit and Ashford (2004), FindAPile.com by the DFI, ADSC and UC Irvine
33	F	N	Naselle, WA	Sand (Silty)	18	75.0	50.0	Steel Pipe Pile	FHWA, Kramer (1991)
34	F	N	Naselle, WA	Sand (Silty)	18	77.0	51.3	Steel Pipe Pile	FHWA, Kramer (1991)
35	F	N	Naselle, WA	Sand (Silty)	8	46.0	69.0	Steel Pipe Pile	FHWA Database
36	F	N	Naselle, WA	Sand (Silty)	8	54.0	81.0	Steel Pipe Pile	FHWA Database
37	F	N	Florence Ave, CA	Sand (Silty)	16	34.0	25.5	RC Drilled Shaft	FHWA Database
38	F	N	Florence Ave, CA	Sand (Silty)	16	34.9	26.1	RC Drilled Shaft	FHWA Database
39	F	N	Atlantic Boulevard, CA	Layered Clay and Sand	15.5	35.0	27.1	RC Drilled Shaft	FHWA Database
40	F	Y	Houston, TX	Sand	24	100.0	50.0	Steel Pipe Pile	Little & Briaud (1988)
41	F	Y	Houston, TX	Sand	36	97.0	32.3	RC Drilled Shaft	Little & Briaud (1988)
42	F	Y	Houston, TX	Sand	42	128.0	36.6	RC Drilled Shaft	Little & Briaud (1988)
43	F	Y	Houston, TX	Sand	42	128.0	36.6	RC Drilled Shaft	Little & Briaud (1988)
44	F	Y	Houston, TX	Sand	42	128.0	36.6	RC Drilled Shaft	Little & Briaud (1988)
45	F	Y	Houston, TX	Layered Clay and Sand	10.75	38.7	43.2	Steel Pipe Pile	Dunnavant & O'Neill (1985)
46	F	N	Roosevelt Bridge, FL	Sand	30	48.0	19.2	Prestressed Concrete Pile	Ruesta & Townsend (1997), Anderson, Townsend, & Grajales (2003)
47	F	Y	UC Davis, CA	Sand	16	18.0	13.5	RC Wished in Place Pile	Chai and Hutchinson (2001)
48	F	Y	UC Davis, CA	Sand	16	18.0	13.5	RC Wished in Place Pile	Chai and Hutchinson (2001)
49	F	Y	UC Davis, CA	Sand	16	18.0	13.5	RC Wished in Place Pile	Chai and Hutchinson (2001)
50	F	Y	UC Davis, CA	Sand	16	18.0	13.5	RC Wished in Place Pile	Chai and Hutchinson (2001)
51	L	N	Newfoundland, Canada	Sand	4.02	2.0	6.0	Steel Pipe Pile	Prasad & Chari (1999)
52	L	Y	UT Austin	Sand	6	0.5	1.0	Steel Suction Caisson	Chen & Gilbert (Unpublished)
53	L	N	Turkey	Sand	1.97	0.7	4.0	Steel Pipe Pile	Uncuoglu & Mustafa (2011)
54	L	N	Turkey	Sand	1.97	0.7	4.0	Steel Pipe Pile	Uncuoglu & Mustafa (2011)
55	L	N	Turkey	Sand	1.97	0.7	4.0	Steel Pipe Pile	Uncuoglu & Mustafa (2011)
56	L	N	Turkey	Sand	1.97	0.7	4.0	Steel Pipe Pile	Uncuoglu & Mustafa (2011)
57	L	N	Turkey	Sand	1.97	0.7	4.0	Steel Pipe Pile	Uncuoglu & Mustafa (2011)
58	L	Y	University of Oxford, UK	Sand	3.15	1.2	4.5	Copper Pipe Pile	LeBlanc, Houlsby and Byrne (2010)
59	F	Y	Seal Beach, CA	Sand (Silty)	24.0	32.0	16.0	Steel Pipe Pile	Ting (1987)

Continued on next page

No.	Field/ Lab	Cyclic Loading	Location	Soil	Diameter (in)	Length(ft)	L/D	Type	Source
60	L	N	University of Liverpool, UK	Sand	48.2	30.0	7.5	Steel Pipe Pile (Prototype Dimensions)	Georgiadis et al.(1991)
61	L	N	University of Liverpool, UK	Sand	48.2	30.0	7.5	Steel Pipe Pile (Prototype Dimensions)	Georgiadis et al.(1991)
62	F	N	Shanghai, China	Layered Clay and Sand (Silty)	110.24	236.0	25.7	Steel Pipe Pile	Pan et al. (2016)
63	F	N	Blessington, Ireland	Sand	13.39	7.2	6.5	Steel Pipe Pile	Doherty & Gavin (2010)
64	L	Y	Houston, TX	Sand	36	86.6	28.9	Pipe Pile (Prototype Dimensions)	Zakeri et al (2016)
65	L	Y	Cambridge University, UK	Sand	2	0.8	4.9	Steel Pipe Pile (Actual Model Dimensions)	Li, Haigh & Bolton (2010)
66	L	Y	Cambridge University, UK	Sand	2	0.8	4.9	Steel Pipe Pile (Actual Model Dimensions)	Li, Haigh & Bolton (2010)
67	L	Y	Cambridge University, UK	Sand	2	0.8	4.9	Steel Pipe Pile (Actual Model Dimensions)	Li, Haigh & Bolton (2010)
68	L	Y	Cambridge University, UK	Sand	2	0.8	4.9	Steel Pipe Pile (Actual Model Dimensions)	Li, Haigh & Bolton (2010)
69	F	N	Garryhesta, Ireland	Sand	9.65	4.9	6.1	Steel Pipe Pile	Murphy et al. (2016)
70	F	N	Garryhesta, Ireland	Sand	9.65	4.9	6.1	Winged Monopile	Murphy et al. (2016)
71	F	N	Garryhesta, Ireland	Sand	9.65	4.9	6.1	Winged Monopile	Murphy et al. (2016)
72	F	N	Blessington, Ireland	Sand	9.65	4.9	6.1	Steel Pipe Pile	Murphy et al. (2016)
73	F	N	Blessington, Ireland	Sand	9.65	4.9	6.1	Winged Monopile	Murphy et al. (2016)
74	F	N	Blessington, Ireland	Sand	9.65	4.9	6.1	Winged Monopile	Murphy et al. (2016)
75	L	N	Bethlehem, PA	Sand	4	5.0	15.0	Steel Pipe Pile	Lin et al. (2015)
76	L	Y	TU Delft	Sand	173	72.0	5.0	Steel (Prototype Dimensions)	Alderlieste et al. (2011)
77	L	Y	TU Delft	Sand	173	72.0	5.0	Steel (Prototype Dimensions)	Alderlieste et al. (2011)
78	F	N	Treasure Island, CA	Silty Sand	12.75	37.7	35.5	Steel Pipe Pile	Alderlieste et al. (2011)
79	L	Y	Aalborg University, Denmark	Sand	2	1.3	7.9	Steel Pipe Pile	Moller and Christiansen (2011)
80	L	Y	Technical University of Denmark, Denmark	Sand	39.37	19.7	6.0	Steel (Prototype Dimensions)	Klinkvort et al. (2010)
81	L	Y	Technical University of Denmark, Denmark	Sand	39.37	26.3	8.0	Steel (Prototype Dimensions)	Klinkvort et al. (2010)
82	L	Y	Technical University of Denmark, Denmark	Sand	39.37	32.8	10.0	Steel (Prototype Dimensions)	Klinkvort et al. (2010)

Concluded

Appendix B

Supplemental Information about Test Sites

B.1 Mustang Island, TX

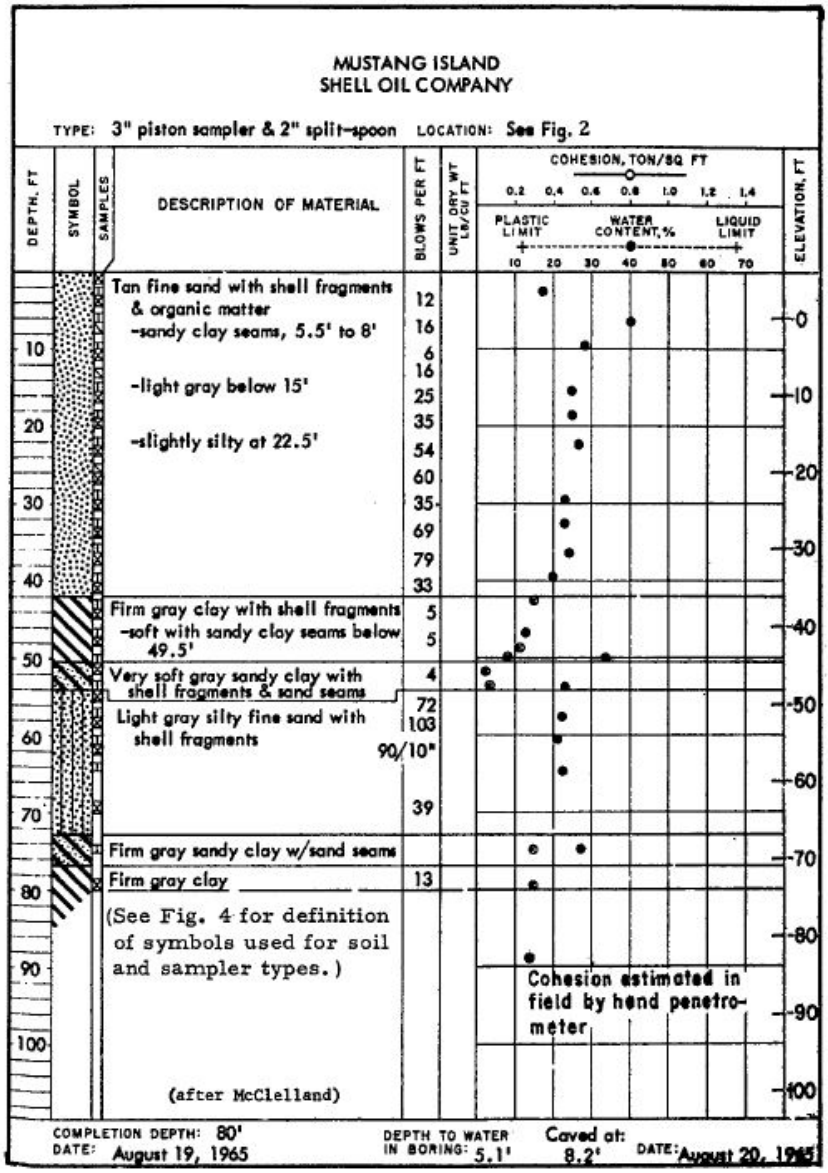

Figure B.1: Boring Log of Borehole 1 at Mustang Island (Cox et al., 1974)

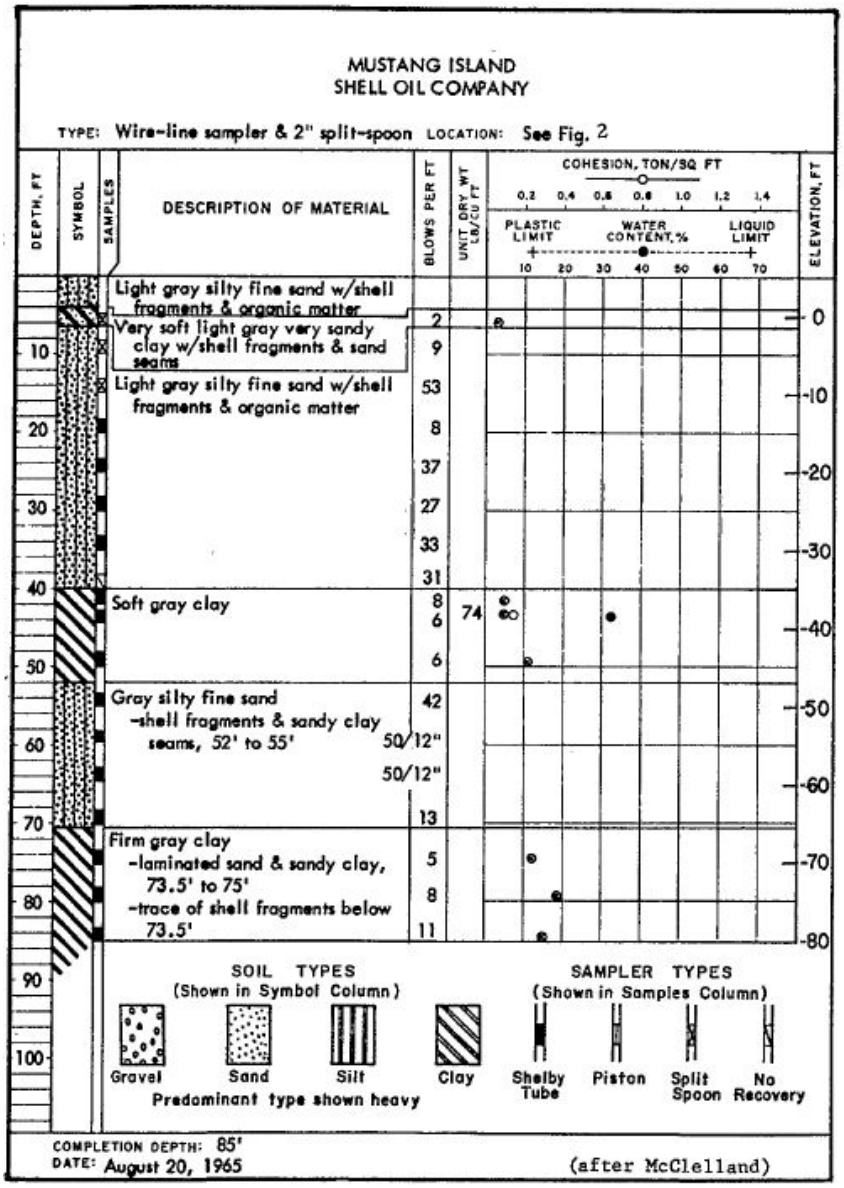

Figure B.2: Boring Log of Borehole 2 at Mustang Island (Cox et al., 1974)

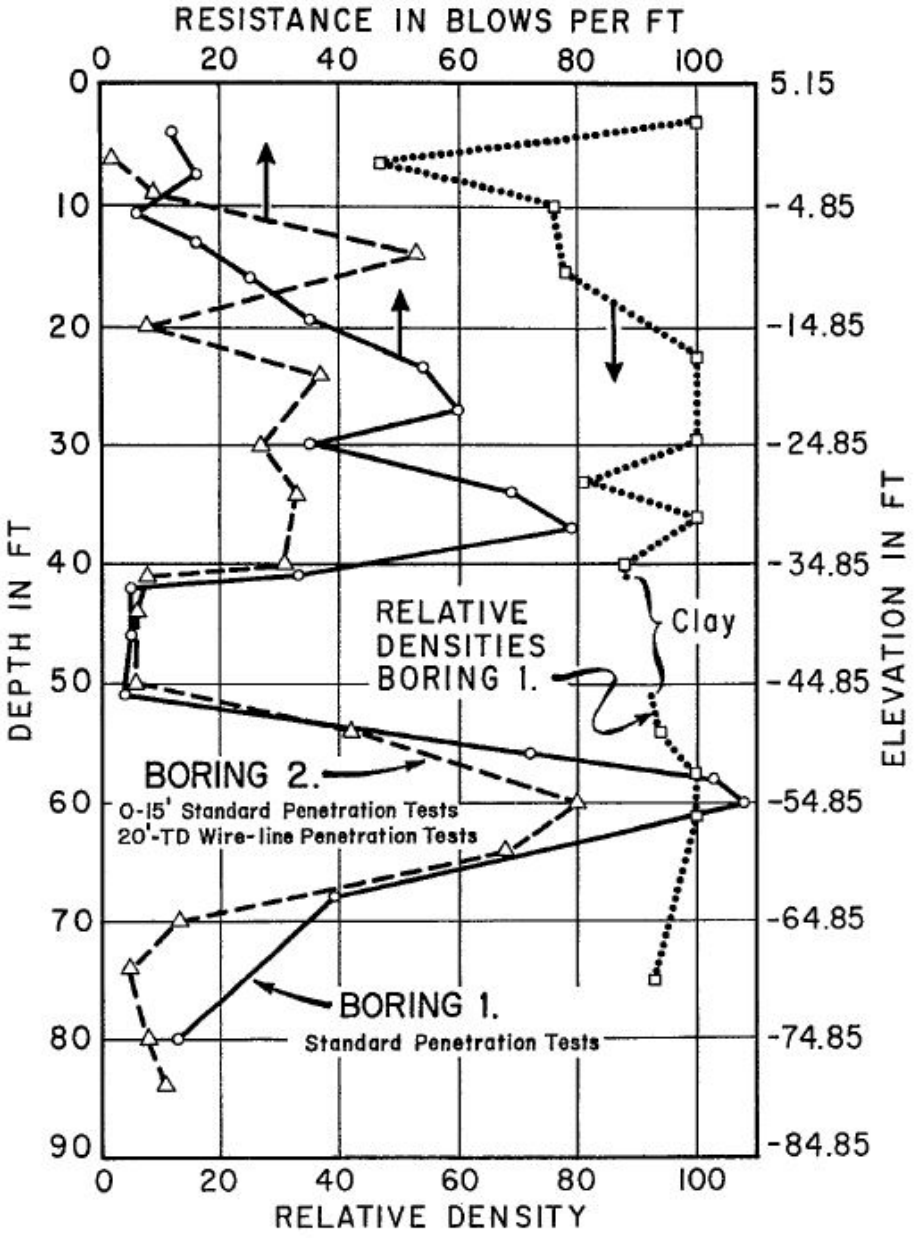

Figure B.3: Results of standard and wire-line penetration test and relative density values from piston samples (Cox et al., 1974)

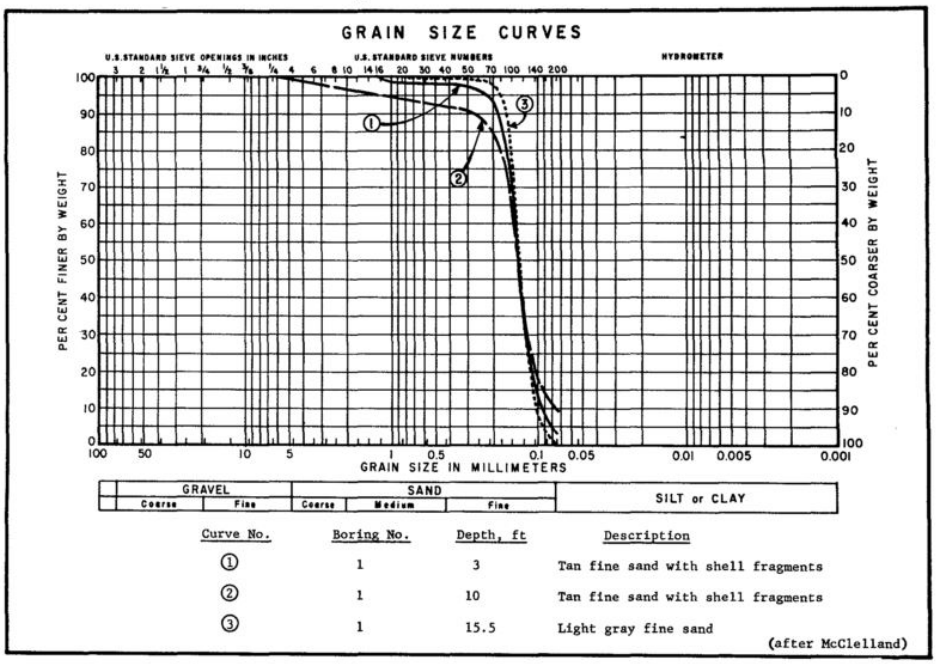

Figure B.4: Original Grain Size Distribution at Mustang Island (Cox et al., 1974)

B.2 Houston, TX

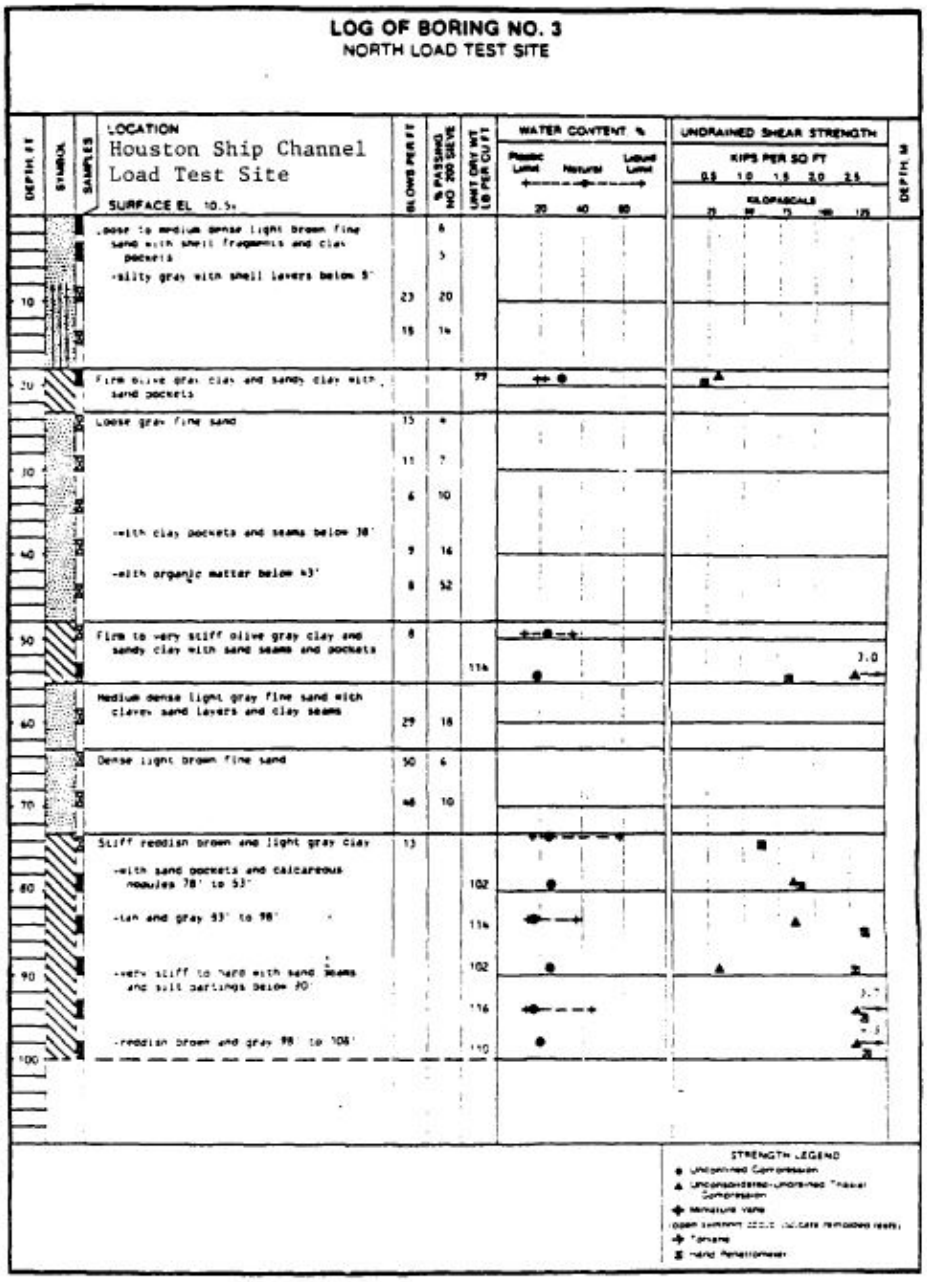

Figure B.5: Borehole Log at Houston (Little and Briaud, 1988)

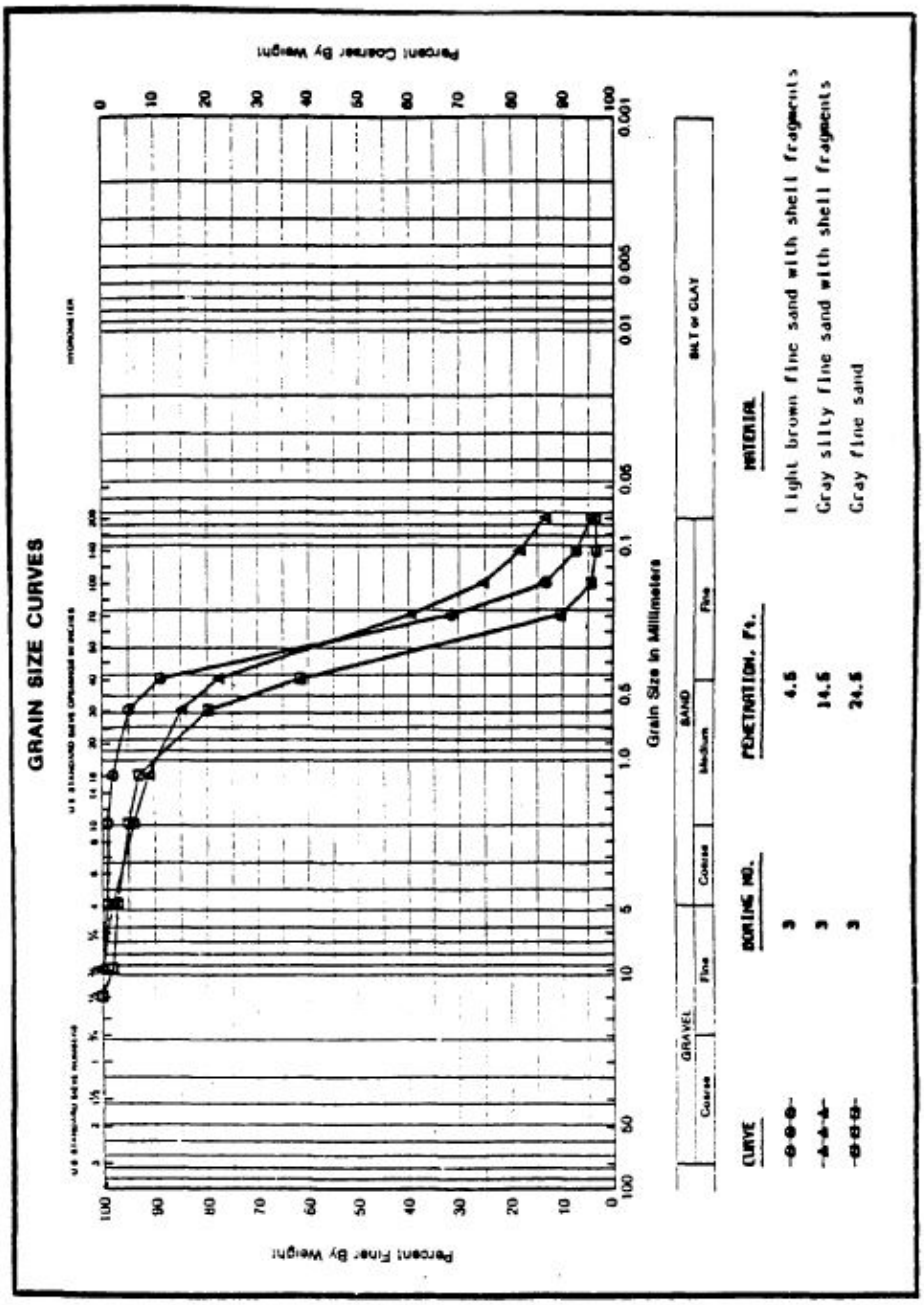

Figure B.6: Original Grain Size Distribution at Houston (Little and Briaud, 1988)

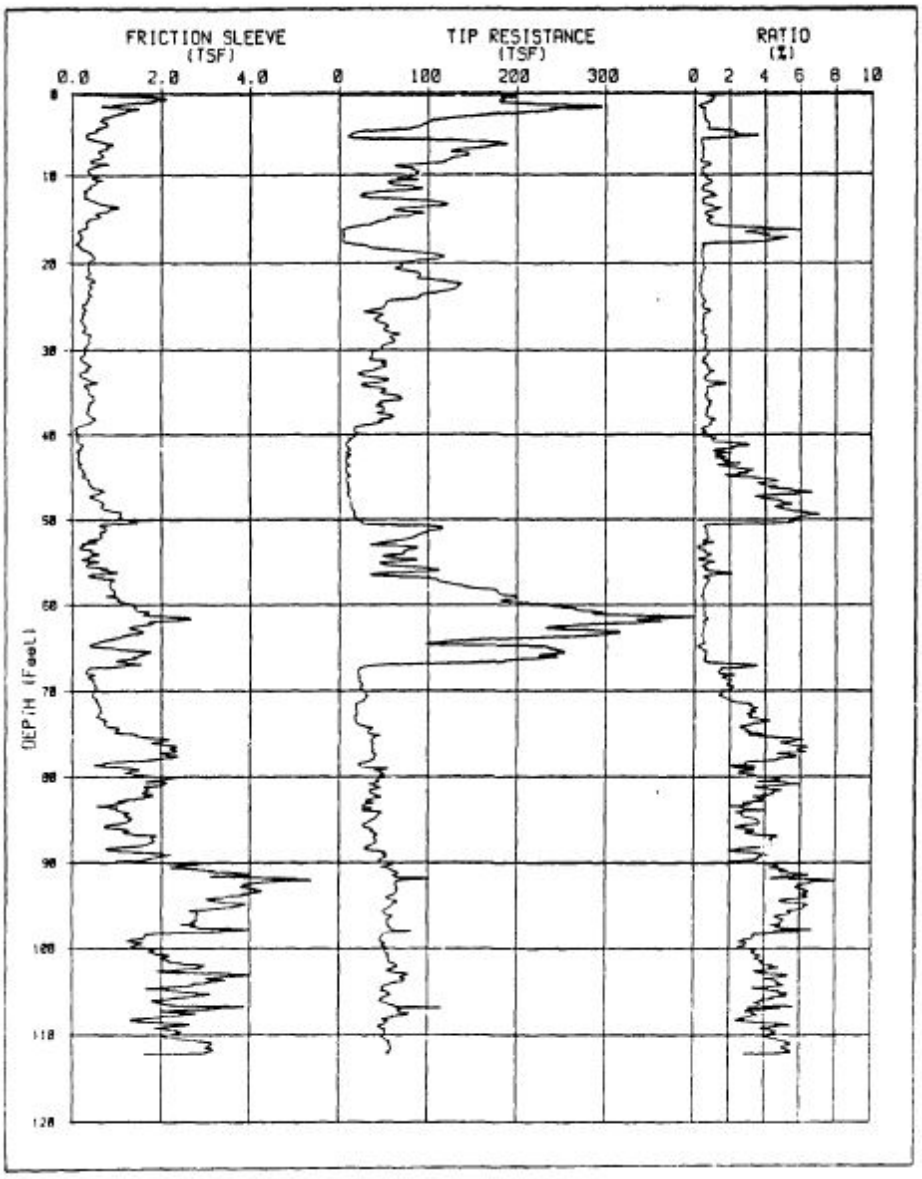

Figure B.7: CPT Profile 1 at Houston (Little and Briaud, 1988)

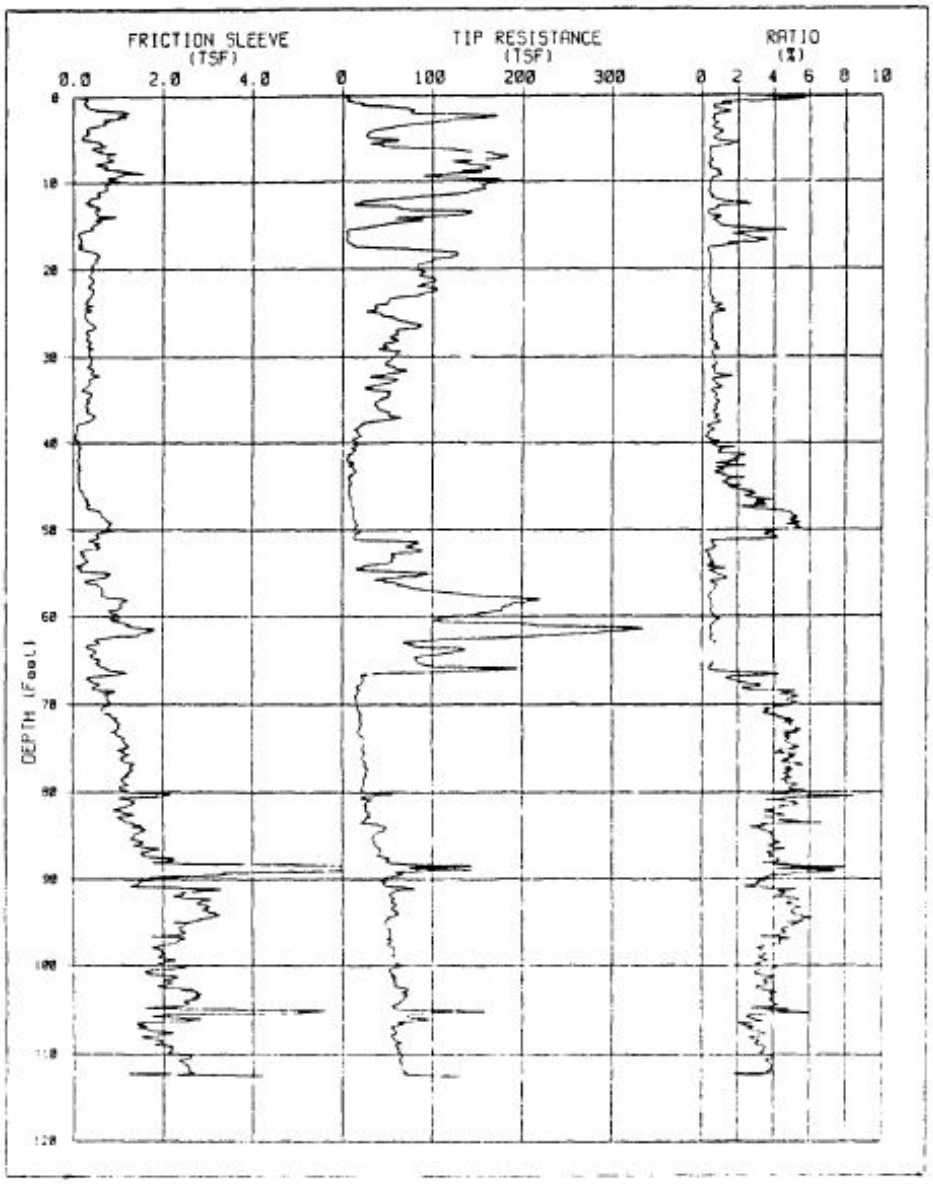

Figure B.8: CPT Profile 2 at Houston (Little and Briaud, 1988)

B.3 Ireland

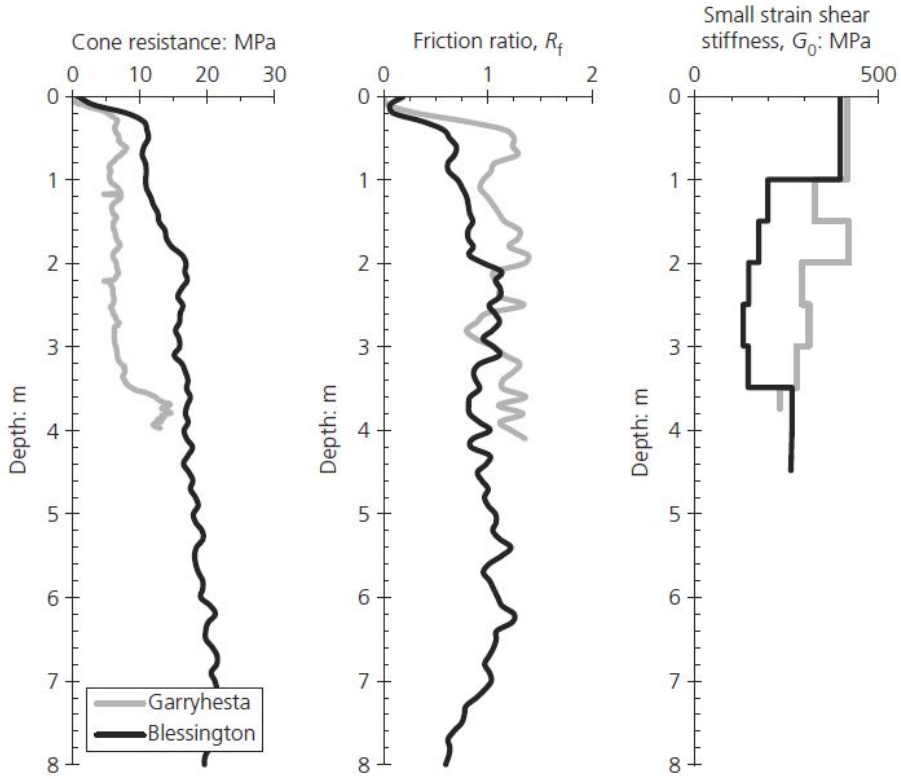

Figure B.9: Comparison of Blessington and Garryhesta Site Characterization (Murphy et al., 2016)

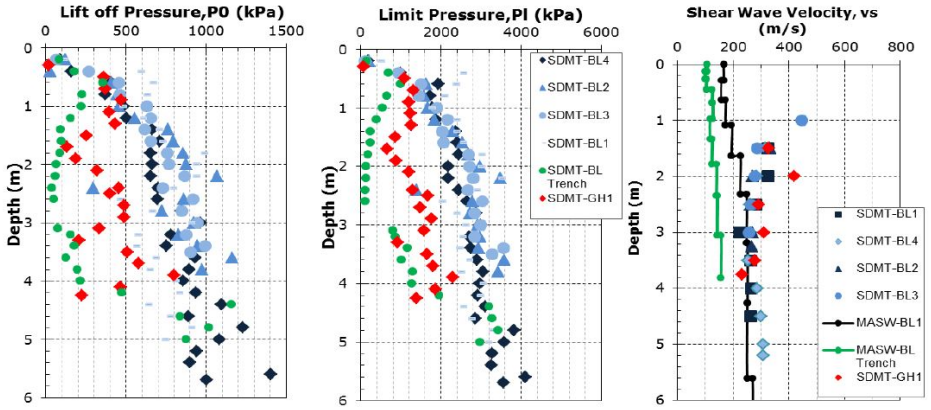

Figure B.10: DMT Data at both Garryhesta (GH) and Blessington (BL) (Murphy et al., 2014)

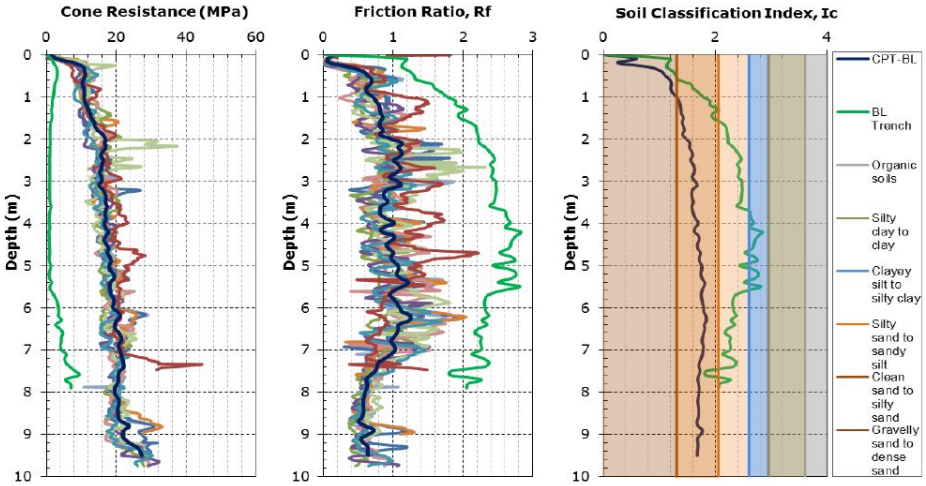

Figure B.11: CPT Data at Blessington (Murphy et al., 2014)

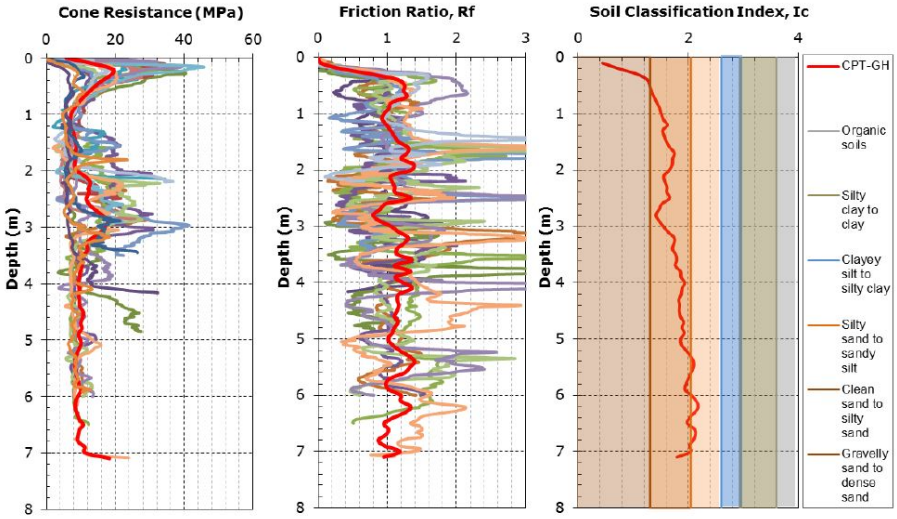

Figure B.12: CPT Data at Garryhesta (Murphy et al., 2014)

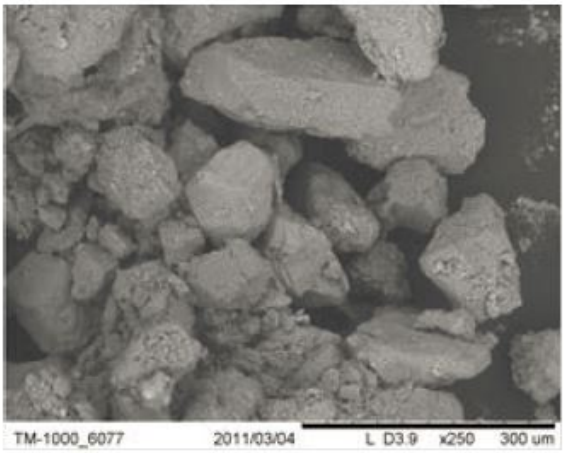

Figure B.13: Scanning Electron Microscope Image of Sands at Blessington (Doherty et al., 2012a)

Bibliography

Abadie, C., Byrne, B., and Levy-Paing, S. (2015). "Model pile response to multi-amplitude cyclic lateral loading in cohesionless soils.

Achmus, M., Abdel-Rahman, K., and Kuo, Y. (2007). "Numerical modelling of large diameter steel piles under monotonic and cyclic horizontal loading." *Tenth International Symposium on Numerical Models in Geomechanics*, Taylor & Francis London, 453–459.

Achmus, M., Abdel-Rahman, K., and Peralta, P. (2005). "On the design of monopile foundations with respect to static and quasi-static cyclic loading." *Proceedings of the Offshore Wind Energy Conference*, Copenhagen:[sn].

Achmus, M., Thieken, K., Lemke, K., et al. (2014). "Evaluation of py approaches for large diameter monopiles in sand." *The Twenty-fourth International Ocean and Polar Engineering Conference*, International Society of Offshore and Polar Engineers.

Ahmed, S. S. and Hawlader, B. (2016). "Numerical analysis of large-diameter monopiles in dense sand supporting offshore wind turbines." *International Journal of Geomechanics*, 16(5), 04016018.

Ahmed, S. S., Hawlader, B., and Roy, K. (2015). "Finite element modeling of large diameter monopiles in dense sand for offshore wind turbine founda-

tions." *ASME 2015 34th International Conference on Ocean, Offshore and Arctic Engineering*, American Society of Mechanical Engineers.

Alderlieste, E. A. (2011). "Experimental modelling of lateral loads on large diameter mono-pile foundations in sand." *Delft University of Technology, Delft*.

Alderlieste, E. A., Dijkstra, J., and van Tol, A. F. (2011). "Experimental investigation into pile diameter effects of laterally loaded mono-piles." *ASME 2011 30th International Conference on Ocean, Offshore and Arctic Engineering*, American Society of Mechanical Engineers, 985–990.

Alizadeh, M. and Davisson, M. (1970). "Lateral load tests on piles-arkansas river project." *Journal of Soil Mechanics & Foundations Div.*

Anderson, J., Townsend, F., and Grajales, B. (2003). "Case history evaluation of laterally loaded piles." *Journal of geotechnical and geoenvironmental engineering*, 129(3), 187–196.

Anderson, J. B. and Townsend, F. (2002). "A laterally loaded pile database." *Deep Foundations 2002: An International Perspective on Theory, Design, Construction, and Performance*, 262–273.

API (2010). "Rp 2a-wsd: Recommended practice for planning, designing and constructing fixed offshore platforms working stress design." *American Petroleum Institute*.

API (2011). "Rp 2geo: Recommended practice for geotechnical and foundation design consideration." *American Petroleum Institute*.

Arshad, M. and OKelly, B. C. (2016). "Model studies on monopile behavior under long-term repeated lateral loading." *International Journal of Geomechanics*, 17(1).

Ashford, S. A. and Juirnarongrit, T. (2003). "Evaluation of pile diameter effect on initial modulus of subgrade reaction." *Journal of Geotechnical and Geoenvironmental Engineering*, 129(3), 234–242.

Bae, K.-t., Lee, M., Lee, J., Kim, Y., Youn, H., Lee, D., et al. (2015). "Lateral behavior of monopile for offshore wind power using centrifugal model tests on sandy soil." *The Twenty-fifth International Offshore and Polar Engineering Conference*, International Society of Offshore and Polar Engineers.

Barton, Y., Finn, W., Parry, R., Towhata, I., et al. (1983). "Lateral pile response and py curves from centrifuge tests." *Offshore Technology Conference*, Offshore Technology Conference.

Beaudry-Losique, J., Boling, T., Brown-Saracino, J., Gilman, P., Hahn, M., Hart, C., Johnson, J., McCluer, M., Morton, L., Naughton, B., Norton, G., Ram, B., Redding, T., and Wallace, W. (2011). "A national offshore wind strategy: Creating an offshore wind energy industry in the united states." *Report No. DOE/GO-102011 2988*, Office of Energy Efficiency and Renewable Energy (EERE), Washington, DC (United States).

Bekken, L. (2009). "Lateral behavior of large diameter offshore monopile foundations for wind turbines.

Blanco, M. I. (2009). "The economics of wind energy." *Renewable and Sustainable Energy Reviews*, 13(6), 1372–1382.

Bouafia, A. and Garnier, J. (1991). "Experimental study of py curves for piles in sand." *Centrifuge*, Vol. 91, 261–268.

Bowman, E. R. (1958). *Investigation of the lateral resistance to movement of a plate in cohesionless soil*.

Brødbæk, K., Augustesen, A. H., Møller, M., and Sørensen, S. H. (2011). "Physical modelling of large diameter piles in coarse-grained soil." *Geotechnical Engineering: New Horizons: Proceedings of the 21st European Young Geotechnical Engineers' Conference, Rotterdam 2011*, IOS Press, 69.

Byrne, B., McAdam, R., Burd, H., Houlsby, G., Martin, C., Gavin, K., Doherty, P., Igoe, D., Zdravkovic, L., Taborda, D., et al. (2015a). "Field testing of large diameter piles under lateral loading for offshore wind applications.

Byrne, B., McAdam, R., Burd, H., Houlsby, G., Martin, C., Zdravkovi, L., Taborda, D., Potts, D., Jardine, R., and Sideri, M. (2015b). "New design methods for large diameter piles under lateral loading for offshore wind applications." *3rd International Symposium on Frontiers in Offshore Geotechnics (ISFOG 2015), Oslo, Norway, June*, 10–12.

Castelli, R. J. and Fan, K. (2002). "O-cell test results for drilled shafts in marl and limestone." *Deep Foundations 2002: An International Perspective on Theory, Design, Construction, and Performance*, 807–823.

Chen, R.-p., Sun, Y.-x., Zhu, B., and Guo, W. D. (2015). "Lateral cyclic pile-soil interaction studies on a rigid model monopile.

Choo, Y. W. and Kim, D. (2015). "Experimental development of the p-y relationship for large-diameter offshore monopiles in sands: Centrifuge tests." *Journal of Geotechnical and Geoenvironmental Engineering*, 142(1), 04015058.

Choo, Y. W., Kim, D., Park, J.-H., Kwak, K., Kim, J.-H., and Kim, D.-S. (2013). "Lateral response of large-diameter monopiles for offshore wind turbines from centrifuge model tests.

Cox, W. R., Reese, L. C., and Grubbs, B. R. (1974). "Field testing of laterally loaded piles in sand." *Offshore Technology Conference*, Offshore Technology Conference.

Curras, C. J., Hutchinson, T. C., Boulanger, R. W., Chai, Y.-H., and Idriss, I. (2001). "Lateral loading & seismic response of cidh pile supported bridge structures." *Foundations and Ground Improvement:*, ASCE, 260–275.

Davis, L. H. (1977). "Tubular steel foundation." *Report no.*

DNV-GL (2016). "Dnv-st-0126-support structures for wind turbines." *Det Norske Veritas - Germanischer Lloyd*.

Doherty, P. and Gavin, K. (2011). "Laterally loaded monopile design for offshore wind farms.

Doherty, P., Kirwan, L., Gavin, K., Igoe, D., Tyrrell, S., Ward, D., and O'Kelly, B. C. (2012a). "Soil properties at the ucd geotechnical research site at blessington." *Bridge and Concrete Research in Ireland 2012, Dublin, Ireland, 6-7 September, 2012*.

Doherty, P., Li, W., Gavin, K., Casey, B., et al. (2012b). "Field lateral load test on monopile in dense sand." *Offshore Site Investigation and Geotechnics: Integrated Technologies-Present and Future*, Society of Underwater Technology.

Dunnavant, T. W. and O'Neill, M. W. (1985). *Performance, Analysis, and Interpretation of a Lateral Load Test of a 72-inch-diameter Bored Pile in Overconsolidated Clay*. University of Houston, Department of Civil Engineering.

Ebin, D. M. (2012). "The response of monopile wind turbine foundations in sand to cyclic loading." Ph.D. thesis, Tufts University, Tufts University.

Edgers, L., Bradshaw, A. S., Ebin, D., et al. (2013). "A simplified approach to modeling long-term monopile serviceability with finite element analysis." *Offshore Technology Conference*, Offshore Technology Conference.

Emery, K. O. (1966). *Atlantic continental shelf and slope of the United States: Geologic background*. Number 529. US Government Printing Office.

Georgiadis, M., Anagnostopoulos, C., and Saflekou, S. (1992). "Centrifugal testing of laterally loaded piles in sand." *Canadian Geotechnical Journal*, 29(2), 208–216.

GIANNAKOS, S., GEROLYMOS, N., and GAZETAS, G. (2011). "On the lateral response of piles: numerical analysis against centrifuge experiments." *Santiago*, 10, 13.

Gilman, P., Maurer, B., Feinberg, L., Duerr, A., Peterson, L., Musial, W., Beiter, P., Golladay, J., Stromberg, J., Johnson, I., Boren, D., and Moore, A. (2016). "A national offshore wind strategy: Facilitating the development of the offshore wind industry in the united states." *Report No. DOE/GO-102016-4866*, U.S. Department of Energy and U.S. Department of Interior,.

GWEC (2017). "Global wind statistics 2016." *Global Wind Report*.

Hansen, M., Wolf, T. K., Rasmussen, K. L., Roesen, H. R., and Ibsen, L. B. (2013). "Physical modelling of cyclic laterally loaded pile in cohesionless soil." *Report no.*, Department of Civil Engineering, Aalborg University.

Hanssen, S. B. and Eiksund, G. (2014). "Dynamic model test of monopile for offshore wind turbines." *ASME 2014 33rd International Conference on Ocean, Offshore and Arctic Engineering*, American Society of Mechanical Engineers.

Hetényi, M. (1946). *Beams on Elastic Foundation;: Theory with Applications*

in the Fields of Civil and Mechanical Engineery. University of Michigan press.

Hutchinson, T. C., Chai, Y., and Boulanger, R. W. (2005). "Simulation of full-scale cyclic lateral load tests on piles." *Journal of geotechnical and geoenvironmental engineering*, 131(9), 1172–1175.

IEA (2016). "Decoupling of global emissions and economic growth confirmed." *Press Release*, International Energy Agency, <http://www.iea.org/newsroom/news/2016/march/decoupling-of-global-emissions-and-economic-growth-confirmed.html> (Paris, 16 March 2016).

Isenhower, W. and Wang, S. (2016a). "Technical manual for lpile 2016 (using data format version 9)." *Ensoft Inc., Austin, TX.*

Isenhower, W. M. and Wang, S. (2016b). "Users manual for lpile 2016 (using data format version 9)." *Ensoft, Austin, TX.*

Ismael, N. F. (1990). "Behavior of laterally loaded bored piles in cemented sands." *Journal of Geotechnical Engineering*, 116(11), 1678–1699.

Ismael, N. F. (2007). "Lateral load tests on bored piles and pile groups in sand." *7th FMGM 2007: Field Measurements in Geomechanics*, 1–11.

Juirnarongrit, T. and Ashford, S. (2004). "Lateral load behavior of cast-in-drilled-hole piles in weakly cemented sand." *Transportation Research Record: Journal of the Transportation Research Board*, (1868), 190–198.

Juirnarongrit, T. and Ashford, S. A. (2001). "Effect of pile diameter on the modulus of sub-grade reaction." *SSRP*, 22.

Kaiser, M. J. and Snyder, B. (2012). "Offshore wind energy cost modeling: installation and decommissioning." Vol. 85, Springer Science & Business Media, Chapter 2, 13–30.

Kalavar, S. and Ealy, C. (2000). "Fhwa deep foundation load test database." *New Technological and Design Developments in Deep Foundations*, 192–206.

Kallehave, D., Byrne, B. W., Thilsted, C. L., and Mikkelsen, K. K. (2015). "Optimization of monopiles for offshore wind turbines." *Phil. Trans. R. Soc. A*, 373(2035).

Keaney, B. and Batts, J. (2007). "Concrete cylinder piles at oregon inlet, north carolina." *Contemporary Issues In Deep Foundations*, 1–10.

Kirkwood, P. and Haigh, S. (2014). "Centrifuge testing of monopiles subject to cyclic lateral loading." *Proceedings of the 8th International Conference of Physical Modelling in Geotechnics (ICPMG)*, Taylor & Francis Group, London, UK, 827–831.

Klinkvort, R. T. (2013). *Centrifuge modelling of drained lateral pile-soil response*. Technical University of Denmark.

Klinkvort, R. T. and Hededal, O. (2013). "Lateral response of monopile supporting an offshore wind turbine." *Proceedings of the Institution of Civil Engineers-Geotechnical Engineering*, 166(2), 147–158.

Klinkvort, R. T., Leth, C. T., and Hededal, O. (2010). "Centrifuge modelling of a laterally cyclic loaded pile." *International Conference on Physical Modelling in Geotechnics*, 959–964.

Kramer, S. L. (1991). *Behavior of piles in full-scale, field lateral loading tests.* Washington State Department of Transportation.

L. Rasmussen, K., Hansen, M., Kirk Wolf, T., Ibsen, L. B., and Roesen, H. R. (2013). "A literature study on the effects of cyclic lateral loading of monopiles in cohesionless soils." *Report no.*, Department of Civil Engineering, Aalborg University.

Lada, A., Ibsen, L. B., and Nicolai, G. (2014). "The stiffness change and the increase in the ultimate capacity for a stiff pile resulting from a cyclic loading." *Report no.*, Department of Civil Engineering, Aalborg University.

LeBlanc, C., Houlsby, G., and Byrne, B. (2010). "Response of stiff piles in sand to long-term cyclic lateral loading." *Geotechnique*, 60(2), 79–90.

Lesny, K. and Hinz, P. (2009). "Design of monopile foundations for offshore wind energy converters." *Contemporary Topics in Deep Foundations*, 512–519.

Lesny, K., Hinz, P., et al. (2007a). "Investigation of monopile behaviour under cyclic lateral loading." *Offshore site investigation and geotechnics, confronting new challenges and sharing knowledge*, Society of Underwater Technology.

Lesny, K., Paikowsky, S., and Gurbuz, A. (2007b). "Scale effects in lateral load response of large diameter monopiles." *Contemporary Issues In Deep Foundations*, 1–10.

Lesny, K. and Wiemann, J. (2006). "Finite-element-modelling of large diameter monopiles for offshore wind energy converters." *GeoCongress 2006: Geotechnical Engineering in the Information Technology Age*, 1–6.

Li, W., Igoe, D., and Gavin, K. (2015). "Field tests to investigate the cyclic response of monopiles in sand." *Proceedings of the Institution of Civil Engineers-Geotechnical Engineering*, 168(5), 407–421.

Li, Z., Haigh, S., and Bolton, M. (2010). "Centrifuge modelling of mono-pile under cyclic lateral loads." *Physical Modelling in Geotechnics*, 965–970.

Lin, H., Ni, L., Suleiman, M. T., and Raich, A. (2014). "Interaction between laterally loaded pile and surrounding soil." *Journal of geotechnical and geoenvironmental engineering*, 141(4).

Lin, S.-S. and Liao, J.-C. (1999). "Permanent strains of piles in sand due to cyclic lateral loads." *Journal of Geotechnical and Geoenvironmental Engineering*, 125(9), 798–802.

Little, R. L. and Briaud, J.-L. (1988). "Full scale cyclic lateral load tests on six single piles in sand." *Report no.*, DTIC Document.

Long, J. and Vanneste, G. (1994). "Effects of cyclic lateral loads on piles in sand." *Journal of Geotechnical Engineering*, 120(1), 225–244.

Malhotra, S. (2007). "Design and construction considerations for offshore wind turbine foundations." *ASME 2007 26th International Conference on Offshore Mechanics and Arctic Engineering*, American Society of Mechanical Engineers, 635–647.

Mansur, C. I. and Hunter, A. H. (1970). "Pile tests-arkansas river project." *Journal of Soil Mechanics & Foundations Div.*

McClelland, B. and Focht, J. A. (1958). "Soil modulus for laterally loaded piles." *Transactions of the American Society of Civil Engineers*, 123(1), 1049–1063.

Meyer, B. J. and Reese, L. C. (1979). "Analysis of single piles under lateral loading." *Report no.*, Center for Highway Research, University of Texas at Austin TX.

Møller, I. F. and Christiansen, T. (2011). "Laterally loaded monopile in dry and saturated sand–static and cyclic loading." *Aalborg Univ., Aalborg, Denmark.*

Murchison, J. M. and O'Neill, M. W. (1984). "Evaluation of py relationships in cohesionless soils." *Analysis and Design of Pile Foundations:*, ASCE, 174–191.

Murphy, G., Cadogan, D., Doherty, P., Gavin, K., Caprani, C., and O'Connor, A. (2012). "Experimental investigation of novel foundation solutions for

offshore wind turbines." *Proceedings of BCRI 2012, 6–7th September 2012, Dublin*.

Murphy, G., Doherty, P., Cadogan, D., and Gavin, K. (2016). "Field experiments on instrumented winged monopiles." *Proceedings of the Institution of Civil Engineers-Geotechnical Engineering*, 169(3), 227–239.

Murphy, G., Doherty, P., Gavin, K., and Ward, D. (2014). "Characterisation of two dense sand sites in ireland using in-situ testing." *Proceedings of the 3rd International Symposium on Cone Penetration Testing*, 12–14.

Musial, W., Heimiller, D., Beiter, P., Scott, G., and Draxl, C. (2016). "2016 offshore wind energy resource assessment for the united states." *Report no.*, NREL (National Renewable Energy Laboratory (NREL), Golden, CO (United States)).

Naramore, S. and Feng, F. (1990). "Field tests of large diameter drilled shafts, part 1-lateral loads." *ReportNo. FHWA/CA/SD-88/02, California Department of Transportation, Sacramento, California*.

Nicolai, G., Ibsen, L. B., et al. (2014). "Small-scale testing of cyclic laterally loaded monopiles in dense saturated sand." *The Twenty-fourth International Ocean and Polar Engineering Conference*, International Society of Offshore and Polar Engineers.

Nicolai, G., Ibsen, L. B., et al. (2015). "Investigation on monopiles behavior under cyclic lateral loads in dense sand." *The Twenty-fifth International*

Ocean and Polar Engineering Conference, International Society of Offshore and Polar Engineers.

Nikitas, G., Vimalan, N. J., and Bhattacharya, S. (2016). "An innovative cyclic loading device to study long term performance of offshore wind turbines." *Soil Dynamics and Earthquake Engineering*, 82, 154–160.

Pan, D., Lucarelli, A., and Cheng, Z. (2016). "Field test and numerical analysis of monopiles for offshore wind turbine foundations." *Geotechnical and Structural Engineering Congress 2016*, 1138–1152.

Peck, R. B., Hanson, W. E., and Thornburn, T. H. (1974). *Foundation engineering*, Vol. 10. Wiley New York.

Petek, K., Mitchell, R., and Ellis, H. (2016). "Fhwa deep foundation load test database version 2.0 user manual." *Report no.*

Portugal, J. "Seco e pinto ps (1993) analysis and design of pile under lateral loads." *Proceedings of the 11th international geotechnical seminar on deep foundation on bored and auger piles, Belgium*, 309–313.

Prasad, Y. V. and Chari, T. (1999). "Lateral capacity of model rigid piles in cohesionless soils." *Soils and Foundations*, 39(2), 21–29.

Prendergast, L. J. and Gavin, K. (2016). "A comparison of initial stiffness formulations for small-strain soil–pile dynamic winkler modelling." *Soil Dynamics and Earthquake Engineering*, 81, 27–41.

Prendergast, L. J., Gavin, K., and Igoe, D. (2014). "Dynamic soil-structure interaction modeling using stiffness derived from in-situ cone penetration tests." *3rd International Symposium on Cone Penetration Testing, Las Vegas, Nevada, USA, 12-14 May, 2014*.

Price, G. and Wardle, I. (1987). "Lateral load tests on large diameter bored piles." *Report no.*

Qin, H. and Guo, W. D. (2016). "Response of static and cyclic laterally loaded rigid piles in sand." *Marine Georesources & Geotechnology*, 34(2), 138–153.

Reese, L. C. (1996). "Compilation of benchmark lateral load tests on piles in sand and clay.." *Report no.*, DTIC Document.

Reese, L. C., Cox, W. R., and Koop, F. D. (1974). "Analysis of laterally loaded piles in sand." *Offshore Technology in Civil Engineering Hall of Fame Papers from the Early Years*, 95–105.

Reese, L. C. and Van Impe, W. F. (2010). *Single piles and pile groups under lateral loading*. CRC Press.

Roesen, H. R., Andersen, L. V., Ibsen, L. B., Foglia, A., et al. (2012). "Experimental setup for cyclic lateral loading of monopiles in sand." *The Twenty-second International Offshore and Polar Engineering Conference*, International Society of Offshore and Polar Engineers.

Roesen, H. R., Ibsen, L. B., and Andersen, L. V. (2013a). "Experimental testing of monopiles in sand subjected to one-way long-term cyclic lateral

loading." *Proceedings of the 18th International Conference on Soil Mechanics and Geotechnical Engineering*.

Roesen, H. R., Ibsen, L. B., Hansen, M., Wolf, T. K., Rasmussen, K. L., et al. (2013b). "Laboratory testing of cyclic laterally loaded pile in cohesionless soil." *The Twenty-third International Offshore and Polar Engineering Conference*, International Society of Offshore and Polar Engineers.

Rollins, K. M., Lane, J. D., and Gerber, T. M. (2005). "Measured and computed lateral response of a pile group in sand." *Journal of Geotechnical and Geoenvironmental Engineering*, 131(1), 103–114.

Ruesta, P. F. and Townsend, F. C. (1997). "Evaluation of laterally loaded pile group at roosevelt bridge." *Journal of Geotechnical and Geoenvironmental Engineering*, 123(12), 1153–1161.

Sahasakkul, W., Nguyen, H., Sari, A., et al. (2016). "An improved methodology on design and analysis of offshore wind turbines supported by monopiles." *Offshore Technology Conference*, Offshore Technology Conference.

Sawin, J. L. (2015). "Renewables 2016 global status report." *REN21*.

Senanayake, A., Rendon, E., Wang, S.-T., Gerkus, H., Stevens, R. F., Gilbert, R. B., et al. (2015). "Design of large diameter monopiles under lateral loads in normally to moderately overconsolidated clay." *Offshore Technology Conference*, Offshore Technology Conference.

Senanayake, A. I. M. J. (2016). "Design of large diameter monopiles for offshore wind turbines in clay." Ph.D. thesis, Ph.D. thesis.

Sørensen, H., Peder, S., Ibsen, L. B., et al. (2012). "Experimental comparison of non-slender piles under static loading and under cyclic loading in sand." *The Twenty-second International Offshore and Polar Engineering Conference*, International Society of Offshore and Polar Engineers.

Sorensen, S. P., Ibsen, L. B., Foglia, A., et al. (2015). "Testing of laterally loaded rigid piles with applied overburden pressure." *International Journal of Offshore and Polar Engineering*, 25(02), 120–126.

Sørensen, S. P. H. and Ibsen, L. B. (2011). "Small-scale quasi-static tests on non-slender piles situated in sand." *Report no.*, Department of Civil Engineering, Aalborg University.

Stevens, R. F., Soosainathan, L., Rahim, A., Saue, M., Gilbert, R., Senanayake, A. I., Gerkus, H., Rendon, E., Wang, S. T., O'Connell, D. P., et al. (2015). "Design procedures for marine renewable energy foundations." *Offshore Technology Conference*, Offshore Technology Conference.

Suryasentana, S. and Lehane, B. (2014). "Verification of numerically derived cpt based p–y curves for piles in sand." *Proceedings of the 3rd international symposium on cone penetration testing*, 3–29.

Suryasentana, S. and Lehane, B. (2016). "Updated cpt-based p–y formu-

lation for laterally loaded piles in cohesionless soil under static loading." *Géotechnique*, 66(6), 445–453.

Tak Kim, B., Kim, N.-K., Jin Lee, W., and Su Kim, Y. (2004). "Experimental load–transfer curves of laterally loaded piles in nak-dong river sand." *Journal of Geotechnical and Geoenvironmental Engineering*, 130(4), 416–425.

Thomassen, K., Roesen, H. R., Ibsen, L. B., and Sørensen, S. P. H. (2011). "Small-scale testing of laterally loaded monopiles in sand." *Symposium Proceedings: 64th Canadian Geotechnical Conference and 14th Pan-American Conference on Soil Mechanics and Engineering*.

Ting, J. M. (1987). "Full-scale cyclic dynamic lateral pile responses." *Journal of Geotechnical engineering*, 113(1), 30–45.

Uncuoğlu, E. and Laman, M. (2011). "Lateral resistance of a short rigid pile in a two-layer cohesionless soil." *Acta Geotechnica Slovenica*, 2, 19–43.

Velarde, J. (2016). "Design of monopile foundations to support the dtu 10 mw offshore wind turbine." M.S. thesis, NTNU, NTNU.

Versteijlen, W., Van Dalen, K., Metrikine, A., and Hamre, L. (2014). "Assessing the small-strain soil stiffness for offshore wind turbines based on in situ seismic measurements." *Journal of Physics: Conference Series*, Vol. 524, IOP Publishing.

Villalobos Jara, F. A. (2006). "Model testing of foundations for offshore wind turbines." Ph.D. thesis, University of Oxford, University of Oxford.

Wichtmann, T., Niemunis, A., and Triantafyllidis, T. (2008). "Prediction of long-term deformations for monopile foundations of offshore wind power plants." *11th Baltic Sea Geotechnical Conference: Geotechnics in Maritime Engineering*.

Xue, J., Gavin, K., Murphy, G., Doherty, P., and Igoe, D. (2016). "Optimization technique to determine the py curves of laterally loaded stiff piles in dense sand.

Yan, L. and Byrne, P. M. (1992). "Lateral pile response to monotonie pile head loading." *Canadian Geotechnical Journal*, 29(6), 955–970.

Yang, M., Ge, B., Li, W., and Zhu, B. (2016). "Dimension effect on p-y model used for design of laterally loaded piles." *Procedia Engineering*, 143, 598–606.

Yu, L.-q., Wang, L.-z., Guo, Z., Bhattacharya, S., Nikitas, G., Li, L.-l., and Xing, Y.-l. (2015). "Long-term dynamic behavior of monopile supported offshore wind turbines in sand." *Theoretical and Applied Mechanics Letters*, 5(2), 80–84.

Zakeri, A., Clukey, E. C., Kebadze, E. B., and Jeanjean, P. (2016a). "Fatigue analysis of offshore well conductors: Part i–study overview and evaluation of series 1 centrifuge tests in normally consolidated to lightly over-consolidated kaolin clay." *Applied Ocean Research*, 57, 78–95.

Zakeri, A., Clukey, E. C., Kebadze, E. B., and Jeanjean, P. (2016b). "Fatigue analysis of offshore well conductors: Part ii–development of new approaches for conductor fatigue analysis in clays and sands." *Applied Ocean Research*, 57, 96–113.

Zdravković, L., Taborda, D., Potts, D., Jardine, R., Sideri, M., Schroeder, F., Byrne, B., McAdam, R., Burd, H., Houlsby, G., et al. (2015). "Numerical modelling of large diameter piles under lateral loading for offshore wind applications." *Proceeding 3rd International Symposium on Frontiers in Offshore Geotechnics. Norway:[sn]*.

Vita

Udit Shankar Dasgupta was born in Delhi, India and grew up in Mumbai, India. He received his Bachelor of Engineering (Hons.) degree in Civil Engineering from the Birla Insitute of Technology and Science, Pilani, India in 2015. Right after completing his undergraduate program, he moved to Austin, Texas to pursue his master's degree in geotechnical engineering.

Permanent address: usd@utexas.edu
udasgupta93@gmail.com

This thesis was typeset with LaTeX[†] by the author.

[†]LaTeX is a document preparation system developed by Leslie Lamport as a special version of Donald Knuth's TeX Program.